Competition and conjugation between agrobacterial cooperators and cheaters

by

Priscila Amanda Guzman

B.S., Middle Georgia State University, 2014
A.S., Middle Georgia State University, 2015

AN ABSTRACT OF A DISSERTATION

submitted in partial fulfillment of the requirements for the degree

DOCTOR OF PHILOSOPHY

Division of Biology
College of Arts and Sciences

KANSAS STATE UNIVERSITY
Manhattan, Kansas

2022

Abstract

Natural selection favors selfish behaviors that undermine the stability of cooperative systems. Despite this, cooperation is widespread throughout nature, including in the microbial world. This dissertation examines the interactions between bacterial cheaters and cooperators, and how these interactions influence the evolution of cooperation and virulence. Bacterial cooperators often pay a fitness cost to provide a benefit, a public good, that benefits the cooperator and other nearby individuals. These public goods drive the emergence of cheaters, individuals that do not pay the costs of cooperation but do benefit from the public goods produced by cooperators. Because cheaters have an inherent competitive advantage over cooperators, they threaten the stability of cooperative systems. Cooperative individuals may employ strategies that antagonize cheaters, thereby preventing cheaters from spreading through the population. In Agrobacterium tumefaciens, a plant pathogen and the causative agent of crown gall disease, cooperation is a key feature of its infection of host plants. Cooperative agrobacteria carry the tumor inducing (Ti) plasmid that encodes the virulence genes required for the genetic transformation of plants. The act of infecting the plants is metabolically costly, involving the expression of the vir genes required to form a type IV secretion system and the effectors that mediate delivery of the T-DNA (transferred DNA) into the plant's genome. This genetic transformation of the plant by the T-DNA results in the misregulation of plant hormones and the production of opines, small compounds that serve as a nutrient source for agrobacteria. Cheater agrobacteria, individuals that do not infect plants, but do catabolize opines, replicate faster than their cooperative counterparts. Yet, despite this

expected competitive advantage, natural cheaters have not been observed dominating the agrobacterial populations associated with natural galls.

My research focuses on three main areas related to the interaction between agrobacterial cooperators and cheaters: the population ecology of cheaters, conjugation of the Ti plasmid into cheaters, and screening platforms for the study of competitive interactions between cheaters and cooperators. Broadly, I demonstrated that ΔvirA mutants are cheaters that have a large fitness advantage over virulent agrobacteria. Further, I showed that in gall-like environments the expression of virulence is very costly for agrobacterial cooperators. As a result, agrobacterial cheaters readily arise de novo in these environments. I explored the antagonistic interactions between cheaters and cooperators, focusing on whether pathogenic agrobacteria used horizontal gene transfer as a policing mechanism to prevent cheaters from taking over. In A. tumefaciens, conjugation is regulated in response to bacterial cell density by quorum sensing (QS). To understand the effects of conjugation on cheater policing, I carried out competitions involving mutants lacking TraR. I found that TraR is necessary for conjugation and that traR+ cooperators compete more favorably against ΔvirA cheaters than do traR- cooperators. However, conjugation alone will not antagonize cheater spread when they are already present in a population. In contrast, when cheaters arise via de novo mutations, conjugation can serve as a policing mechanism against freeloaders. Finally, driven by the limitations of current platforms for the screening of microbial interactions, I collaborated on the development of a new tool for the screening of microbial interactions. I used a photodegradable hydrogel that allows for high-throughput screening of bacterial populations in just one experimental trial. As a proof-of-principle, I studied a known interaction between an

agrobacterial cooperator and a cheater and demonstrated that our approach allows the screening of entire transposon mutant libraries in a single experiment. In a first screen of this kind, I was able to identify, extract, and characterize rare cells (9/28,000) using this high-throughput approach. Thus, photodegradable hydrogels offer a powerful, straightforward, and adaptable approach that can be used not only for the screening of cheater-cooperator competitive interactions, but also more broadly for the study of other microbial interactions.

Competition and conjugation between agrobacterial cooperators and cheaters

by

Priscila Amanda Guzman

B.S., Middle Georgia State University, 2014
A.S., Middle Georgia State University, 2015

A DISSERTATION

submitted in partial fulfillment of the requirements for the degree

DOCTOR OF PHILOSOPHY

Division of Biology
College of Arts and Sciences

KANSAS STATE UNIVERSITY
Manhattan, Kansas

2022

Approved by:

Major Professor
Dr. Thomas G. Platt

Copyright

Abstract

Natural selection favors selfish behaviors that undermine the stability of cooperative systems. Despite this, cooperation is widespread throughout nature, including in the microbial world. This dissertation examines the interactions between bacterial cheaters and cooperators, and how these interactions influence the evolution of cooperation and virulence. Bacterial cooperators often pay a fitness cost to provide a benefit, a public good, that benefits the cooperator and other nearby individuals. These public goods drive the emergence of cheaters, individuals that do not pay the costs of cooperation but do benefit from the public goods produced by cooperators. Because cheaters have an inherent competitive advantage over cooperators, they threaten the stability of cooperative systems. Cooperative individuals may employ strategies that antagonize cheaters, thereby preventing cheaters from spreading through the population. In Agrobacterium tumefaciens, a plant pathogen and the causative agent of crown gall disease, cooperation is a key feature of its infection of host plants. Cooperative agrobacteria carry the tumor inducing (Ti) plasmid that encodes the virulence genes required for the genetic transformation of plants. The act of infecting the plants is metabolically costly, involving the expression of the vir genes required to form a type IV secretion system and the effectors that mediate delivery of the T-DNA (transferred DNA) into the plant's genome. This genetic transformation of the plant by the T-DNA results in the misregulation of plant hormones and the production of opines, small compounds that serve as a nutrient source for agrobacteria. Cheater agrobacteria, individuals that do not infect plants, but do catabolize opines, replicate faster than their cooperative counterparts. Yet, despite this

expected competitive advantage, natural cheaters have not been observed dominating the agrobacterial populations associated with natural galls.

My research focuses on three main areas related to the interaction between agrobacterial cooperators and cheaters: the population ecology of cheaters, conjugation of the Ti plasmid into cheaters, and screening platforms for the study of competitive interactions between cheaters and cooperators. Broadly, I demonstrated that ΔvirA mutants are cheaters that have a large fitness advantage over virulent agrobacteria. Further, I showed that in gall-like environments the expression of virulence is very costly for agrobacterial cooperators. As a result, agrobacterial cheaters readily arise de novo in these environments. I explored the antagonistic interactions between cheaters and cooperators, focusing on whether pathogenic agrobacteria used horizontal gene transfer as a policing mechanism to prevent cheaters from taking over. In A. tumefaciens, conjugation is regulated in response to bacterial cell density by quorum sensing (QS). To understand the effects of conjugation on cheater policing, I carried out competitions involving mutants lacking TraR. I found that TraR is necessary for conjugation and that traR+ cooperators compete more favorably against ΔvirA cheaters than do traR- cooperators. However, conjugation alone will not antagonize cheater spread when they are already present in a population. In contrast, when cheaters arise via de novo mutations, conjugation can serve as a policing mechanism against freeloaders. Finally, driven by the limitations of current platforms for the screening of microbial interactions, I collaborated on the development of a new tool for the screening of microbial interactions. I used a photodegradable hydrogel that allows for high-throughput screening of bacterial populations in just one experimental trial. As a proof-of-principle, I studied a known interaction between an

agrobacterial cooperator and a cheater and demonstrated that our approach allows the screening of entire transposon mutant libraries in a single experiment. In a first screen of this kind, I was able to identify, extract, and characterize rare cells (9/28,000) using this high-throughput approach. Thus, photodegradable hydrogels offer a powerful, straightforward, and adaptable approach that can be used not only for the screening of cheater-cooperator competitive interactions, but also more broadly for the study of other microbial interactions.

Table of Contents

List of Figures

List of Tables

Acknowledgements

I am eternally grateful for the guidance, advice, and support of my advisor Tom Platt. Over the last six years, you have been a source of inspiration and helped me become a better scientist, mentor, and person. Thank you for your encouragement, for allowing me to cultivate my interests outside of the lab, for the many, many letters of recommendation, and for trusting me to be a good mentor to the undergrads in the lab. You have undoubtedly been integral to my development as a scientist, but what I am most grateful for are the conversations and the support you gave me when life got rough. Thank you for being an excellent mentor.

Thank you also to my supervisory committee – Revathi Govind, Ryan Hansen & Lydia Zeglin. You have been generous with your time and expertise. I am grateful for your support.

A special thanks to members, past and present, of the Platt Lab. You have been a crucial part of my graduate journey, and I am so incredibly happy to be a part of the same science fam! A special shoutout to Veronica Mateo, Annie Dillon, Chris Carter, Isam Madi, and Dana Johnson. Thanks to members of the Hansen Lab -Niloy Barua, Niloufar Fattahi & Andre van der Vlies, and the Fuqua Lab -Ian Barton. I learned a lot from our collaborations and enjoyed meeting you all.

I was lucky enough to be a part of the Yale Ciencia Academy, the STEM Advocacy Institute, EDSIN Power of Data, CommSciCon, AAAS CASE, KAWSE, KSCI, GSC, Eli Lilly's MIH LDA, CienciaPR, and KSACNAS. I am forever grateful to these organizations for the opportunities, conversations, and friendships that they have given me. Also, a big thank you to my funding sources who allowed me to do work not only in the lab, but with the Manhattan community: NSF GRFP, BGSA, GSC, BioKansas, SACNAS, Eli Lilly, SAi, and KSU.

To my friends in Puerto Rico- gracias! The joyful conversations, the board games and movie nights helped make this journey a bit more fun! I especially appreciate you all agreeing to the litany of karaoke nights! To Raul, Xiomara, Joel, Amanda, Alberto, Jariel, Jovaniel, Stacey, Shirley, Ilaisa, Juan, Isra & Gherardee – los adoro. I also want to thank the BGSA community who made these last years a fun experience. To Shilpa, Nirupama, Dustin, Candy, Anne, Josh, Elsie, Alicia, Henry, Nick, Leah, Seton, Anil, Babita, Pragyesh and many others – thank you!

To Reilly Jensen, my undergraduate mentee – mil gracias! Your help with experiments and data collection was crucial. I hope you learned from me as much as I learned from you.

To my partner in science – Aakash. Meeting you is one of the highlights of my graduate journey. I will not forget the conversations, photo shoots, food dates, margarita Mondays, and the supportive text messages. You, my friend, are a rare gem and I will miss you deeply.

To the biggest bullies and greatest allies, my sisters. Life would be dull without you. Thank you for listening to my school rants and for your input on figures and presentations.

To my life partner- Jordan. Thank you for listening to my presentations and for labeling all those petri plates. I couldn't be here without your support. I love you lots! Keep flying high!

Last, but certainly not least, to those who shaped me into who I am today. To my parents, my grandparents, and my uncle. I can't begin to put into words what you mean to me. You all sacrificed so much so that I could be here, and here we are. This achievement is yours. You are the force that drives me to be better and do better. You are a constant source of inspiration and strength. You are the foundation of my successes, and the biggest blessing God has bestowed on me. My only wish is to repay all that which you have done for me.

I love you all endlessly....

Dedication

A mis padres,

Luis Ángel Nieves Vélez & Edna Luz Otero Maldonado

A mis abuelos,

Ángel Luis Otero Feliciano, Aida Luz Maldonado Dávila & Eduvijis Vélez Echevarría

Vivo eternamente agradecida por todos los sacrificios que han hecho por mí. Soy y siempre seré un reflejo de ustedes; de sus valores y creencias, de sus sueños y su arduo trabajo. Este logro no es mío, es nuestro. Es la culminación de todos los proyectos, de los viajes a la universidad, las amanecidas estudiando y las competencias escolares. Este título sería irrelevante sin ustedes, sin su apoyo.; pero hoy es la celebración de muchos sacrificios. ¡Quien diría que un papel pudiera significar tanto! Estoy aquí gracias al favor y la gracia del Señor, sin Él no soy nada; pero también estoy aquí gracias a ustedes y a los valores que inculcaron en mí.

Ustedes son el fundamento de mis dichas y logros, son el tesoro más grande que jamás tendré. Mi único anhelo es tenerlos conmigo por mucho tiempo y poder celebrar muchos triunfos y alegrías a su lado. Si algo he aprendido en estos últimos años es que la vida es efímera, el amor es inefable y el estar presentes es el mejor regalo que podemos dar. Dicho esto, quiero agradecerles por siempre estar presente, por amarme incondicionalmente y por apoyarme en todas las etapas de mi vida. Con orgullo y una alegría que no me cabe en el pecho, quiero inmortalizar mi agradecimiento hacia ustedes y decirles que los amo infinitamente.

Preface

Microbial interactions are as ubiquitous as the participants themselves. Microbiomes, diverse microbial communities, are shaped by these complex intra- and interspecific interactions that have a major impact on individuals, populations, and communities as well as the environments in which they occur (Coyte et al., 2015; Venturi & Bez, 2021). Given the breadth and diversity of microbes, it is no surprise these exchanges can lead to not only different types of interactions, but also large-scale impacts. Positive or beneficial interactions include mutualism, syntrophism, commensalism, and cooperation, whereas negative or detrimental interactions may involve predation, parasitism, and interference and resource competition (Faust & Raes, 2012; Tshikantwa et al., 2018). Bacteriocin production highlights one way in which microbes can compete with one another, while the production of extracellular iron-scavenging molecules is an example of microbial cooperation (Buckling et al., 2007; Kobayashi, 2021).

In this dissertation, I examined the ecologic, evolutionary, and genetic consequences of interactions between bacteria. Specifically, I examined cooperative and competitive interactions using the plant pathogen *Agrobacterium tumefaciens*. *A. tumefaciens* is the causative agent of crown all disease and a model organism for studies on quorum sensing (H.-B. Zhang et al., 2002), virulence (Gelvin, 2006), and plant transformation (Gelvin, 2003). The cooperative pathogenesis of *A. tumefaciens* is well-characterized, however most studies focus on its role as a pathogen or as a tool for plant genetic engineering. My dissertation aims to elucidate how interactions among agrobacteria influence the evolution of cooperation and agrobacterial virulence. Moreover, my focus on the interactions between agrobacterial

cheaters and cooperators aims to understand the population ecology of cheaters and the effects of conjugation of the Ti plasmid. I also developed a high throughput screening platform for the study of competitive interactions between agrobacterial cheaters and cooperators.

Chapter 1- *Freeloading agrobacteria outcompete agrobacterial pathogens*

A. tumefaciens cooperators carry the tumor inducing (Ti) plasmid that encodes the genes needed to infect plant hosts. Infecting plants is metabolically costly, but results in the misregulation of plant hormones and the production of opines, small compounds that serve as a nutrient source for agrobacteria. As a result, agrobacterial cheaters, individuals that do not infect plants, but catabolize opines, have a fitness advantage over cooperators in the disease environment.

I examined the emergence of cheaters and the costs associated with virulence expression in this system. I found that the fitness costs related to the expression of the virulence genes drive the emergence and spread of cheaters. Cheater phenotypes result from the loss of virulence genes needed for pathogenesis or the curing of the cooperative plasmid. I found that avirulent mutants can only use opines as a nutrient source if they emerge in their presence. Thus, only mutants that arise in the presence of opines will retain the ability to catabolize them. This chapter therefore highlights that the costs and benefits of cooperation will impact the fitness of both cheaters and cooperators and underscores that ecological and genetic dynamics of this system depend on the selective context in which they take place.

Chapter 2- *Plasmid conjugation antagonizes the invasion of greenbeard cheater mutants*

Quorum sensing is a gene regulatory system in which bacteria coordinate gene expression in response to self-produced chemical cues (Moré et al., 1996; H.-B. Zhang et al., 2002). In *A. tumefaciens*, Ti plasmid conjugation is regulated by a quorum sensing system carried on the Ti plasmid. This gene regulatory system ensures that conjugation occurs when cell density is high and opines are present. One of the main players in Ti plasmid conjugation is the transcription factor TraR. Binding of acyl homoserine lactone cues drives TraR dimerization. This dimer complex initiates the expression of the genes required for conjugation and is thus necessary for the conjugation of the Ti plasmid. This chapter aims to understand the effects of Ti plasmid conjugation on the interactions between cooperators and cheaters. In Chapter 1, I established that agrobacterial cheaters genotypes readily arise *de novo* in environments containing both opines and the plant cues that trigger the expression of the genes required for pathogenesis. In this chapter we examine whether quorum sensing regulated conjugation of the Ti plasmid antagonizes the spread of cheaters.

I found that conjugation will not antagonize cheater spread if cheaters are initially present in the population. However, if cheaters arise spontaneously via mutation, conjugation has a significant antagonistic effect on cheater emergence. Conjugation of the Ti plasmid into cheater mutants transforms cheaters to cooperators that induce *vir* expression and can cause the formation of plant tumors. These findings demonstrate that Ti plasmid conjugation can help stabilize agrobacterial cooperation and virulence.

Chapter 3- *Photodegradable hydrogels for rapid screening, isolation, and genetic characterization of bacteria with rare phenotypes*

Screening bacterial populations is a lengthy and arduous process if one relies on standard microbiology approaches. Some of these conventional approaches have limitations that prevent their use for the study of important microbial interactions like those that involve rare phenotypes. Motivated by the limitations of current plating-based approaches for the screening of microbial interactions, I collaborated on the development of a novel technique for the screening of microbial interactions. This technique uses a photodegradable hydrogel that encapsulates cells but allows for their growth. In addition, the hydrogel allows for high-throughput screening of bacterial populations. As a proof-of-principle, I studied the well-known interaction between an agrobacterial cooperator and a cheater. I found that this new approach allows for the screening of entire mutant libraries in a single experiment. In addition, using this new high-throughput technique, I was able to identify, extract, and characterize rare cells (9/28,000) with the target phenotype. This chapter proves that photodegradable hydrogels are a powerful and adaptable approach that could be used in the screening of cheater-cooperator competitive interactions and more broadly for the study of other microbial interactions.

My dissertation aims to elucidate the competitive and conjugative interactions between agrobacterial cooperators and cheaters. I tackled this subject looking not only at the population and individual levels, but also at the genetic level. My dissertation advances our understanding of the competitive and cooperative interactions of agrobacteria and how these interactions drive the evolution of cooperative pathogenesis.

Chapter 1 - Freeloading Agrobacteria Outcompete Agrobacterial Pathogens

Introduction

The evolutionary stability of cooperative behaviors is undermined by the inherent fitness advantage cheaters have over cooperative individuals (Damore & Gore, 2012; Platt & Bever, 2009). Despite this, cooperation is widespread at all levels of biological organization. Cooperation and social interactions more generally have a strong impact on the population dynamics and evolution of a wide range of bacterial traits, including mechanisms mediating nutrient acquisition(Cordero et al., 2012), the production of biosurfactants required for swarming (Xavier et al., 2011), or secretion of exoproteases (Loarca et al., 2019). Bacterial cooperation often involves one or more individuals incurring a fitness cost to make a public good available (Damore & Gore, 2012; Oliveira et al., 2014; Smith & Schuster, 2019). These public goods are often secreted molecules that benefit both the cooperators that make them available and neighboring bacteria in the population. Cheaters exploit cooperative behaviors as they benefit from public goods without paying the fitness costs associated with their production. Cheaters can arise via mutation or arrive via migration and are a threat to the evolutionary stability of these cooperative traits due to their innate fitness advantage over cooperative individuals (Friesen, 2020; Mc Ginty et al., 2011; Ostrom, 2008). Invasion by cheaters can lead to a decrease in public goods availability and even potential population collapse (Madgwick et al., 2018; Smith & Schuster, 2019).

Agrobacterium tumefaciens is a plant pathogen whose infection of hosts depends on cooperation. Most of the genes required to infect hosts are carried on the tumor inducing (Ti) plasmid (Escobar & Dandekar, 2003; Platt, Bever, et al., 2012). The Ti plasmid-encoded VirA/VirG two-component system regulates responses to several cues associated with the rhizosphere of wounded plant roots (e.g. including high levels of plant phenolics like acetosyringone). VirA is a periplasmic histidine kinase that activates VirG, a sequence-specific DNA-binding regulatory protein, in response to plant phenolics, low pH, and other cues (Gelvin, 2003; Jin, Prusti, et al., 1990; Jin, Roitsch, et al., 1990; S. Winans et al., 1994). Phosphorylated VirG initiates the expression of several genes, including those required for the expression of a type IV secretion system that delivers the T-DNA (transferred DNA), a part of the Ti plasmid, into the plant's genome (Barton et al., 2018a; Escobar & Dandekar, 2003; Gordon & Christie, 2014; Platt, Bever, et al., 2012). Transformed plant cells misregulate key growth hormones resulting in formation of a tumor. Transformed plant cells also produce and secrete small metabolites known as opines which *A. tumefaciens* uses as a nutrient source (Barton et al., 2018a; Escobar & Dandekar, 2003; Platt, Bever, et al., 2012). Thus, the benefits of agrobacterial infections arise from the breakdown of public goods -opines- produced by the infected plant cells.

Agrobacterial pathogenesis and opine catabolism genes are encoded in the Ti plasmid. The Ti plasmid is an example of a multigene greenbeard, since the genes required for cooperative pathogenesis (the *vir*-genes) are genetically linked to the genes required to access the benefits of cooperation, the opine catabolism genes (Platt, Bever, et al., 2012; Platt & Bever, 2009). However, some strains have evolved the ability to breakdown opines while

lacking the genes that encode agrobacterial cooperative pathogenesis (Barton et al., 2018a; Gordon & Christie, 2014; Merlo & Nester, 1977; Platt, Bever, et al., 2012). These strains are cheaters that bypass the fitness costs associated with plant infection but benefit from the public goods produced. In this study, we examined the costs of virulence expression, the environmental factors that lead to emergence of cheaters, and describe the mutations that produce cheaters. Although cheaters in this system do not directly affect availability of public goods, they can still evade the high fitness costs associated with agrobacterial pathogenesis. By taking advantage of the opines and replicating faster than cooperators, these freeloaders could dramatically alter the structure of the agrobacterial populations in the plant tumor environment (Guyon et al., 1993; Savka & Farrand, 1997).

In this paper we show that the costs and benefits associated with cooperation directly impact the fitness of agrobacterial cheaters and cooperators. Moreover, the fitness costs associated with the expression of the virulence genes drives the origin and spread of cheaters during experimental evolution. These cheater phenotypes are the result of the loss of genes required for cooperative pathogenesis. If they emerge in the absence of opines, these avirulent mutants are not able to use opines as a nutrient source and are thus not able to freeload on infections established by the cooperative pathogen. Only mutants that emerge in environments where opines are present retain the ability to catabolize them. Thus, we show that the ecological and genetic dynamics of cooperative bacteria will largely depend on the selective context in which they take place.

Materials & Methods

Strains, plasmids, reagents, media, and growth conditions

The bacterial strains and plasmids used in this study are described in Tables 5.1-5.3. We obtained chemicals, antibiotics, and culture media from Fisher Scientific (Pittsburgh, PA), Sigma Aldrich (St. Louis, MO), VWR (Wayne, PA), Midwest Scientific (Valley Park, MO), and Goldbio (St. Louis, MO), unless otherwise noted. Oligonucleotide primers were ordered from Integrated DNA Technologies (Coralville, IA). Unless specified otherwise, strains were cultured and genetically manipulated using the methods described by Morton & Fuqua (2012). Plasmids were introduced to *E. coli* strains via transformation of chemically competent cells and to *A. tumefaciens* via conjugation. Genetic changes in *A. tumefaciens* were performed via allelic replacement (Morton & Fuqua, 2012a). All mutant strains used in this study have been sequenced confirmed. The 15955 Δ*virA* mutant used in competition experiments is isogenic to the ancestral 15955 wildtype except for the in-frame *virA* deletion, thereby allowing attribution of observed fitness consequences to the effects of lacking *virA*.

Unless noted otherwise, all agrobacterial strains were grown on AT minimal media with 0.5% (w/v) glucose and 15 mM ammonium sulfate (Morton & Fuqua 2012). *E. coli* strains were cultured in Luria-Bertani broth. Antibiotics for *E. coli* were used at the following concentrations: ampicillin (100 μg/ml), gentamicin (50 μg/ml), kanamycin (50 μg/ml), spectinomycin (100 μg/ml), and streptomycin (25 μg/ml). Antibiotics for *A. tumefaciens* were used at the following concentrations: ampicillin (150 μg/ml), gentamicin (100 μg/ml), kanamycin (200 μg/ml), spectinomycin (100 μg/ml), and streptomycin (2500 μg/ml).

Opine catabolism assay

We evaluated how well strains grow on octopine as a sole carbon and nitrogen source as described by Platt et al. (Platt, Bever, et al., 2012) with some minor modifications. We grew the strain to mid-log phase (OD_{600} = 0.5 - 0.8) and then diluted them to an OD_{600} of approximately 0.05. The cells were collected via centrifugation and washed with 78.6 mM KH_2PO_4 buffer (pH 7.0) 8 times to remove carryover carbon or nitrogen. Washed cells were then diluted to OD_{600} = 0.0005 in either 2 ml (culture tubes) or 0.7 ml (96-well deep-well plates) of AT minimal media (Morton & Fuqua 2012) supplemented with 0 (AT–O) or 300 mM (AT+O) of octopine as a sole source of carbon and nitrogen. The cultures were incubated at 28°C overnight with shaking. The OD_{600} of the cultures was monitored using a spectrophotometer or a plate reader.

Competition experiment

In order to assess the fitness costs associated with expression of *virA*, we competed Δ*virA* cells against its parental genotype in a variety of environmental conditions differing in the presence or absence of plant cues (acetosyringone) and opines (octopine). We followed the approach described by Platt, Bever, et al. (2012) with some modifications. The competition media control contained AT salts, 27.5 mM glucose, 0.6 mM $(NH_4)_2SO_4$, 0.5 mM NaH_2PO_4, 0.05 per cent DMSO, and was buffered to pH 5.6 by 2-(*N*-morpholino)ethanesulfonic (MES) (Morton & Fuqua, 2012b). The + Plant Cue media was the competition control media supplemented with 200 µM acetosyringone. The + Opines media was the competition control media supplemented with 0.6 mM octopine. Lastly, the + Plant Cue + Opines media was the competition media supplemented with 200 µM acetosyringone and 0.6 mM octopine.

We grew the strains to mid-log phase (OD_{600} = 0.5 - 0.8) and then diluted each to an OD_{600} of approximately 0.05. Cells were collected via centrifugation and washed with 78.6 mM KH_2PO_4 buffer (pH 7.0) 8 times to remove carryover carbon or nitrogen. Washed cells were then diluted in their respective media to an OD_{600} = 0.005. Competitions consisted of approximately half wildtype cells and half Δ*virA* cells carrying a spectinomycin and streptomycin resistance cassette (ERM117) or half wildtype cells carrying the same antibiotic resistance cassette (ERM115) and half 15955 Δ*virA* (TGP103) cells. Competition mixtures were diluted to an OD_{600} of 0.005 and incubated at 28°C overnight. Competition cultures were sub-cultured 1: 100 into 2 ml of the appropriate media one time. We plated serial dilutions of all initial cell mixtures, each culture after 24 hours of incubation, and 24 hours after the passage. Cultures were plated onto ATGN (± appropriate antibiotics) to estimate the density of each genotype in each culture.

Evolution experiment

Wildtype *A. tumefaciens* 15955 was grown overnight at 28°C to mid-log phase (OD_{600} = 0.5 - 0.8). After overnight incubation, cultures were diluted to an OD_{600} of approximately 0.05 in media that varies in the presence or absence of both acetosyringone and octopine. Control evolution media was composed of AT salts, 27.5 mM glucose, 0.6 mM $(NH_4)_2SO_4$, 0.5 mM NaH_2PO_4, 0.05 per cent DMSO, and 1X Hutner Base (Morton & Fuqua, 2012b). The media was buffered to pH 5.6 by 2-(*N*-morpholino)ethanesulfonic (MES). + Plant Cue media is control evolution media supplemented with 200 µM acetosyringone. Similarly + Opines media is the control media supplemented with 0.6 mM octopine and + Plant Cue + Opines media is control media supplemented with both 200 µM acetosyringone and 0.6 mM octopine. The 96-well

plates were then incubated overnight at 28°C. After overnight incubation, the cultures were passaged into a new 96 well plates with fresh media at a 1 : 100 ratio of inoculate to fresh media. This process was then repeated for a total of 14 passages. At each passage, 25% glycerol stock of each replicate were frozen at -80°C. After the final passage, *vir*-gene induction was measured as the β-galactosidase activity resulting from expression of a P*virB*::*lacZ* reporter carried on pSW209Ω (Y. Wang et al., 2000). Each population was mated with S17-1 λpir pSW209 on LB to deliver the P*vir*B reporter. Matings were incubated on LB media overnight at 28 °C. The next day, the cells were collected, serially diluted, and plated on P*virB*-*lacZ* medium to measure P*virB* expression and select for agrobacterial cells as S17-1 λpir cannot grow on this minimal media. P*virB*-lacZ media contains AT minimal media salts, 0.5% (w/v) glucose, 20 mM MES pH 5.6 buffer, 500 µM phosphate, 200 µM acetosyringone, 200 µg/ml kanamycin, and 40 mg/ml X-gal (5-bromo-4-chloro-3-indolyl-galactopyranoside). After a 4–5-day incubation period we counted the numbers of white and blue colonies. Cells that can express the P*virB*::*lacZ* construct will form blue colonies; whereas cells that do not express these genes will form white colonies.

To understand the evolutionary consequences of evolution with plant cues and opines on opine catabolism and pathogenicity phenotypes, we evaluated these phenotypes on a subset of isolates recovered from the '+ Plant Cue' and '+ Plant Cue + Opines' evolution treatments. We performed these assays on two P*virB*$^{-}$ isolates and one P*virB*$^{+}$ isolate per independent evolution line, for a total of 48 evolved isolates (16 P*virB*$^{-}$ and 8 P*virB*$^{+}$ per environment treatment). The octopine catabolic assay was performed as described above.

The pathogenicity assay was performed as described by Anand & Heberlein (1977), with minor modifications. Liquid cultures of each isolate were grown overnight to mid-log phase (OD_{600} = 0.5 - 0.8) and diluted to OD_{600} = 0.05. Red potatoes were surfaced sterilized by soaking them in a 1.05% sodium hypochlorite solution for 20 minutes. Then, we removed 3 cm from both ends of the potato with a surface sterilized scalpel. We used a surface sterilized cork borer (11 mm diameter) to obtain an internal segment of potato tissue. Both ends of the potato cylinder were discarded, and the remaining part was sliced with a sterilized scalpel into 2 mm thick disks. Two potato disks were placed into a 60 x 15 mm 1.5 % agar water Petri plate and each potato disk was inoculated with 35 µL of an OD_{600} = 0.05 cell suspension. Plates were placed in a sterilized container along with a cup of saturated K_2SO_4 solution to ensure the plates did not dry out while incubating. The plates were incubated at room temperature for 21 days. After incubation, we recorded the presence or absence of tumors on the potato disks.

Sunflower i*n planta* competition experiment

We competed wildtype 15955 cells against either 15955 Δ*virA* or a pTi15955-cured derivative of 15955 on *Helianthus annuus* plants as described by (Morton et al., 2014). To prepare seedlings, we germinated surface sterilized seeds in sterile soil and allowed them to grow for two weeks. Each seedling was then wounded with a 0.5 - 1 cm cut at the root-shoot joint using a sterile razor blade. We then transferred the wounded seedling to a double deep pot where 10 ml of inoculum was delivered directly onto the wound site. After the plant was positioned into the pot, we then flooded the soil surface with a mixture of 25 ml of sterile MqH_2O and 10 ml of cell inoculum. Sterile control pots received 25 ml of sterile MqH_2O and 20 ml of AT minimal

medium. To prepare inoculum, we grew all strains to mid-log phase (OD600 = 0.5 - 0.8) in AT minimal medium, normalized all cultures to an OD600 of 0.25, and mixed the appropriate strains at a 1 : 1 ratio. Each experimental trial involved ERM115 competing with either TGP101 or TGP103 or 15955 competing with ERM116 or ERM117. We used selective plating (AT minimal media ± appropriate antibiotics) of the mixed inoculum to quantify the initial density of each strain present. Eleven weeks after plants were inoculated, we collected 1 – 3 grams of soil that was not associated with the plant, 1 – 3 grams of plant roots, and the plant gall. We then made a 1 : 10 (w : v) slurry of the soil sample, roots, and gall in MqH_2O that was vigorously shaken for 1 hour prior to being serially diluted and plated onto medium 1A supplemented with 315.2 µM tellurite which is semi-selective for biovar 1 agrobacteria (Shams et al., 2012). We then patched 300 colonies from each sample onto AT minimal media ± appropriate antibiotics to determine the frequency of each strain present. A second *in planta* competition experiment involving only wildtype 15955 and 15955 pTi15955- cells was set up in the same manner as described above, except using a rectangular pot (15 x 22.5 x 15 cm) so that we could sample the microbial population at a range of distances from the sunflower plant.

Genome sequencing

DNA samples were sequenced by the Microbial Genomic Sequencing Center (MiGS) in Pittsburgh, PA. The DNA concentrations of all samples were measured via Qubit fluorometric quantification. Samples were normalized to the same concentration and enzymatically fragmented using an Illumina tagmentation enzyme. Sample unique indices were attached to the pools of fragmented DNA, and the resulting barcoded pools were combined to multiplex on

an Illumina NextSeq 550 flow cell. Evolved isolates and the 15955 reference strain were sequenced using Illumina Sequencing on the NextSeq 2000 platform. The 15955 reference genome was also sequenced using Long Read Sequencing on the Oxford Nanopore platform.

Bioinformatics analyses

All bioinformatic analyses were performed on the Beocat High-Performance Computing cluster. We evaluated the quality of the long read sequences using Nanoplot (De Coster et al., 2018) and both the long and short read sequences using FastQC (Andrews, 2010). Then, the long read sequence adapters were removed using PoreChop (R. Wick et al., 2017). We then trimmed the short reads with Trimmomatic (Bolger et al., 2014) and used Filtlong to remove long reads with either a mean quality weight less than 12 or with read lengths less than 1000 bp (R. Wick, 2017). The quality score of trimmed short reads and the filtered long reads was evaluated once more as previously described. We then used unicycler to produce a *de novo* hybrid assembly based on the trimmed short reads and the filtered long reads (R. R. Wick et al., 2017). Finally, the assembled genome was annotated with Prokka (Seemann, 2014).

Prior to genomic analyses of evolved isolates, we used FastQC to evaluate the quality scores of the and used Trimmomatic to trim the reads. We performed read mapping by aligning the trimmed Illumina reads to the wildtype reference genome using the Burrows-Wheeler Aligner's Smith Waterman Alignment (BWA-SW) algorithm (H. Li & Durbin, 2009). This algorithm aligns the Illumina sequence reads to the reference genome. We then used the Genome Analysis Toolkit (GATK) pipeline for variant calling. GATK compares the alignment of the samples to the reference genome while simultaneously performing a quality score calibration, indel

realignment, duplicate removal, and SNP and INDEL discovery (McKenna et al., 2010). Finally, mutations, deletions, and genomic rearrangements were visualized using Mauve alignments (Darling et al., 2004).

Statistical analyses

We observed at least five, and typically more, independent biological replicates of all treatments. Finally, statistical significance was evaluated using 2-sided, paired *t*-tests, ANOVA followed by Tukey HSD Post-Hoc test, Kruskal-Wallis (Kruskal & Wallis, 1952), or Mann-Whitney U tests (Mann & Whitney, 1947).

Results

Avirulent agrobacterial mutants can catabolize octopine

To confirm that 15955 Δ*virA* can catabolize octopine, we compared its growth on media containing octopine as the sole source of carbon and nitrogen with that of its parental strain (15955) and a strain that has been cured of pTi15955 (TGP101). The growth of 15955 and the 15955 Δ*virA* mutant was similar in media supplemented with octopine as the sole source of carbon and nitrogen (+ Opines) (Figure 1.1). As expected, the negative control strain cured of its Ti plasmid did not grow in AT+O media. In the baseline media with no octopine (Baseline) all three strains had little to no growth.

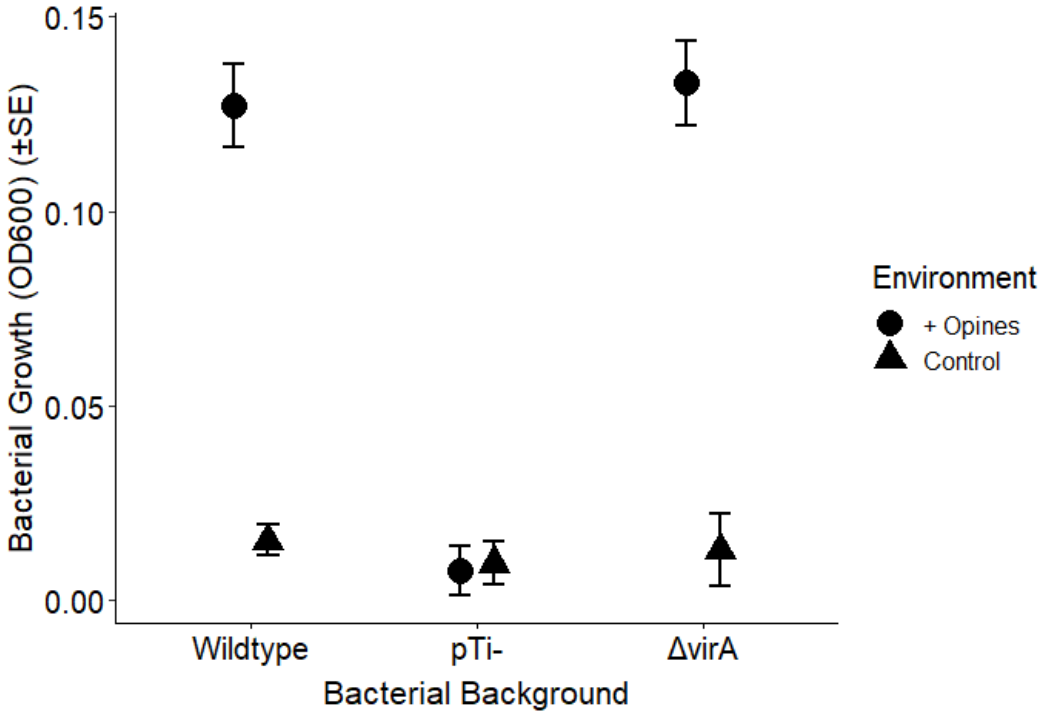

Figure 1.1. The 15955 Δ*virA* mutant and 15955 wildtype parental strain can successfully use octopine as a nutrient source. Wildtype and the Δ*virA* mutant showed little to no growth on the minimal baseline media. The 15955 pTi- strain did not grow in either medium. The baseline media is AT minimal media without any supplementation, while the + Opines media is the baseline media supplemented with 300 µM octopine. OD_{600} was measured 12 hours after inoculation. Values represent mean ± s.e. of ten replicates.

The expression of cooperative pathogenesis genes is costly

To measure the costs associated with expressing the *vir*-genes, we competed the 15955 Δ*virA* mutant (TGP103) against its parental strain (15955) in range of conditions differing in the presence or absence of acetosyringone (AS) and octopine. Deletion of *virA* results in loss of *vir*-gene expression (Gelvin, 2006; Jin, Roitsch, et al., 1990). The phenolic compound acetosyringone (AS) induces the expression of the virulence genes, with little to no expression occurring when it is absent under these conditions (Barton et al., 2018a; Bolton et al., 1986; Platt, Bever, et al., 2012; S. C. Winans, 1992). 15955 and 15955 Δ*virA* have equal fitness when acetosyringone is not present (Figure 1.2). In contrast, when grown in media supplemented with acetosyringone, 15955 Δ*virA* cheater has a large fitness advantage over 15955 (Figure 1.2).

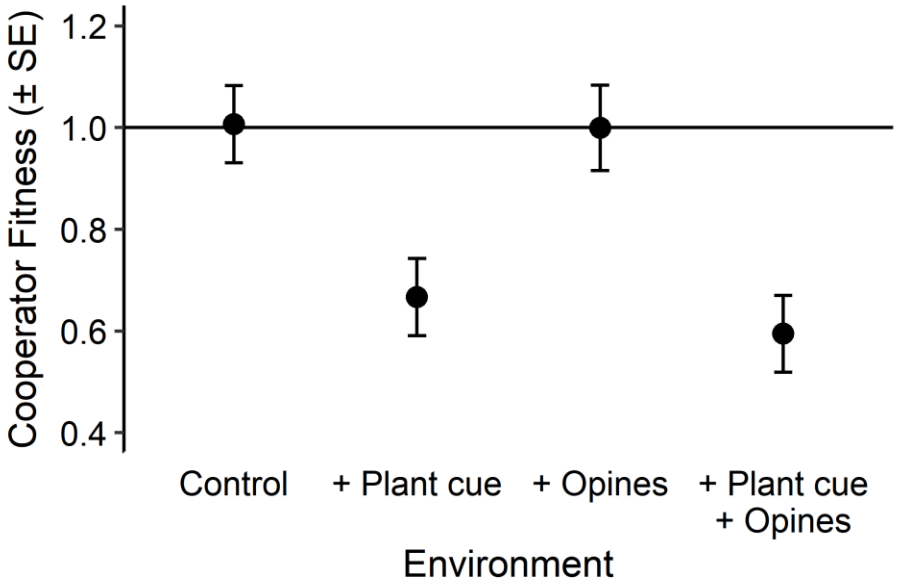

Figure 1.2. 15955 Δ*virA* has a fitness advantage over 15955 in environments that contain the plant cue acetosyringone. The presence or absence of the opines does not provide an advantage to either strain. 'Control' refers to the competition control media. '+ Plant cue' is the control media supplemented with 200 µM acetosyringone. '+ Opines' is the control media supplemented with 50mM octopine. '+ Plant cue + Opines is the control media supplemented with acetosyringone and octopine. Values represent fitness means ± s.e. of 10 replicates.

In-planta agrobacterial competition

15955 Δ*virA* has a competitive advantage over 15955 when grown in culture media supplemented with acetosyringone (Figure 1.2). To evaluate if this advantage translates into a fitness advantage on infected plants, we competed 15955 with 15955 Δ*virA* derivatives on initially healthy sunflowers that subsequently developed galls. Congruent with media-based competition experiments (Platt et al. 2012; Figure 1.2), we observed that 15955 has a competitive advantage over the 15955 pTi- (TGP101) derivative but a competitive disadvantage against 15955 Δ*virA* (TGP103) in soil washed directly from the plant tumor (Figure 1.3).

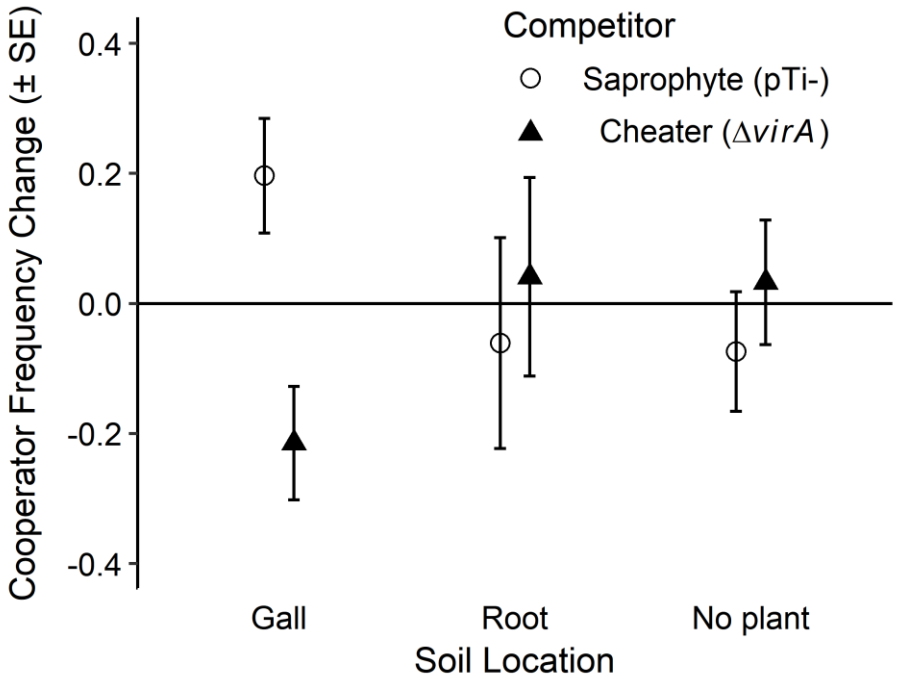

Figure 1.3. 15955 Δ*virA* has a fitness advantage over 15955 in soil directly associated with sunflower galls. In contrast, pTi- saprophytes are at a disadvantage to cooperators in sunflower galls. Each competition was initiated with equal densities of each strain present. 'No plant' refers to agrobacteria competing in bulk soil not associated with the plant, 'Root' refers to the soil washed from the sunflower roots excluding any galls, and 'Gall' refers to diseased sunflower tumors. Values represent fitness means ± s.e. of 10 replicates.

Experimental evolution of virulence gene expression

To examine the potential for *de novo* mutation to generate cheater strains and how opines may influence the spread of such mutants, we evolved 15955 for approximately 60 generations in three environments that differ in the presence or absence of acetosyringone and opines. We observed that 15955 evolved in baseline media retained the ability to induce the *vir*B promoter (Figure 1.4). In contrast, 15955 evolved in the presence of acetosyringone largely lost this ability (Figure 1.4) Overall, presence of the plant cue acetosyringone caused a decrease in *A. tumefaciens'* ability to induce P*virB*. When evolved in media supplemented with the plant cue alone, the proportion of agrobacteria expressing the *virB* promoter was almost zero. In comparison, if the *vir*-inducing media was supplemented with octopine in addition to the plant cue, P*vir*B expression levels tripled (Figure 1.4). The proportion of P*virB*$^{+}$ agrobacteria was significantly different between the two environments that contain plant cues (ANOVA, Tukey's HSD, $p < 0.0001$, 95% C.I. = [0.0323, 0.0531]). These results demonstrate that mutation can readily yield avirulent agrobacteria and that in unstructured populations these mutants can quickly displace cooperators. This pattern was similar in a smaller-scale evolution experiment that we passaged for approximately 120 generations (Figure 5.1).

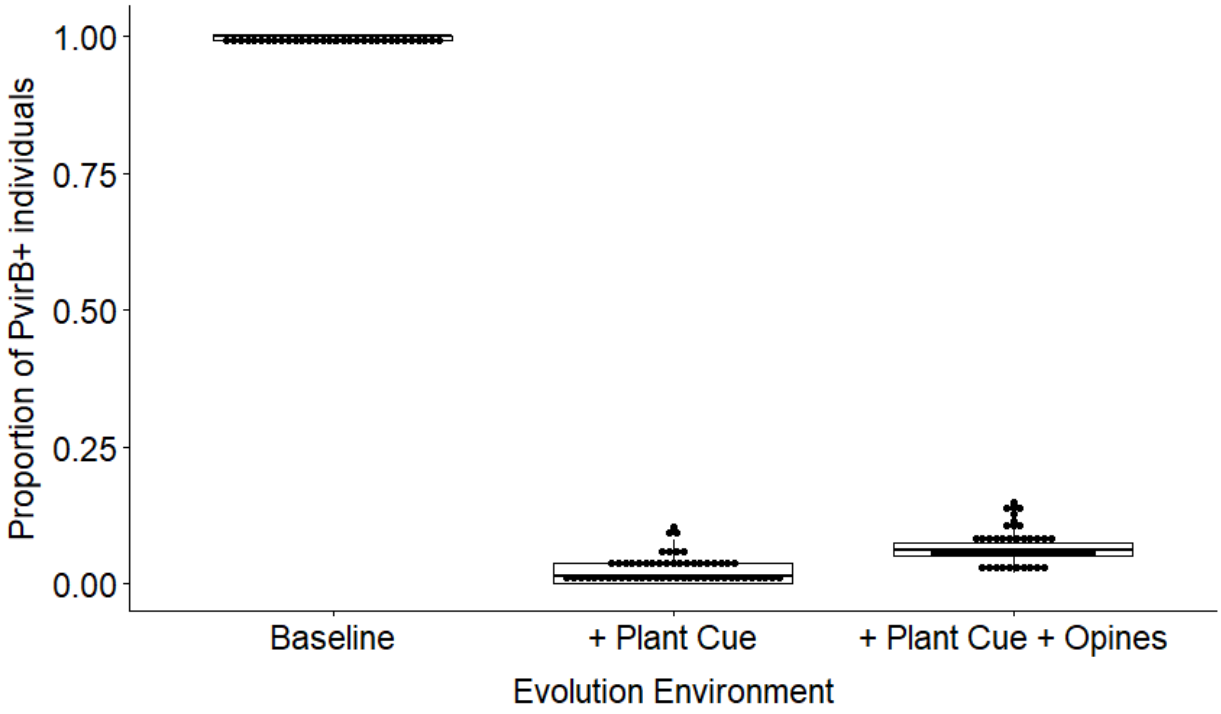

Figure 1.4. Populations evolving in the presence of either the plant cue (200 µM acetosyringone) or the plant cue and opine (50 mM octopine) are largely composed of individuals unable to induce the *virB* promoter after approximately 60 generations. In contrast, populations evolving without these chemicals retain the ancestral ability to induce this promoter. All means are statistically different from one another ($p < 0.05$). Values represent fitness means ± s.e. of 55 replicates. Each point corresponds to an independent evolution population.

Opine catabolism capabilities of evolved strains

We evaluated the opine catabolism ability of all P*virB*$^{-}$ clones recovered from the evolution experiment (Figure 1.4). 16 came from the '+ Plant Cue' evolution populations (orange) and 16 from the '+Plant Cue + Opines' evolution populations (blue) (Figure 1.5). Avirulent mutants only retained the ability to break down opines when they evolved in their presence. All isolates had little to no growth in the no opine baseline media. P*virB*$^{-}$ isolates from the '+ Plant cue + Opines' treatment grew well in media supplemented with opines, whereas isolates evolved in the

presence of the plant cue alone did not grow in media supplemented with opines. For the '+ Opines' media, the growth difference between the isolates from '+ Plant Cue' and '+ Plant Cue + Opines' is significant (Kruskal-Wallis Test, $p < 0.01$). P*virB*$^{+}$ isolates grew in media with opines irrespective of the environment they were evolved in (Figure 5.2).

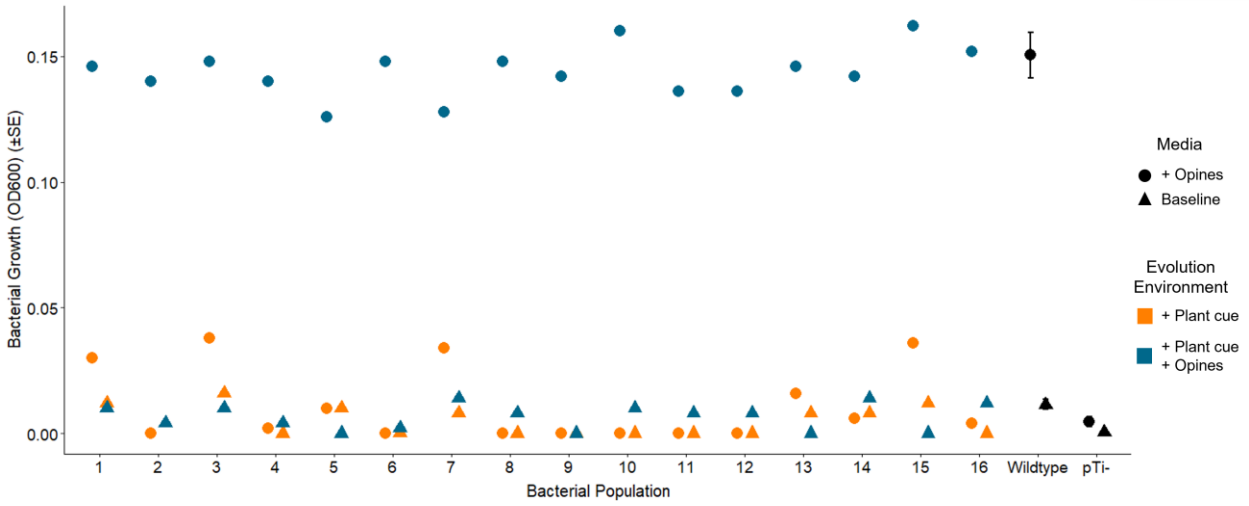

Figure 1.5. Opine catabolic capabilities of 16 independent P*virB*$^{-}$ isolates evolved in the presence of 200 µM acetosyringone (+ Plant Cue) and 16 independent isolates evolved in the presence of acetosyringone and 50 mM octopine (+ Plant Cue + Opines). When evolved in the presence of the plant cue acetosyringone, isolates fail to grow in media with or without opines (Orange). In contrast, when evolved in the presence of both plant cue and opines, all isolates show significant growth when octopine is present (Blue). Wildtype (15955) and 15955pTi^{-} (TGP101) strains were used as positive (+) and negative (-) controls in these experiments. OD_{600} was measured 24 hours after inoculation. Values represent means ± s.e. of at least eight replicates.

Bioinformatics analysis of evolved isolates

To determine the genetic basis of the changes in P*virB* expression (Figure 1.4) and opine catabolism (Figure 1.5), we used variant calling to compare the genomes of a subset of evolved isolates to the ancestral 15955 genome. When evolved in media supplemented with the plant cue acetosyringone alone, all P*virB*$^{-}$ isolates (16/16) showed large-scale deletions (270 Kb) in the AT plasmid and curing of the Ti plasmid (Figure 1.6). P*virB*$^{+}$ isolates, on the other hand, showed two distinct types of genetic changes. Some of the isolates (2/8) incurred simultaneous large-scale deletions on the AT plasmid and Ti plasmid curing, like those observed in the P*virB*$^{-}$ isolates, while others (6/8) only incurred a small 1 kb deletion (Table 5.4). When evolved in media supplemented with plant cues and opines, P*virB*$^{+}$ isolates had no genetic changes. In contrast, some P*virB*$^{-}$ isolates (3/16) incurred the large-scale deletions and curing events previously described, while most isolates (13/16) only incurred a 2.5 kb deletion that included the *virA* locus. Isolates recovered from 15955 populations evolved in environments that do not induce virulence expression do not have mutations of major effect with respect to *vir*-gene expression (Genotype 1). Overall, when evolved in the presence of plant cues that induce virulence expression, we see the spread of mutants that do not express *vir*-genes (Figure 1.4), due to either a loss of *virA* (Genotype 2) or the loss of the Ti plasmid (Genotype 3) (Figure 1.6).

A. Ancestral Genome

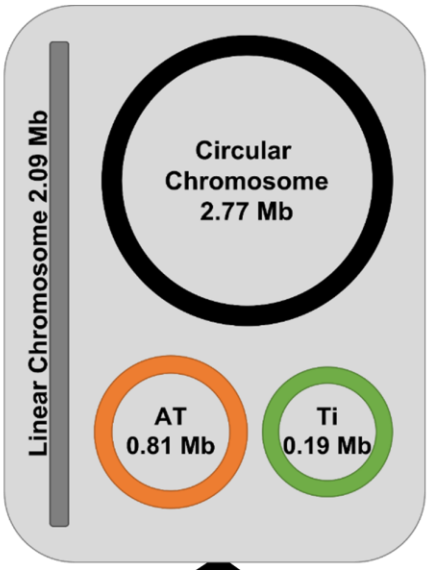

B. Derived Genomes

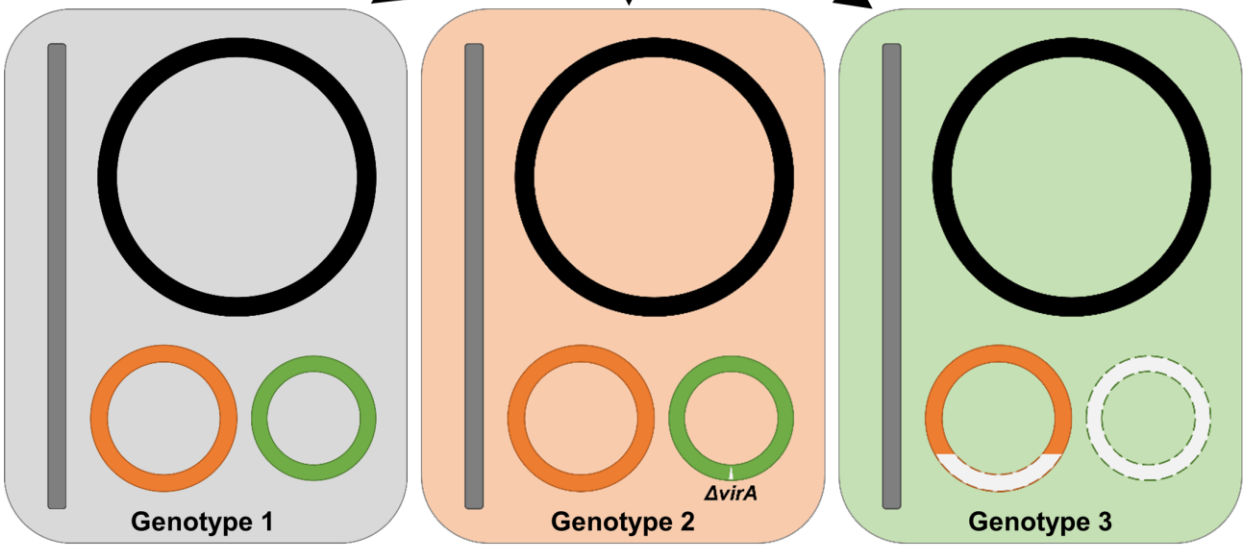

C. Genotype Frequencies by Environment

Baseline	
P*virB*$^{+}$ 0.99	P*virB*$^{-}$ 0.00
G1: 8/8	G1: 0/16
G2: 0/8	G2: 0/16
G3: 0/8	G3: 0/16

+ Plant Cue	
P*virB*$^{+}$ 0.02	P*virB*$^{-}$ 0.97
G1: 6/8	G1: 0/16
G2: 0/8	G2: 0/16
G3: 2/8	G3: 16/16

+ Plant Cue + Opines	
P*virB*$^{+}$ 0.06	P*virB*$^{-}$ 0.93
G1: 8/8	G1: 0/16
G2: 0/8	G2: 13/16
G3: 0/8	G3: 3/16

Figure 1.6. (A) Depiction of the four replicons within the ancestral genome (15955). The parental strain carries a 2.77Mb circular chromosome, a 2.09 Mb linear chromosome, a 0.81 Mb AT plasmid, and a 0.19 Mb Ti plasmid. (B) Evolution of the ancestral strain gave rise to three distinct genotypes: Genotype (grey) 1 had no major mutations likely to impact *vir*-gene expression, Genotype 2 (orange) showed a 2.5 kb deletion from the Ti plasmid resulting in loss of *vir*A, and Genotype 3 (green) presented a 270 Kb deletion in the AT plasmid and curing of the Ti plasmid. (C) Summary of derived genomes for each evolution environment condition. The P*virB* phenotype frequencies and the number of observed genotypes is given for each environment. Evolution in the baseline media resulted in P$virB^{+}$ isolates with no major mutations (grey). In contrast, evolution in the presence of acetosyringone resulted in populations principally composed of P$virB^{-}$ isolates that had incurred curing of the Ti and large-scale deletions in the AT plasmid (green). Evolution in the presence of both acetosyringone and octopine resulted in populations mostly composed of P$virB^{-}$ isolates that either lacked *virA* or had cured the Ti along with major deletions in the AT plasmid (orange/green). These populations also have some P$virB^{+}$ cells that had not incurred any mutations likely to impact *vir*-gene expression (grey). Evolution environment: Baseline is the control media, + Plant Cue is baseline media supplemented with 200 µM acetosyringone, and +Plant Cue + Opines is baseline media supplemented with 200 µM acetosyringone and 50mM octopine.

Discussion

Cooperative behaviors are costly for the individual and benefit other individuals in the population (Damore & Gore, 2012; Y.-H. Li & Tian, 2012; Rainey & Rainey, 2003; West, Griffin, et al., 2007). Cheaters have an inherent advantage in cooperative systems because they avoid the costs of cooperation but reap its benefits. Consequently, cheating undermines the evolutionary stability of cooperative systems. In this study, we examined the ecological and evolutionary dynamics of cheating by agrobacteria that avoid the costs of establishing plant infections but retain the ability to benefit from host infection. We used a synthetic biology approach to demonstrate that avirulent Δ*vir*A mutants have a fitness advantage over pathogenic cooperators when they compete on infected plant hosts. Similar experiments demonstrated that the pathogen has a competitive advantage over pTi^- derivatives in soil directly associated with infected host tissues. We also used experimental evolution to determine that avirulent agrobacteria readily arise via mutation and competitively displace pathogenic cooperators in environments where a plant cue that stimulates expression of the genes needed to initiate pathogenesis is present. However, these mutants retain their ability to benefit from host infection only when they evolved in the presence of opines, the public good catabolites that plants produce following infection. These avirulent agrobacteria arise from either the loss of *vir*A or the complete loss of the Ti plasmid.

The selective pressures present in the tumor environment have direct effects on the pathogen's fitness and growth rates (Morton et al., 2014; Platt, Fuqua, et al., 2012). The cooperative pathogenesis of *A. tumefaciens* requires the maintenance and expression of genes carried on the Ti plasmid. The Ti plasmid carries most of the genes involved in infection and genes that

confer the ability to catabolize the public goods the plant produces following infection (Christie, 1997; Gelvin, 2000, 2003; Nester, 2015). The expression of *vir*-genes imposes a significant fitness cost on the agrobacterial host cell (Figure 1.2) (Barton et al., 2018a; Gordon & Christie, 2014; Morton et al., 2014; Platt, Bever, et al., 2012; Platt et al., 2014). We observed that avirulent strains can readily arise and outcompete virulent cooperators when the environment stimulates the pathogen to express its *vir*-genes (Figure 1.4). Further illustrating the importance of these costs, avirulent, opine catabolic cheaters outcompete the cooperative pathogen in the gall environment. In contrast, the cooperative pathogen outcompetes a pTi- derivative in the gall environment, reflecting the importance of opine catabolism to the ecology of the cooperative pathogen (Figure 1.3). The fitness advantage of cheaters over cooperators within the diseased environment suggests that the persistence of pathogenic agrobacteria in natural systems depends on there being sufficient spatial structure to allow cooperation to often benefit related agrobacteria (Damore & Gore, 2012; Hamilton, 1964; Nowak, 2006). These findings underscore the importance of the context-dependent costs and benefits associated with the Ti plasmid that vary with environmental conditions and competitors present (Platt et al. 2012).

Several studies have reported that freeloading mutants can arise as a result of mutations to genes essential to the expression of cooperation and virulence (Celiker & Gore, 2013; Harrison & Buckling, 2005; Rainey & Rainey, 2003). In *A. tumefaciens*, emergence of avirulent mutants can be caused by mutations in the VirA/VirG two component system (Fortin et al., 1992; S. C. Winans et al., 1988). Congruent with this, we observe that evolution in presence of plant cues results in a decrease in the proportion of virulent cooperative, pathogenic individuals (Figure

1.4 & 1.6). This loss in virulence reflects the benefit of not paying the costs associated with the expression of the virulence genes when their expression does not result in availability of the public good. Cheaters may also arise from deletion mutations impacting the virulence region or the curing of a virulence plasmid (Breen et al., 2016; Schuch & Maurelli, 1997). We observe such genomic outcomes in our evolution experiment, especially following evolution in environments lacking opines. Further, genomic studies of Ti plasmid evolution and diversification have reported natural isolates that have incurred mutations resulting in loss of pathogenesis functions (Weisberg et al., 2020, 2022). Nevertheless, recent genomic analyses suggest that interactions among plasmids have produced Ti plasmids with new combinations of *vir* genes that could facilitate infection of new plant hosts (Weisberg et al., 2022).

The gall environment has both opines and plant cues present. Populations of wildtype *A. tumefaciens* evolving with both these molecules present come to be composed primarily of Δ*vir*A or pTi- mutants (Figure 1.6). The complete loss of the Ti plasmid results not only in the loss of the pathogenesis genes needed for plant infection, but in the loss of the genes necessary for the catabolism of opines. We observed that the opine catabolic abilities of evolved P*vir*B- isolates differ depending on the environment they evolved in. Most P*vir*B- isolates that arose in the presence of opines and the plant cue lost *vir*A but retained the rest of the Ti plasmid including opine catabolism genes. In contrast, P*vir*B- isolates that emerged in the presence of plant cues alone all lost the Ti and AT plasmids, which results in loss of both the opine catabolism genes and the *vir*-genes. In this way, the Ti plasmid acts as a multigene greenbeard where the genes required for the cooperative trait (the *vir*-genes) are genetically linked to those required to access the benefits of cooperation (Platt, Bever, et al., 2012; Platt, Fuqua, et

al., 2012; Platt & Bever, 2009). While theory predicts that multigene greenbeards should be evolutionarily unstable due to the opportunity for mutation to result in the loss of costly cooperative traits while retaining the genes required to benefit from cooperation. Our observations suggest that, in this system, opines constrain greenbeard evolution, undermining how readily non-cooperative mutants can emerge.

Large-scale deletions of the AT plasmid have been previously observed in *A. tumefaciens* strain 15955 (Barton et al. 2019). Barton et al. (2019) identified a consistent 270 kb deletion in backgrounds cured of the Ti plasmid with similar deletions occurring in another related strain of *A. tumefaciens*. We observed that when evolved in gall-like environment, the parental genotype can lose expression of virulence. In some cases, and especially when opines were not present, we observed that this occurred through the loss of the Ti plasmid. Congruent with the observations of Barton et al. (2019), when this happened there was simultaneous loss of the AT plasmid. Though cross-replicon interactions between these two plasmids have been previously observed, our results highlight not only how these interactions drive the evolution of these replicons, but also the impacts on the population ecology of cheaters and cooperators. This cross-replicon interaction suggests there is a genetic link between the two plasmids, and highlights interdependency affecting plasmid stability. Although there is no definitive answer as to why these interactions occur, Barton et al. (2019) suggest that it could result from homologous recombination or transposition events.

The ecological and genetic dynamics of cooperative plasmids are dependent on the environment in which the host cells reside. As such, the fitness of both cheaters and cooperators depends on the costs associated with the expression of cooperative traits and the

benefits cooperation yields. The Ti plasmid carries the genes mediating both these fitness consequences, but we observed that mutation can readily uncouple these traits to generate cheater strains. Cheaters arise because of the loss of the genes that encode cooperative pathogenesis, or the loss of the cooperative plasmid. However, when evolved in the absence of these public goods, evolved mutants are unable to catabolize opines, and are thus phenotypic saprophytes. Mutants that arise in the presence of opines retain the ability to catabolize them, suggesting that the selective environment of infected hosts constrains the emergence of cheaters.

Funding

This work was supported by the National Science Foundation (NSF) Graduate Research Fellowship Program (GGVP004842 to PN-O), Kansas IDeA Networks of Biomedical Research Excellence (KINBRE) Bioinformatics Scholar Award (to RSJ, P20GM103418), and the Kansas NSF EPSCoR First Award Program (OIA-1656006 to TP). We also thank KINBRE Bioinformatics Core (P20GM103418) for help with using scripts used in the bioinformatic analyses. The computing for this project was performed on the Beocat Research Cluster at Kansas State University, which is funded in part by NSF grants CNS-1006860, EPS-1006860, EPS0919443, ACI-1440548, CHE-1726332, and NIH P20GM113109.

Chapter 2 - Plasmid conjugation antagonizes the invasion of greenbeard cheater mutants

Introduction

Many cooperative microbial systems involve the costly production of public goods which can benefit not only the individuals that pay this cost but also other nearby individuals. Cooperative systems are vulnerable to evolutionary invasion by cheaters, individuals that benefit from cooperative behaviors that they do not themselves perform. These cheaters have an intrinsic within group fitness advantage over cooperators in that they avoid the costs of cooperation but still realize its benefits. Kin selection theory centers on the idea that natural selection favors cooperation when cooperative individuals are genetically related to the beneficiaries of the cooperative behavior (Damore & Gore, 2012; Hamilton, 1964; Nowak, 2006). That is, cooperation allows individuals to indirectly promote the transmission of their genes when they help close relatives (Damore & Gore, 2012). Altruistic behaviors may also be maintained because they provide direct benefits that outweigh the associated costs (West, Diggle, et al., 2007). Enforcement mechanisms act to reduce cheating within cooperative systems, potentially by ensuring that individuals cooperate (Ågren et al., 2019). Toxin-antidote systems, specialized spatial structure of communities, metabolic trade-offs, and horizontal gene transfer are all potential enforcement mechanisms methods employed by cooperators (Abisado et al., 2018; Friesen, 2020; Mc Ginty et al., 2011; Mehdiabadi et al., 2006; Strassmann & Queller, 2011; Travisano & Velicer, 2004; West, Griffin, et al., 2007).

Horizontal gene transfer plays a key role in the acquisition of new traits, including antibiotic resistance and pathogenesis functions. Additionally, horizontal gene transfer is an important biological tool that has been applied to bioremediation andplant genetic engineering (French et al., 2020; Gelvin, 2003; Shoeb et al., 2012). Enforcement of cooperation by cooperators may prevent freeloaders from dominating populations, potentially resulting in insufficient public good production and population collapse (Mc Ginty et al., 2011; Wang et al., 2015). Bacterial cooperative behaviors are often encoded by genes carried on plasmids. Consequently, horizontal transfer of these plasmids into cheaters can re-introduce cooperative genes back into defectors and thus reestablish cooperative phenotypes (Lee et al., 2021; Mc Ginty et al., 2011).

The cooperative pathogenesis of *Agrobacterium tumefaciens* is encoded by the tumor inducing (Ti) plasmid. *A. tumefaciens* cooperators genetically transform plants by inserting a region of the Ti plasmid (the transferred DNA or T-DNA) into the plant's genome. This transformation leads to changes in the regulation of plant hormones and the secretion of small metabolites (opines) that serve as a nutrient source for the agrobacteria. Freeloaders, agrobacteria that consume but do not infect plants, do not pay the costs associated with cooperation (Barton et al., 2018). We hypothesize that conjugation of the Ti plasmid into cheaters reduces the chance that cheaters outcompete cooperators on infected hosts. The horizontal transfer of the Ti is regulated by a Ti plasmid encoded quorum sensing system, such that conjugation occurs when agrobacterial populations are dense and opines are present (Dessaux & Faure, 2018; Farrand et al., 2002; Faure & Lang, 2014). TraI, a LuxI-type enzyme, produces N-3-oxo-octanoyl homoserine lactone (3OC8HSL), a QS signal (Moré et al., 1996;

Zhang et al., 1993). When 3OC8HSL is sufficiently concentrated (e.g. when cells are at high density) it binds to the transcription factor TraR which initiates expression of the genes required for conjugation of the Ti plasmid and increased plasmid copy number (C. Fuqua & Winans, 1996; W. C. Fuqua et al., 1994). For many Ti plasmids, this can only occur when opines are present because *traR* expression depends on opine-dependent transcriptional control (Faure & Lang, 2014).

This chapter focuses on the impact of quorum sensing regulation of Ti plasmid conjugation on interactions between cooperative and cheater agrobacteria. Specifically, we will test the hypothesis that quorum sensing regulated conjugation of the Ti plasmid is an enforcement mechanism that antagonizes the spread of cheaters within populations. We demonstrate that conjugation of the Ti plasmid from cooperative agrobacteria to a nearly isogenic cheater strain converts the avirulent cheater into a cooperator. This antagonism is dependent on the expression of TraR, a quorum sensing transcriptional regulator necessary for Ti plasmid conjugation. We observe that when cheaters are present in the population when public goods are made available, conjugation is not an effective enforcement mechanism. In contrast, when cheaters arise from *de novo* mutations, conjugation significantly antagonizes cheater emergence. This enforcement not only stabilizes cooperation in the population, but also re-introduces the pathogenesis genes back into mutants, transforming them into pathogenic cooperators—potentially yielding genotypes with novel combinations of plasmid and chromosomal genes.

Materials & Methods

Strains, plasmids, reagents, media, and growth conditions

Chemicals, antibiotics, and culture media were purchased from Fisher Scientific (Pittsburgh, PA), Sigma Aldrich (St. Louis, MO), VWR (Wayne, PA), Midwest Scientific (Valley Park, MO), and Goldbio (St. Louis, MO), unless otherwise noted. All oligonucleotide primers were purchased from Integrated DNA Technologies (Coralville, IA). The molecular cloning and genetic manipulation of all bacterial strains and plasmids was performed as described by Morton & Fuqua (2012), unless noted otherwise. Plasmids were introduced to *Escherichia coli* strains using chemical transformation and *Agrobacterium tumefaciens* strains via conjugation. Genetic manipulations of *A. tumefaciens* were performed following the allelic replacement protocol (Morton & Fuqua, 2012a). All strains, plasmids and primers used in this study have been sequence confirmed and are described in Tables 5.5 – 5.7.

A. tumefaciens strains were grown on AT minimal media with 0.5% (w/v) glucose and 15 mM ammonium sulfate, unless otherwise noted. Conjugation media contains AT minimal media salts, 20 mM MES pH 5.6 buffer, 500 µM phosphate, 0.5% (w/v) glucose, 0.6 mM $(NH_4)_2SO_4$, 200 µM AS, 3.25 mM octopine, and 2 ml/L Hutner Base (Morton & Fuqua, 2012b). *E. coli* strains were grown in standard LB media. Antibiotic concentrations for *E. coli* were as follows: ampicillin (100 µg/ml), gentamicin (50 µg/ml), kanamycin (50 µg/ml), spectinomycin (100 µg/ml), and streptomycin (25 µg/ml). Antibiotic concentrations for *A. tumefaciens* were as follows*:* ampicillin (150 µg/ml), gentamicin (100 µg/ml), kanamycin (200 µg/ml), spectinomycin (100 µg/ml), and streptomycin (2500 µg/ml). When specified, agrobacterial media was supplemented with octopine (3.25 mM) and/or acetosyringone (200 µM).

Genetic manipulations and conjugation assay

The 15955 Δ*traR* mutants and expression constructs used in this study are described in Barton et al. (Barton et al., 2021). In this study, we measured the conjugation frequencies of the *traR* mutants and compared them to those of complemented *traR* mutants and the wildtype parental strain to see the effects of TraR on Ti plasmid conjugation. Cultures were grown overnight to mid-log phase (OD_{600} = 0.5 - 0.8) and then diluted to an OD_{600} of approximately 0.05. We mixed equal volumes of wildtype *A. tumefaciens*, *traR* mutants, and complemented *traR* mutants, with a pTi- background (ERM116), and spotted the mixture onto a filter disc. Mating mixtures were incubated overnight in the presence or absence of 400 µM IPTG (Morton & Fuqua, 2012a). After incubation, the mating disk was placed in a 1.5 mL microcentrifuge tube and was washed by vortexing with 1 mL of sterile MqH_2O. The cell suspension was then serially diluted and plated onto selective media allowing for quantification of donor, recipient, and transconjugants densities.

Tumorigenesis assay

We followed the tumorigenesis assay described by Anand & Heberlein (1977), with some minor modification. Liquid cultures of PAG10 and PAG12 were grown overnight to mid-log phase (OD_{600} = 0.5 - 0.8) and diluted to OD_{600} = 0.05. We surface sterilized potatoes by soaking them in a 1.05% sodium hypochlorite solution for 20 minutes. Then, we removed 3 cm from both ends of the potato with a surface sterilized scalpel. We used a surface sterilized cork borer (11 mm diameter) to obtain an internal segment of potato tissue. The ends of each potato cylinder were

discarded, and the remaining part of the potato cylinder was sliced with a sterilized scalpel into 2 mm thick disks.

We placed two potato disks into 60 X 15 mm Petri plates containing 1.5 % agar water. Each potato disk was inoculated with 35 µL of a bacterial culture dilution. All plates were placed in a sterilized container along with a cup of saturated K_2SO_4 solution to ensure the plates did not dry out while incubating. The plates were incubated at room temperature for 21 days. After incubation, if tumors were observed, one potato disk from each Petri plate was placed into a 1.5 mL tube with 1 mL of sterile water, then vortexed vigorously for 1 minute. We made a frozen archive of the strains present by mixing 500 µL of the resulting bacterial suspension with 500 µL of 50 % glycerol. Finally, we used 100 µL of the remaining bacterial cell suspension to inoculate a plate mating with *E. coli* S17-1 λpir pSW209, as described by Morton & Fuqua (2012). After overnight incubation at 28 °C, the cells were collected, serially diluted, and plated on P*virB-lacZ* medium to recover the agrobacteria present (S17-1 λ*pir* cannot grow on this minimal media). P*virB-lacZ* media contains AT minimal media salts, 0.5% (w/v) glucose, 20 mM MES pH 5.6 buffer, 500 µM phosphate, 200 µM acetosyringone, 200 µg/ml kanamycin, and 40 mg/ml X-gal (5-bromo-4-chloro-3-indolyl-galactopyranoside). Agrobacterial cells capable of expressing the P*virB*::*lacZ* construct carried by pSW209 form blue colonies, while those that cannot form white colonies on this media.. Plates were incubated at 28 °C for 3-4 days, after which the number of blue and white colonies were counted.

Competition experiment

Bacterial cultures were grown overnight at 28 °C to mid-log phase (OD_{600} = 0.5 - 0.8). After overnight incubation, cells were collected via centrifugation and resuspended to an OD_{600} of 0.02 in conjugation media, which has 100 µM acetosyringone and 3.25 mM octopine. Cells were incubated at 28 °C for three hours and then diluted once more to OD_{600} = 0.02 for a final volume of 1.8 mL. 15955 Δ*virA* strains (e.g. TGP103) were further diluted such that these cells will make up 25%, 2.5%, and 0.25% of the final population mixture. In all cases, 500 µL of a cell suspension of a genotype capable of pathogenesis (IB123, a kanamycin resistant 15955 derivative carrying a gentamycin resistance gene on its Ti plasmid) was combined with 500 µL of a cell suspension of a genotype that cannot express *vir*-genes (ERM117, a streptomycin and spectinomycin resistant 15955 Δ*virA* derivative). The mixture was vortexed and serially diluted prior to plating onto selective media and incubated at 28 °C for 3-4 days. 700 µL of the remaining bacterial mixtures were centrifuged (11,000 rpm for 2 minutes) and resuspended in 100 µL MqH_2O, which we then pipetted onto a PES filter disk on a conjugation media plate and incubated for 3-4 days at 28 °C. After incubation, the PES filter disk was placed in a 1.5 mL tube with 1 mL MqH_2O and vortexed vigorously. Serial dilutions were then made from these suspended cells, plated on ATGN plates with antibiotics that allowed for selection of donors (kanamycin and gentamycin), recipients (streptomycin and spectinomycin), and transconjugants (streptomycin, spectinomycin, kanamycin, and gentamycin). Plates were incubated at 28 °C for 3-4 days. After incubation, all colonies were counted.

Evolution experiment

Mid-log phase (OD_{600} = 0.5 – 0.8) cultures of WT (PAG10) and ΔpTi*traR* (PAG12) were diluted to an OD_{600} = 0.04. Potato disks were prepared as described in the tumorigenesis assay. We placed three potato disks on each Petri plate (60 x 15 mm) containing 1.5% water agar. We inoculated each disk with 35 µL of the one strain's cell suspension. The plates were placed in a sterilized container with a cup of saturated K_2SO_4 solution to prevent dehydration of the agar and incubated at room temperature for 7 days. After 7 days, we collected the bacteria from each potato disk and inoculated a fresh potato disks. To do this, each potato disks was placed into a sterile 1.5 mL tube with 1 mL of sterile water, then vortexed vigorously for 1 minute. We then diluted this cell suspension 100-fold with fresh media and inoculated a set of new potato disks as described above. We repeated this for a total of 4 passages. We preserved 25 % glycerol stocks of all evolved populations at -80 °C. On the 7^{th} day after the 4^{th} passage, we mated 100 µL of the cell suspension washed from the potato disk with 100 µL of mid-log phase *E. coli* S17-1 λpir pSW209 cells to quantify the density of transconjugants capable of activating the *virB* promoter, as described above.

Genome sequencing

All isolates were sequenced by the Microbial Genomic Sequencing Center (MiGS) in Pittsburgh, PA. The DNA concentration of all samples was measured via Qubit fluorometric quantification and normalized to the same concentration. Samples were enzymatically fragmented using an

Illumina tagmentation enzyme. Sample unique indices were attached to the segmented DNA, and barcoded pools were combined to multiplex on an Illumina NextSeq 550 flow cell.

Bioinformatics analyses

All bioinformatic analyses were run on Beocat, the High-Performance Computing cluster at Kansas State University. We read mapped the sequences by aligning the sample genomes to the wildtype reference genome using the Burrows-Wheeler Aligner's Smith Waterman Alignment (BWA-SW) algorithm (H. Li & Durbin, 2009). This algorithm aligns sequences to a reference genome. Then, we performed a variant calling using the Genome Analysis Toolkit (GATK) pipeline. GATK compares the alignment of the samples to the reference genome while simultaneously performing a quality score calibration, indel realignment, duplicate removal, and SNP and INDEL discovery (McKenna et al., 2010). Further, the GATK pipeline identifies mutations with high confidence. Following variant calling and read map alignment, the mutated regions that potentially result in loss of virulence were identified.

Statistical analyses

We observed at least five, and typically more, independent biological replicates of all treatments. Statistical significance was evaluated using 2-sided, paired *t*-tests, Kruskal-Wallis (Kruskal & Wallis, 1952), or Mann-Whitney U tests (Mann & Whitney, 1947).

Results

TraR is necessary for conjugation

To confirm that *traR* is necessary for the conjugation of the pTi15955, we created in frame deletion mutants of both the pTi*traR* locus and the pAT*traR* locus and compared their conjugation rates with each *traR* mutant carrying the appropriate plasmid-borne P*lac*::*traR* expression construct and their wildtype parental strain. The conjugation rates of the ΔpATtraR and ΔpTitraR mutants significantly decreased when compared to wildtype (Figure 2.1). The conjugation rates of strains carrying IPTG-inducible *traR* expression constructed showed a similar reduction when incubated in media with no IPTG. In contrast, IPTG induction significantly increased the conjugation rate, though not to wildtype levels.

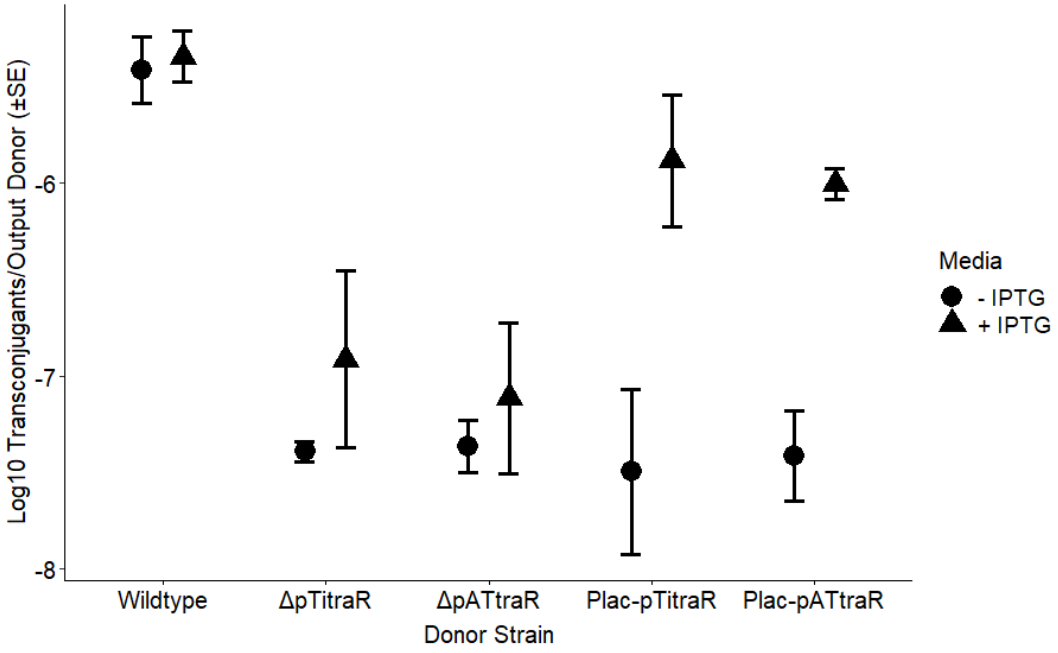

Figure 2.1. Wildtype (15955) displayed significantly higher conjugation rates than either of the Δ*traR* mutants. Both mutant strains (15955 ΔpTi*traR* and 15955 ΔpAT*traR*) displayed higher conjugation rates when induced to express a corresponding plasmid-borne P*lac*::*traR* construct. All matings were initiated with equal densities of donor and recipient strains. -IPTG is conjugation media (circles) and +IPTG is conjugation media with 400 µM IPTG (triangles). Values represent means ± s.e. of 4 independent replicates.

TraR+ cooperators have a fitness advantage over traR- mutants

To measure the effects of Ti plasmid conjugation on cheater population dynamics, we competed the 15955 Δ*traR* mutant (PAG12) and its parental strain (15955) against a nearly isogenic cheater strain (15955 Δ*virA*; TGP103) present at a range of initial densities. Deletion of *traR* results in a significantly lower conjugation rate (Figure 2.1). Both strains have fare equally well in competition with cheaters when cheaters are rare (0.25% and 2.5% of the initial population; Figure 2.2). In contrast, when cheaters are common (25%) 15955 Δ*traR* mutants compete less well with the cheater strain (Figure 2.2).

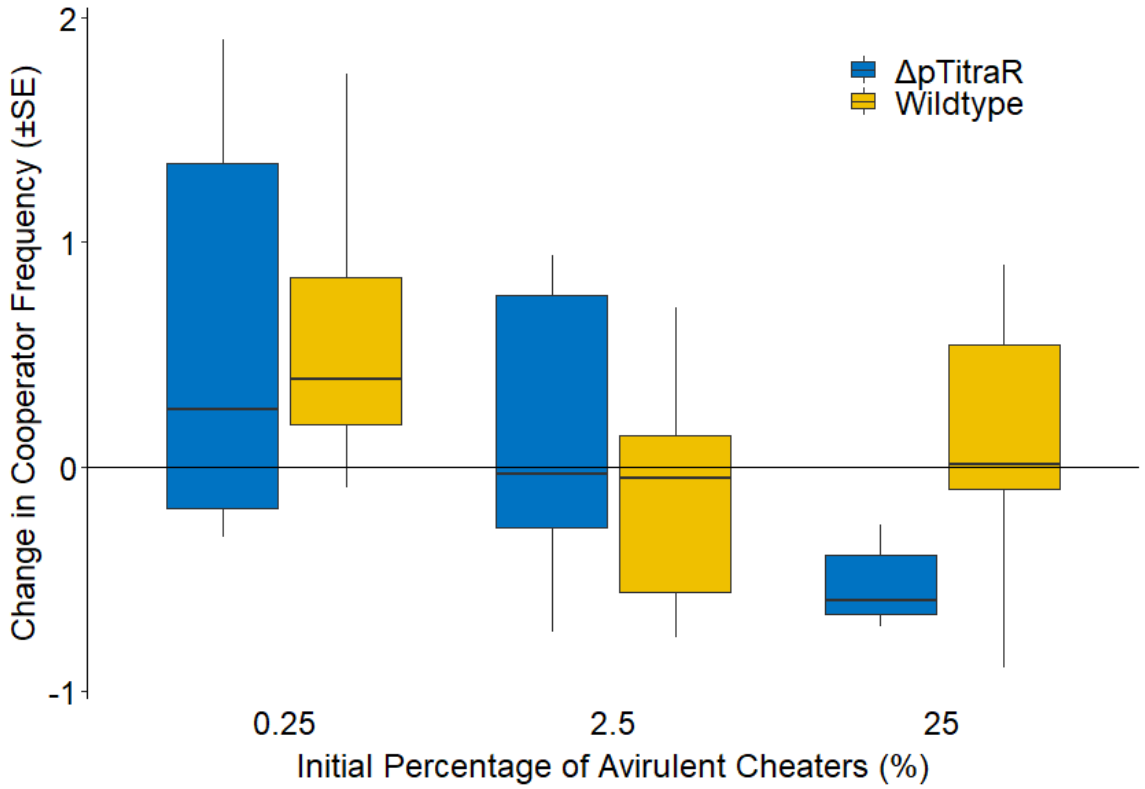

Figure 2.2. Cooperators lacking *traR* (ΔpTi*traR*) decline in frequency when cheaters are common (25%). Neither strain has a competitive advantage in environments where cheaters are initially rare (0.25% and 2.5%). Values represent mean change in cooperator frequency ± s.e. of 8 replicates. The widltype and ΔpTi*traR* means in the "25" treatment are significantly different from one another ($p < 0.05$), whereas the means of the other two treatments are not significantly different from one another.

Conjugation can delay emergence of *de novo* cheaters

We examined if conjugation could be employed by cooperators to antagonize cheaters already present in a population by converting them into cooperators (Figure 2.2). Here, we evaluate if conjugation antagonizes cheaters that emerge *de novo* due to mutations, by evolving a Δ*traR* mutant (PAG12) and its parental strain (PAG10) capable of conjugation in potato tissue for approximately 50 generations (Figure 2.3). Deletion of *traR* leads to a decrease in the rate of conjugation (Figure 2.1); thus, ΔpTi*traR* mutants are deficient in conjugation. We observed that populations whose initial genotype was the wildtype background retained the ability to activate the *virB* promoter at a higher frequency than populations initially composed of ΔpTi*traR* cells. These results suggest that mutation can readily yield P*virB*- isolates and that in gall-like environments avirulent mutants can outcompete cooperators.

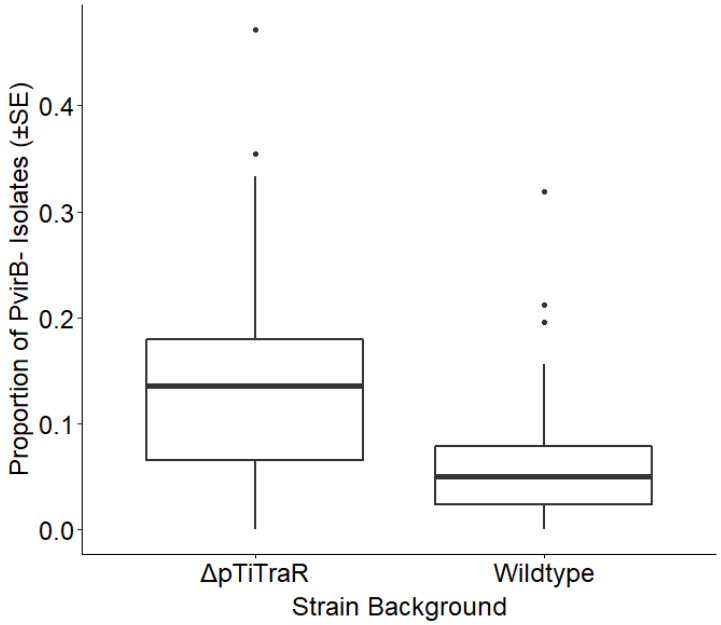

Figure 2.3. Cooperators with an intact *traR* delay cheater invasion via conjugation of the cooperative genes carried on the Ti plasmid. Wildtype is the parental genotype to the ΔpTi*traR* isogenic mutant. Strains were evolved in potato tissue for approximately 50 generations. Values represent fitness means ± s.e. of 35 independent replicates. Strain means are significantly different ($p < 0.01$).

Transconjugants are pathogenic

We evaluated expression of *A. tumefaciens* cooperative pathogenesis, by assessing the ability of four distinct transconjugants to induce tumors in potato tissue (Figure 2.4). We compared transconjugants' pathogenic abilities to those of the parental wildtype strain (15955), and a nearly isogenic 15955 Δ*virA* (TGP103) mutant, the genetic background of all transconjugants before conjugation. Deletion of *virA* results in loss of *vir*-gene expression (Gelvin, 2006; Jin et al., 1990) and consequently, Δ*virA* mutants do not induce formation of tumors. In contrast, wildtype agrobacteria and all four transconjugants induced tumor formation at the same frequency (Figure 2.4). These results demonstrate that conjugation of the Ti plasmid into cheaters backgrounds can phenotypically convert avirulent cheaters into cooperative pathogens.

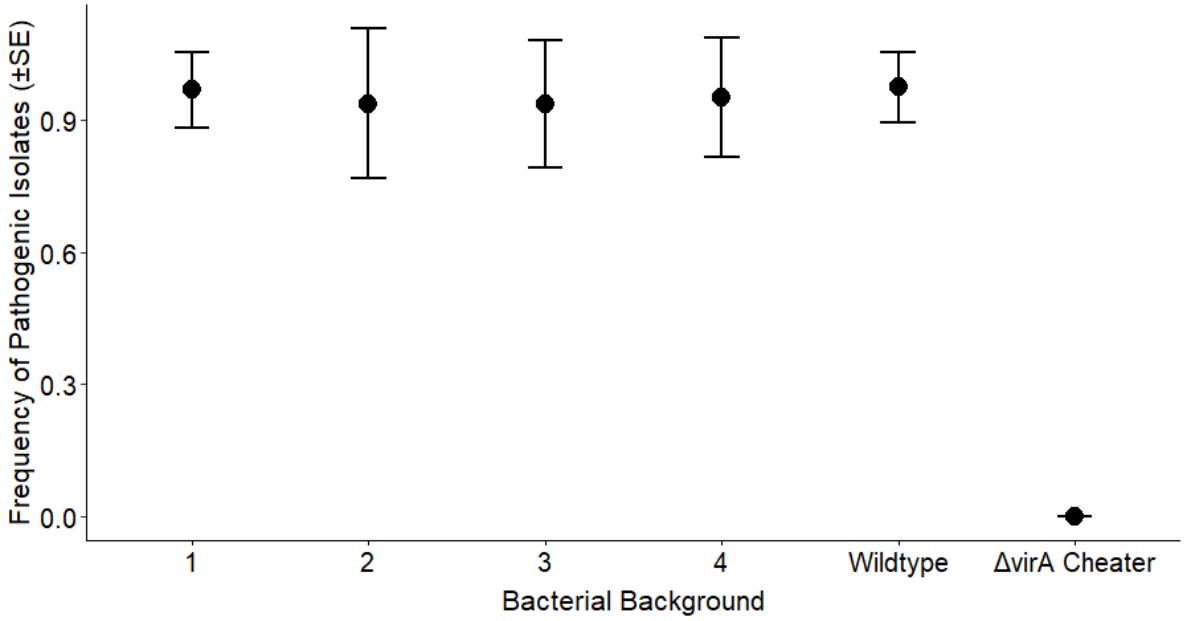

Figure 2.4. 15955 Δ*virA* pTi transconjugants are pathogenic. 1-4 refers to four independent transconjugants. Wildtype is the parental genotype to Δ*virA* mutants. Values represent the mean frequency of isolates capable of inducing tumor formation ± s.e. of 8 independent replicates. The mean of the Δ*virA* strain is significantly lower than each of the other means ($p < 0.001$). All other means are not significantly different ($p > 0.05$).

Genomic consequences of pTi conjugation

To understand the genomic consequences of the horizontal transfer of the Ti plasmid into a similar genetic background (15955 Δ*virA*) and a more distantly related background (C58) we introduced pTi15955 into each of these strains, experimentally evolved the resulting transconjugants under a range of environmental contexts, and sequenced the genome of the evolved transconjugants. Ti plasmid carrying strains transform plant hosts and induce plants to produce opines, small compounds the bacteria uses as a nutrient source. C58 is a nopaline-type agrobacterial strain, whereas 15955 is an octopine-type strain with a key difference between these strains being the suite of opines they induce plants to make (Gordon & Christie, 2014). Both C58 and 15955 can cause crown gall disease in plant hosts, however they carry distinct Ti plasmids (Gordon & Christie, 2014) and belong to different *A. tumefaciens* genomospecies (Lassalle et al., 2011). In addition, pTiC58 and pTi15955 are incompatible with each other such that they are not able to be stably inherited together (Gallie et al., 1985).

We conjugated pTi15955 into these the 15955 Δ*virA* mutant background (ERM117) and the C58 background. We then experimentally evolved the transconjugants for approximately 150 generations in four environments that differ in the presence or absence of acetosyringone and opines, and sequenced isolates recovered from the evolved populations. We observed that the horizontal transfer of the Ti plasmid into the Δ*virA* background (ERM117) did not result in significant genomic changes, irrespective of the evolution environment (data not shown). However, the consequences of the transfer of the Ti plasmid into a C58 background (ERM77), depended on the environmental conditions in which the transconjugants subsequently evolved (Table 5.8). When evolved in the evolution control media or in an evolution environment

supplemented with opines and the plant cue acetosyringone, most transconjugants lost the pTi15955 plasmid. Those that retained the plasmid incurred significant mutational changes throughout pTiC58 and pATC58 plasmids. When evolved in presence of plant cues, all transconjugants lost the pTi15955 plasmid with few mutations occurring on pTiC58 or pATC58. In contrast, if the evolution media was supplemented with opines alone, most transconjugants retained the pTi15955. However, these transconjugants incurred significant mutational changes in the pTiC58 and pATC58, with some curing pTiC58 and deleting a large portion of pATC58 (Table 5.8).

Discussion

The expression of *Agrobacterial tumefaciens* cooperative genes is costly (Figure 1.2). As a result, in environments where plant cues are present, avirulent cheaters readily arise via mutation and displace pathogenic cooperators (Figure 1.4). In this study, we examined the genomic and phenotypic consequences of Ti plasmid conjugation. Using synthetic biology approaches, we demonstrate that quorum sensing deficient Δ*traR* mutants largely lose the ability to transfer the Ti plasmid. In addition, we demonstrate that though conjugation alone will not antagonize cheaters already present in a population, cooperators that transfer the plasmid compete more favorably against Δ*vir*A cheaters than do cooperators that cannot transfer the plasmid. Using experimental evolution, we determined that when avirulent individuals arise via mutation, conjugation can reduce the density of freeloaders by transforming avirulent cheaters into cooperative pathogenic individuals. The horizontal transfer of the Ti plasmid into isogenic mutants does not have major genomic consequences. Yet, when the Ti plasmid is introduced into other backgrounds, it can lead to major mutations, including the loss of resident plasmids.

The Ti plasmid is a greenbeard in that the cooperative pathogenesis it confers benefits all opine catabolic individuals in close proximity (Gardner & West, 2010; Queller, 2011). The physical structure of the Ti plasmid genetically links the genes underlying cooperative pathogenesis (the *vir*-genes) to those needed to access the public goods produced as a result of cooperation (Platt, 2010; Platt, Bever, et al., 2012; Platt, Fuqua, et al., 2012; Platt & Bever, 2009). Consequently, the beneficiaries of agrobacterial cooperation will often also be cooperative individuals that themselves carry a greenbeard Ti plasmid. However, this will not always be the

case as mutation can uncouple pathogenesis and opine catabolic functions resulting in plasmids that confer only opine catabolic functions, which are often observed in natural systems. Although the presence of opines constrains greenbeard evolution (Chapter 1), we observed that evolution in the presence of plant cues and opines leads to the emergence of isogenic avirulent genotypes capable of cheating (Figure 1.4 & Figure 1.6). Because agrobacteria with cheater plasmids can catabolize opines without paying the costs of cooperation (Figure 1.5), they competitively displace virulent agrobacteria (Figure 1.4). Still, several models have shown that horizontal transfer of the plasmids carrying virulence genes can be employed as a cooperation enforcement mechanism by which cheaters are transformed into cooperators (Dimitriu et al., 2014; Mc Ginty et al., 2011; Nogueira et al., 2009; Smith, 2001). These models examine the hypothesis that transfer of a cooperative plasmid into cheaters can force them to cooperate (Mc Ginty et al., 2011; Smith, 2001).Conjugation can favor cooperation by increasing assortment among cooperative alleles (Dimitriu et al., 2014). Moreover, carriage of public good genes on plasmids can lead to indirect selection for plasmid conjugation (Dimitriu et al., 2018). Conjugation of the Ti plasmid requires activation of the *A. tumefaciens* quorum sensing system (Dessaux & Faure, 2018; Farrand et al., 2002; W. C. Fuqua & Winans, 1994). In particular, the conjugal transfer of *A. tumefaciens* Ti plasmid is regulated by the transcriptional activator TraR (W. C. Fuqua & Winans, 1994; Piper et al., 1993). Moreover, conjugation of the Ti plasmid is regulated by a Ti plasmid-encoded quorum sensing system, that ensures that conjugation only happens when opines are present and bacterial numbers are high (Dessaux & Faure, 2018; Farrand et al., 2002). Congruent with this, we observed that the conjugation rates of Δ*traR* mutants were significantly less than those of wildtype bacteria (Figure 2.1). The levels of

conjugation of Δ*traR* strains carrying the expression plasmids were significantly higher than the mutant strains; however, the conjugation frequencies were not the same as those of wildtype 15955 (Figure 2.1). Ectopic expression of *traR* genes in these complemented strains bypasses the need for conjugal opines or AHL (W. C. Fuqua et al., 1994). The partial complementation we observed suggests that the exogenous complementation did not achieve wildtype levels of QS induction.

Even when *tra* gene expression and conjugation are stimulated, the horizontal transfer of *A. tumefaciens* Ti plasmid is not very efficient (C. Fuqua & Winans, 1996). For this reason, conjugation of the Ti plasmid into cheaters may only anatagonize cheater invasion when cheaters are rare and cooperators are common. Our observations are congruent with this hypothesis in that conjugation was most effective when cheaters arose via de novo mutation and generally less effective when cheaters were initially present (Figure 2.2) and conjugation alone will not be able to antagonize cheaters (Figure 2.2, Figure 2.3). When cheaters were initially present, we only observed a significant difference between wildtype and the ΔpTi*traR* mutant when cheaters were 25% of the initial populations, however the effect size of this difference was modest. It may be that we failed observe differences in treatments where cheaters are rarer (0.25% and 2.5% of the initial population) because these low densities resulted in cheater and transconjugant density measurements close to the limit of detection, introducing measurement error and making it difficult to observe modest differences between strains.

The horizontal transfer of the Ti plasmid occurs not only between cheaters and cooperators, but also between cooperators and other agrobacterial strains. We studied the genomic

consequences of Ti plasmid conjugation into the *A. tumefaciens* C58 strain. The consequences of Ti plasmid conjugation vary considerably depending on the environment in which the transconjugant host evolves (Table 5.8). Consistent with our previous findings (Chapter 1), the presence of plant cues results in pTi15955 curing, while presence of opines results in the maintenance of the plasmid, however with significant mutational changes occurring in the plasmid. Some of the cells evolving with opines even lose the pTiC58 and a large portion of the pATC58. Isolates that evolved in environments with plant cues and opines had mutations similar to the mutations of isolates evolved in the evolution control media (Table 5.8). Although we did not observe any patterns suggesting recombination between pTi15955 and pTiC58, such recombination events have played a significant role in Ti plasmid diversification (Weisberg et al., 2020, 2022). However, those observations involve comparison over much longer evolutionary time scales than that of our study.

Conjugation plays a role in the diversification of the Ti plasmid, in the stabilization of agrobacterial virulence, in the maintenance of cooperation, and in the antagonism of cheaters. Our results indicate that conjugation has, at best, a very modest effect on cheater spread when cheaters are initially present. In contrast, when cheaters arise via mutation, conjugation has a significant effect on cheater spread (Figure 2.3). Conjugation-deficient cooperators (ΔpTi*traR*) have higher cheater load than wildtype cooperators that can transform *de novo* cheaters to cooperators. Consistent with this, we observed that recovered transconjugants can not only induce expression of the *virB* promoter but also are able to induce potato tumor formation at a rate similar to the parental wildtype strain (Figure 2.4). This suggests that although conjugation occurs at a relatively low rate, the horizontal transfer of the Ti plasmid can both evolutionarily

stabilize agrobacterial cooperative virulence genes and introduce the virulence into avirulent strains.

Funding

This work was supported by the National Science Foundation (NSF) Graduate Research Fellowship Program (GGVP004842 to PN-O), Kansas IDeA Networks of Biomedical Research Excellence (KINBRE) Bioinformatics Scholar Award (to RSJ, P20GM103418), and the Kansas NSF EPSCoR First Award Program (OIA-1656006 to TP). We also thank KINBRE Bioinformatics Core (P20GM103418) for help with using scripts used in the bioinformatic analyses. The computing for this project was performed on the Beocat Research Cluster at Kansas State University, which is funded in part by NSF grants CNS-1006860, EPS-1006860, EPS0919443, ACI-1440548, CHE-1726332, and NIH P20GM113109.

Chapter 3 - Photodegradable Hydrogels for Rapid Screening, Isolation, and Genetic Characterization of Bacteria with Rare Phenotypes[§]

Abstract

Screening mutant libraries (MLs) of bacteria for strains with specific phenotypes is often a slow and laborious process that requires assessment of tens of thousands of individual cell colonies after plating and culturing on solid media. In this report, we develop a three-dimensional, photodegradable hydrogel interface designed to dramatically improve the throughput of ML screening by combining high-density cell culture with precision extraction and the recovery of individual, microscale colonies for follow-up genetic and phenotypic characterization. ML populations are first added to a hydrogel precursor solution consisting of polyethylene glycol (PEG) *o*-nitrobenzyl diacrylate and PEG-tetrathiol macromers, where they become encapsulated into 13 μm thick hydrogel layers at a density of 90 cells/mm^2, enabling parallel monitoring of 2.8×10^4 mutants per hydrogel. Encapsulated cells remain confined within the elastic matrix during culture, allowing one to track individual cells that grow into small, stable microcolonies (45 ± 4 μm in diameter) over the course of 72 h. Colonies with rare growth profiles can then be identified, extracted, and recovered from the hydrogel in a sequential manner and with minimal damage using a high-resolution, 365 nm patterned light source. The light pattern can be varied to release motile cells, cellular aggregates, or

---

[§] Manuscript: Fattahi, N.; Nieves-Otero, P. A.; Masigol, M.; Van der Vlies, A. J.; Jensen, R. S.; Hansen, R. R.; Platt, T. G. Photodegradable Hydrogels for Rapid Screening, Isolation, and Genetic Characterization of Bacteria with Rare Phenotypes. *Biomacromolecules* 2020. https://doi.org/10.1021/acs.biomac.0c00543. Reproduced with permission from the American Chemical Society. Copyright 2020 American Chemical Society.

microcolonies encapsulated in protective PEG coatings. To access the benefits of this approach for ML screening, an *Agrobacterium tumefaciens* C58 transposon ML was screened for rare, resistant mutants able to grow in the presence of cell free culture media from *Rhizobium rhizogenes* K84, a well-known inhibitor of C58 cell growth. Subsequent genomic analysis of rare cells (9/28,000) that developed into microcolonies identified that seven of the resistant strains had mutations in the *acc* locus of the Ti plasmid. These observations are consistent with past research demonstrating that the disruption of this locus confers resistance to agrocin 84, an inhibitory molecule produced by K84. The high-throughput nature of the screen allows the *A. tumefaciens* genome (approximately 5.6 Mbps) to be screened to saturation in a single experimental trial, compared to hundreds of platings required by conventional plating approaches. As a miniaturized version of the gold-standard plating assay, this materials-based approach offers a simple, inexpensive, and highly translational screening technique that does not require microfluidic devices or complex liquid handling steps. The approach is readily adaptable to other applications that require isolation and study of rare or phenotypically pure cell populations.

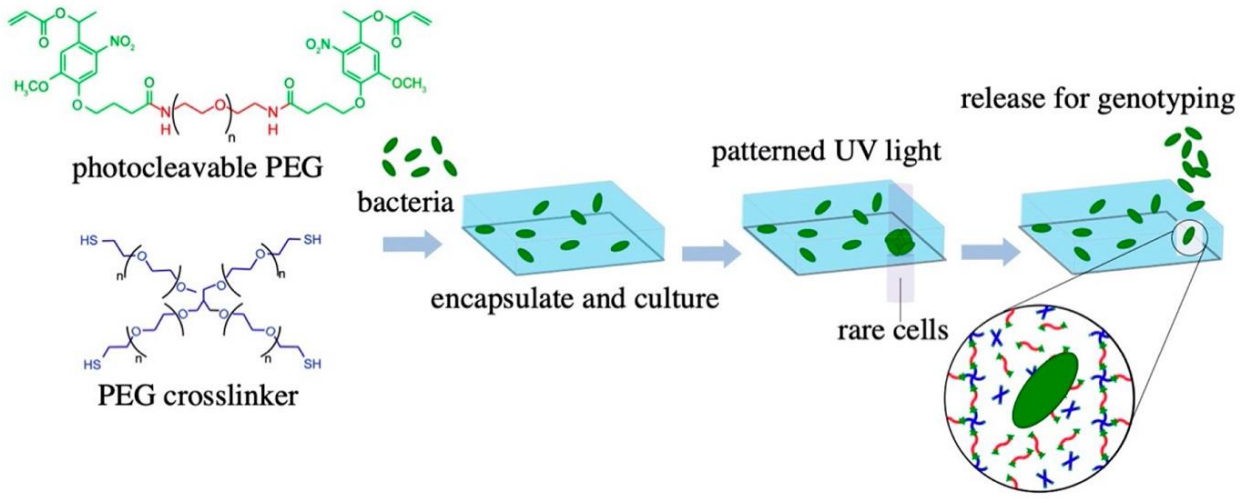

Figure 3.1. Photodegradable hydrogel interface for cell screening and isolation. As seen from left to right: Hydrogel precursor material. Hydrogel gelation and cell encapsulation. UV light exposure on target cell colony. Cell extraction and recovery.

Introduction

The identification and isolation of microorganisms with rare or unique functions from heterogenous populations is a critical step required to connect an organism's genotype with its phenotype.[1] These connections will enable researchers to gain a fundamental, predictive understanding of microbe function, to identify biomarkers that relate to specific diseases, and to engineer bacteria for applications in biotechnology. While phenotypic heterogeneity is prevalent in many microbial populations and communities, including among cells in populations that are genetically homogeneous or nearly homogeneous,[2,3] practical microbiological methods for screening and isolating phenotypically uniform groups of microbial cells is under-developed.

This technical limitation poses a challenge to genotype-to-phenotype determination which thus remains a broad knowledge gap in microbiology and biology more generally.[4]

Established methods of microbial cell isolation include flow-based sorting techniques such as fluorescence-activated cell sorting (FACS), which relies on signal from fluorescently labeled proteins or fluorescence in situ hybridization probes to isolate cells with specific features from its environment.[5,6] FACS allows for high-throughput, single cell analysis capable of sorting of up to 50,000 cells per second.[7] However, subsequent cultivation and enrichment of recovered cells is often inhibited, as the labeling step compromises cell viability.[4] Further, FACS is limited by the inability to sort cells by time-dependent cellular properties.[8] Consequently, FACS is not directly amenable to growth-based screening. In addition, FACS is an impractical option for many laboratories due to its high cost (~$100-200/hr) and availability often being limited to core research facilities. Motivated by these limitations, numerous micro- and nanoscale devices have been developed to isolate and study bacteria in recent years.[9–11] One common approach uses droplet-based microfluidic devices to partition cells into picoliter droplets, offering control over the chemical microenvironment and high-throughput, single cell analysis.[12] However, most devices have several limitations—a major one being that retrieval of individual cells from the device is difficult.[13] Ultimately, this inhibits follow-up genotyping and other -omics level characterizations after on-chip observation. These constraints impose a major limitation for screening and discovery applications. Recently, Lim *et al*. developed an innovative microwell platform for rapid screening of *E. coli* mutant libraries for mutants with growth rate differences,[14] demonstrating the benefits of off-chip recovery of individual cell populations for follow-up genotypic analysis. However, many micro- and nanoscale approaches

require complex fabrication and liquid handling capabilities, thus they often fail to translate into non-expert microbiology laboratories.[4]

Hydrogel materials can provide an alternative strategy to microbe screening and isolation.[15,16] Here, individual cells from a suspension are encapsulated into an elastic, nanoporous hydrogel matrix, most commonly alginate or agarose, that facilitates diffusive biomolecular exchange.[17] Cells can then be cultured into high-density microcolonies, where enough biomass accumulates for cell preservation and follow-up characterization. Cells can be encapsulated into microscale hydrogel droplets using bulk emulsions,[18] or 3D-bioprinters.[19] However, sorting and isolation of individual droplets containing a desired cell or cell population still remains a limitation and is most often achieved using FACS.[20] Photodegradable hydrogels enable an alternative mode of targeted cell recovery thereby alleviating limitations associated with other hydrogel materials. Photodegradable hydrogels are designed to erode on exposure to light, enabling on-demand release of encapsulated cargo or manipulation of the biochemical and biophysical features of the microenvironment.[21] Because light can be patterned at single micron length scales, the approach affords a high level of spatial and temporal control over on-demand release.[22] This capability provides a distinct advantage for microbial selection and isolation applications in which specific cells must be released and retrieved from a screening interface with a high spatial precision. Recently, we reported the use of photodegradable hydrogels as a membrane to retrieve cell populations loaded and cultured in a microwell array format.[23] The hydrogel was generated by combining a poly(ethylene glycol)-*o*-nitrobenzyl diacrylate (PEG-*o*-NB-diacrylate) macromer with a four-arm PEG-thiol macromer, which generates a crosslinked PEG network through thiol-acrylate Michael-type addition reactions.[24]

Using a patterned 365 nm light source, cell populations cultured in individual microwells can be released from wells and into solution on-demand, then plated and recovered.

Building off of these findings, here we investigate the use of photodegradable hydrogels to screen and isolate phenotypically rare bacteria strains present in mutant libraries (ML) for follow-up genotypic analysis (Figure 3.1). The approach uses thiol-acrylate reactions to encapsulate a ML population into a three-dimensional PEG matrix over a thiolated glass coverslip. Encapsulated cells are co-cultured in a defined media for screening, and individual cells with unique growth profiles are targeted for removal and downstream analysis. Each step in the screening procedure, including parallel growth monitoring of bacterial microcolonies, the effect of light pattern and exposure on the arrangement and viability of bacteria released from hydrogels, and sequential extraction of multiple microcolonies is developed towards high-throughput screening and recovery of viable cells. This enabled observation and recovery of any one of 3×10^4 mutants across a ~310 mm^2 hydrogel area, a throughput that can accommodate enough mutant strains to rapidly screen even large bacterial genomes to saturation in a single assay (e.g. *Streptomyces* sp., genome of ~8.7-11.9 Mbps,[25] requiring around 60,000 mutants to achieve saturation). This capability offers a significant reduction in the time and labor required to screen to saturation using standard plating techniques.

To demonstrate the benefits and feasibility of this approach, a ML of *Agrobacterium tumefaciens* C58 is screened for resistance to the antagonistic impacts of cell free culture fluid (CFCF) from *Rhizobium rhizogenes* K84. K84 produces multiple chemicals inhibiting the growth of C58, including the bacteriocin agrocin 84.[26,27] While C58 cells are susceptible to agrocin 84, rare mutations give rise to agrocin-resistant mutants. To identify these rare mutations, the

phenotype of tens of thousands of mutants must first be evaluated. In a single test, we were able to screen, identify, then isolate nine resistant C58 mutants from a ML containing ~28,000 unique strains. Subsequent analysis of whole genome sequences identified mutations in the *acc* locus of the Ti plasmid conferring agrocin 84 resistance. This serves as the first successful example of a successful phenotype-to-genotype determination using this rapid screening approach.

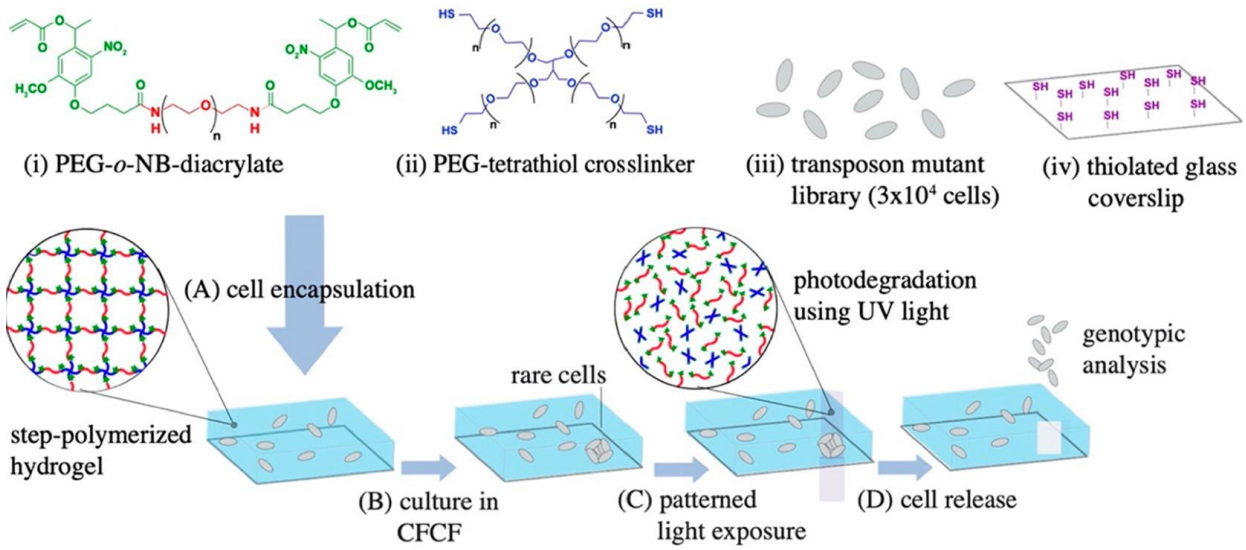

Figure 3.2. Overall approach to screening and isolation of rare cells from transposon mutant libraries. Precursor materials consisting of (i) PEG-*o*-NB-diacrylate, (ii) PEG-tetrathiol crosslinker, (iii) a bacteria transposon mutant library and (iv) a thiolated glass coverslip are prepared. (A) Precursor components are then mixed, resulting in the formation of a step-polymerized photodegradable hydrogel layer over the coverslip. (B) Cells are cultured in cell free culture fluid (CFCF) from an antagonistic species, to identify mutants with rare growth profiles. (C) Patterned light is then used to spatially degrade portions of the hydrogel, (D) releasing resistant cells into solution for recovery and follow-up genotyping.

Experimental Section

Materials

Pentaerythritol tetra (mercaptoethyl) polyoxyethylene (4 arm PEG, - $((CH_2)_2\text{-}SH)_4$ was purchased from NOF America Corporation. PEG-diacrylate (PEGDA, MW 3400) was purchased from Laysan Bio. Fluorescein-5-Maleimide was purchased from Cayman. Ethanol (EtOH), isopropanol, dimethylformamide (DMF), dichloromethane (CH_2Cl_2), diethyl ether (Et_2O), sodium hydrogen sulfate ($NaHSO_4$), anhydrous sodium sulfate (Na_2SO_4), and acetic acid (AcOH) were purchased from Fisher. D-(+)-glucose, biotin ($C_{10}H_{16}N_2O_3S$), (3-Mercaptopropyl) trimethoxysilane, sodium phosphate monobasic dihydrate ($NaH_2PO_4 \cdot 2H_2O$), sodium hydroxide (NaOH), alconox detergent, toluene anhydrous, N-hydroxysuccinimide (NHS), dicyclohexyl carbodiimide (DCC) and PEG-diamine (MW 3400), deuterated chloroform ($CDCl_3$), phosphorpentoxide (P_4O_{10}), 4Å molecular sieves, ninhydrin, and triethylamine (Et_3N) were purchased from Sigma-Aldrich. Silica TLC plates were from Merck. Ammonium sulfate ($(NH_4)_2SO_4$), magnesium sulfate heptahydrate ($MgSO_4{\cdot}7H_2O$), calcium chloride dihydrate ($CaCl_2{\cdot}2H_2O$), manganese (II) sulfate monohydrate ($MnSO_4{\cdot}H_2O$), kanamycin sulfate, spectinomycin sulfate, and iron (II) sulfate ($FeSO_4$) were purchased from VWR. DNeasy Blood & Tissue Kits was purchased from QIAGEN. The LIVE/ DEAD BacLight Bacterial Viability Kit was purchased from ThermoFisher Scientific. All chemicals were used as received unless stated otherwise. 4Å molecular sieves were heated under vacuum at 200^oC for 4 h to remove water. CH_2Cl_2 was dried with 4Å molecular sieves. Et_3N was distilled from ninhydrin at atmospheric pressure and stored over KOH pellets. NHS, DCC and PEG-diamine were dried under vacuum in the presence of P_4O_{10} at 40 °C for 19 h. NB-COOH was

prepared as previously reported.[16] The ninhydrin staining solution was prepared by dissolving 300 mg ninhydrin in 97 mL EtOH and 3 mL AcOH and stored in the dark.

Synthesis of the photodegradable poly(ethyleneglycol) diacrylate

PEG-*o*-NB-diacrylate was prepared with slight modifications from that previously reported[23] and is shown in Figure 5.4. 519 mg (1.5 mmol) NB-COOH and 175 mg (1.5 mmol) NHS were dissolved in 4 mL DMF and 8 mL CH_2Cl_2. The clear solution was cooled on ice for 15 min and a solution of 304 mg (1.5 mmol) DCC in 2 mL CH_2Cl_2 was added dropwise over the course of 5 min. After stirring for 21 hr at room temperature a solution of 508 mg (0.15 mmol, 0.30 mmol NH_2 groups) PEG-diamine and 51 μL (0.37 mmol) Et_3N in 9 mL CH_2Cl_2 was added dropwise over the course of 10 min to the turbid reaction mixture. After stirring for 20 hr, spotting of the reaction mixture on a silica TLC plate followed by ninhydrin staining and heating showed the absence of amine groups. The mixture was concentrated in a flow of nitrogen to remove CH_2Cl_2 and the residue was diluted with 16 mL 1 M $NaHSO_4$ (aq). The suspension was passed through a glass filter and the white residue was washed with 9 mL 1 M $NaHSO_4$ (aq). The slightly hazy filtrate was then passed through a syringe filter (0.45 μm). After washing the syringe filter with 1 M $NaHSO_4$, the clear yellow filtrate (30 mL) was extracted with CH_2Cl_2 (5 x 30 mL). The extracts were combined, dried over Na_2SO_4, filtered through Whatman paper and concentrated under reduced pressure at 30°C. The oily residue was dissolved in 8 mL CH_2Cl_2 and the solution slowly diluted by adding 200 mL Et_2O. The precipitate was collected on a glass filter, washed with Et_2O (3 x 10 mL) and dried. This Et_2O precipitation was repeated one more time to yield PEG-*o*-NB-diacrylate (539 mg) as a light-yellow solid. ^1H NMR ($CDCl_3$) δ= 7.58 (s, CH_{aromat}), 7.00

(s, 1H, CH_{aromat}), 6.52 (m, CH), 6.45 (bs, NH), 6.44 (d, $CH=CH_{trans}$), 6.16 (dd, $CH=CH_2$), 5.87 (d, $CH=CH_{cis}$), 4.10 (t, $CH_2CH_2CH_2O$), 3.92 (s, OCH_3), 4.22-3.20 (CH_2CH_2O + OCH_2CH_2N), 2.39 (t, CH_2CO), 2.17 (m, $CH_2CH_2CH_2$), 1.65 (d, CH_3CH). The degree of functionalization using MW=3400 was 80% by comparing the integral ratios of the aromatic and CH_2CH_2O PEG protons. The ^1H NMR spectrum is shown in Figure 5.5. ^1H NMR spectra were measured on a Varian System 500 MHz spectrometer in deuterated chloroform ($CDCl_3$). A total of 32 scans was collected and the D1 was set to 10s. Chemical shifts (δ) are reported in ppm and are referenced against the residual $CHCl_3$ peak at 7.26 ppm.

Bacterial strains and culture conditions

All strains and plasmids used in this study are described in Table 5.9. Wildtype *A. tumefaciens* C58 (herein referred to as C58) was used for the live/dead assay. *A. tumefaciens* C58 cells constitutively expressing the fluorescent protein GFPmut3 (herein referred to as C58-GFP) were used as controls in the hydrogel experiments. Populations of fluorescent *A. tumefaciens* C58-GFP *Himar1* mutant library cells (described below and herein referred to as C58 ML) were used in seeding, culture, and screening experiments within the hydrogels. *A. tumefaciens* strain NT1 was used as an agrocin 84 resistant control in the agrocin 84 bioassay. Unless noted otherwise, the *A. tumefaciens* strains were grown on AT minimal medium[28] supplemented with 0.5% (w/v) glucose and 15 mM ammonium sulphate (ATGN). *Rhizobium rhizogenes* strain K84 (herein referred to as K84) bacterial cells were cultured in suspension at 28°C (215 rpm) for 24-48 hrs to reach an OD_{600} of 0.7 in ATGN media supplemented with kanamycin (150 µg/ml), spectinomycin (100 µg/ml), biotin (2 µg/ml), and iron as Fe (II) sulfate (0.022 mM).

The optical density of bacteria cultures (100µL) at 600 nm (OD_{600}) were measured using an Epoch2 microplate reader (Biotek) in 96-well plates for all experiments. After K84 reached an OD_{600} of 0.7, the bacterial culture was centrifuged at 2000 g for 10 min and the supernatant containing cell free culture fluid (CFCF) from K84 was sterile filtered two times, first with a 0.45 µm syringe filter, and a second time with a 0.2 µm syringe filter before being used in screening experiments.

Media for screening experiments

8X ATGN media was prepared as the undiluted base media. For unconditioned media, 8X ATGN was diluted to 1X with sterile ultrapure water then supplemented with iron (0.022 mM), biotin (2 µg/mL), kanamycin (150 µg/mL) and spectinomycin (100 µg/mL). For conditioned media, 8X ATGN was diluted with the CFCF acquired from K84 to get 1X ATGN that was subsequently supplemented with iron (0.022 mM), biotin (2 µg/mL), kanamycin (150 µg/mL) and spectinomycin (100 µg/mL).

Transposon mutagenesis

The *mariner* transposon *Himar1* was used to mutagenize C58-GFP cells using previously described methods.[29] In brief, *E. coli* S17-1/λpir pFD1 and C58-GFP cells were mixed and incubated overnight at 28°C on a 0.2 µm polyethersulfone (PES) disk filter (PALL) placed on a LB plate. Following incubation, cells were collected and frozen at −80°C in 25% glycerol.

Thiol surface functionalization

Thiol functionalized surfaces can be used as a route for secondary surface modifications through thiol-acrylate addition reactions,[30] and are used here to provide covalent attachment of the hydrogel to the coverslip surface. Glass coverslips (1.8×1.8 cm) were cleaned with oxygen plasma for 3 min using a PDC-001-HGP Plasma Cleaner (Harrick Plasma). Coverslips were then cleaned and hydroxylated in Piranha solution, a 30:70 (v/v) mixture of H_2O_2 and H_2SO_4 at 60-80°C for 30 min (*Caution! Strongly corrosive*).[31] Coverslips were then rinsed and stored in ultrapure water at room temperature. For functionalization with thiol groups, coverslips were then dried under a N_2 stream and immersed into a 269 mM of (3-mercaptopropyl) trimethoxysilane (MPTS) solution in dry toluene (5 v/v) for 4 hrs at room temperature. Substrates were then rinsed with toluene, ethanol/toluene 1:1, and ethanol, 4 times each.[31] They were then dried under a N_2 stream and stored at 4°C for further use.

Hydrogel preparation and growth monitoring

All hydrogels were made in 1X ATGN phosphate buffer, pH 8. This was made by first adding NaH_2PO_4 to 2X ATGN, adjusting to pH 8 using 5 M NaOH (aq), which was then sterile filtered and stored at -20°C until further use. Bacteria were encapsulated into the hydrogels by first inoculating 1 mL of 2X ATGN media with 2 µL of cells from the 25% glycerol stock stored frozen at -80°C, for both the C58 ML and the C58-GFP control. This resulted in a C58 ML concentration of 3.63×10^7 CFU/mL in 1X ATGN media, pH 8. Then, a hydrogel precursor solution was prepared by adding photodegradable PEGDA (M_n 3400 Da, 8.4 µL, 49 mM) in water into 18.75 µL of the inoculated ATGN. Lastly, PEG-tetrathiol (M_n 10000 Da, 10.35 µL, 20 mM) in water was

added to the mixture, resulting in an equimolar acrylate:thiol ratio. The concentrations of acrylate and thiol groups in the final solution were each 22 mM. The final solution volume was 37.5 µL.

The cell suspension was added to thiol-functionalized coverslip to allow for covalent attachment of the hydrogel to the glass surface through thiol-acrylate addition (Figure 5.6). First, 7 µL of the cell suspension was pipetted onto a chemically inert perfluoroalkylated glass slides, made as previously reported.[23] This coverslip was then contacted with the thiolated coverslip, separated by a fixed distance of 12.7 µm using Stainless Steel Thickness Gage Blades (Precision Brand). The solution was incubated for 25 min. at room temperature to allow for crosslinking of the PEG polymers and hydrogel formation. After gelation, the thiolated glass slide and attached hydrogel were gently removed from the perfluoroalkylated glass slide. Care was taken during this step to prevent the hydrogel from rupturing. With these conditions, it was noted that spacers thicker than 12.7 µm resulted in an overlay of cells, which was not desired because cells colonies above or beneath the target colony are also released during light exposure, which may result in cross-contamination during cell retrieval (Figure 5.7). For screening experiments, hydrogels were placed in 60×15 mm petri dishes and cultured in ATGN media or ATGN/CFCF media in an incubator at 28ºC. For growth monitoring, cells were cultured in ATGN media at 28°C in a live cell incubation chamber (Tokai Hit) placed over a Nikon Eclipse Ti-E inverted fluorescent microscope. Time lapse fluorescent images of the bacteria during growth into microcolonies within the hydrogel were taken with 10× | NA 0.3 or 20× | NA 0.45 lens using NIS-Element software. Growth rates were quantified using Growthcurver software (Figure 5.9).[32]

Hydrogel degradation and cell release with the Polygon 400 light patterning device

Hydrogels were exposed to various patterns of UV light from a 365 nm LED light source using the Polygon400 patterned illumination tool (Mightex Systems) configured to an Olympus BX51 upright microscope. The tool exposes 365 nm light at micron-scale resolution across a user-defined area for a given exposure time, enabling spatiotemporal control of hydrogel degradation (Figure 5.8). Intensity of the 365 nm irradiated light was controlled using Mightex PolyScan2 software and varied between 0.7-7 mW/mm^2. Prior to hydrogel degradation, the tool was calibrated to the specific objective using a mirror and the calibration software to obtain a clean and sharp pattern exposed on the mirror with the selected objective. Hydrogels were then placed in a PDMS holder and covered with ATGN media to prevent the hydrogel from dehydration (Figure 5.10). Targeted microcolonies were identified with the microscope, then focused on within the three-dimensional hydrogel. This focusing step was important to maintain a sharp UV exposure pattern over the targeted cells, as regions above and below the focused region of the hydrogel become exposed to out of focus UV light, causing degredation pattern to become scattered in these regions (Figure 5.12). This is an inherent limitation of the upright microscope. Exposure occurred with a 10× NA 0.3 or 20× NA 0.5 objective. Brightfield images and movies were taken during photodegradation by using Infinity Capture Software.

Labeling the hydrogel with fluorescent dye

Fluorescent microscopy was used to image the hydrogel after UV light exposure and degradation by labeling with fluorescein-5-maleimide, which couples to pendant thiol groups within the hydrogel.[33] 4 μL of a 10 mM stock solution of fluorescein maleimide in DMF was

added to 1 mL PBS buffer (pH 7.3) then added to the hydrogel for 2 hrs at room temperature in a dark environment. The hydrogel was then rinsed with 1X PBS to remove unbound fluorophores and imaged.

Live/Dead assay

To investigate cell viability after exposure of micro-colonies to UV light, a live/dead assay was used. Here, C58 cells were encapsulated in hydrogels containing non-photodegradable PEGDA (M_n=3400 Da) instead of PEG-*o*-NB-diacrylate, thus colonies remained within the hydrogel after UV exposure for staining and imaging. The stain mixture was prepared as recommended by the manufacturer. 300 µL of the mixture was added over each hydrogel and incubated in the dark for 15 minutes. SYTO 9 labels both intact and compromised cells, while propidium iodide labels only cells with damaged membranes, resulting in reduction of expressed fluorescence by SYTO 9.[34] After staining, the hydrogels were washed thoroughly with NaCl 0.85 wt. % solution and imaged using the inverted fluorescence microscope. The percentage of live cells (*p*) was estimated from the fluorescence intensity data according to the following equation:

$$p = 100 - \left(\frac{r_{UV} - r}{r_{dead} - r}\right) \times 100 \quad (1)$$

Where the r_{UV} is the measured red signal following UV exposure, r is the red signal measured when the hydrogel is not exposed to UV, and r_{dead} is the red signal of the dead cell control. For this control, cells were killed by incubating the hydrogel in 70% isopropanol at room temperature for 20 minutes. The hydrogel was then washed with ultra-pure water before staining.

Cell retrieval and recovery

Immediately after light exposure, the free end of a 20 cm long PTFE tubing, 0.05" ID, was placed over the irradiated spot. The other end was attached to a 100 µL microliter syringe that was used three times to aspirate the media containing the released cells. For every exposed microcolony, 300 µL of solution was collected and transferred into an Eppendorf tube. For each sequential microcolony extracted, the syringe, tubing, PDMS holder, and the hydrogel were washed with ultra-pure water at least 3 times to minimize cross-contamination. Following cell retrieval, 300 µL of the bacterial solution was plated onto selective media for recovery. The plating process was also expected to dilute PEG degradation biproducts. 100 µL of the solution was plated on ATGN supplemented with kanamycin and spectinomycin. Cells from the mutant library are expected to be resistant to both antibiotics. In contrast, C58-GFP, the parental strain used to generate the mutant library, is resistant only to spectinomycin. The presence of both antibiotics allowed for recovery of mutants, decreasing the chance of contamination from other sources. After inoculation, the plates were incubated at 28°C for three to five days.

Agrocin 84 bioassay

Agrocin 84 bioassays were performed to determine if recovered mutants are resistant to agrocin 84—a bacteriocin produced by K84 which strongly antagonizes C58. The bioassay protocols were adapted from those reported by Hayman *et al*.[35,36] K84 and recovered C58 ML mutants, were grown in liquid ATGN as previously described for 24 hours. All cultures were normalized to an OD_{600} of 0.6 in ATGN media. Tubes containing 10 mL of molten agar (65°C) were inoculated with 35 µL of the C58 mutant cultures. The tubes were vortexed vigorously for

10 seconds and then poured onto sterile 60 × 15 mm petri dishes. Once the agar solidified, 7.5 µL of K84 cells (OD_{600} = 0.6) was spotted in the center of the plate and allowed to air dry. Once the K84 had dried completely, the plates were wrapped with a plastic wrap to prevent drying of the media, and they were incubated at 28°C for 72 to 120 hrs.

Genomic DNA purification

QIAGEN's DNeasy Blood & Tissue Kit was used to purify bacterial genomic DNA from cellular debris and any residual PEG byproduct. The manufacturer's protocol, including the Gram-negative bacteria pretreatment, was followed with minor modifications. Proteinase K incubation was performed for 60 min at 56 °C and 4 µL of RNase A (100 mg/mL) were added following proteinase K incubation. Lastly, two sequential elution steps via centrifugation were included: the first elution used 150 µL of Buffer AE while 50 µL of Buffer AE were used for the second elution. Genomic DNA samples were stored at -20°C.

Whole genome sequencing

Genomic DNA samples were sent to the Microbial Genomic Sequencing Center (MiGS) in Pittsburgh, PA. Samples were received and immediately frozen until the library preparation began. Qubit fluorometric quantification was used to quantify DNA concentrations. All samples were normalized to the same concentration and enzymatically fragmented using an Illumina tagmentation enzyme. Unique indices were attached to each pool of fragmented genomic DNA using PCR and the resulting barcoded pools were combined to multiplex on an Illumina NextSeq 550 flow cell.

Sequence analysis

Bioinformatic analyses were performed on Beocat, the High-Performance Computing cluster at Kansas State University. Once sequencing reads were acquired from the MiGS, read mapping was performed by aligning the reads to the C58 reference genome using Burrows-Wheeler Aligner's Smith-Waterman Alignment (BWA-SW) algorithm.[37] The BWA-SW algorithm aligns long sequences (up to 1 Mb) against a large reference genome in a fast and accurate manner. A variant calling applying the Genome Analysis Toolkit (GATK) was then applied. GATK is a pipeline that compares the alignment of our reads to the C58 genome at a more detailed level while simultaneously performing a base quality score recalibration, indel realignment, duplicate removal, and SNP and INDEL discovery.[38] Additionally, the GATK pipeline applies standard hard filtering parameters or variant quality score recalibration that result in identification of mutations with high confidence. The purpose of the read mapping and variant calling is to find the mutation responsible for agrocin 84 resistance. Once the mapped reads and the variants were generated, regions with mutations were identified.

Results and discussion

High density cell encapsulation and parallel tracking of cell growth

The first step in developing the hydrogel interface involved achieving high-density encapsulation of viable bacteria cells within the hydrogel for growth monitoring. C58 ML cells were seeded across a 1.8×1.8 cm glass coated with a hydrogel initially 12.7 µm thick, which reached 140 µm in its swollen state after incubation. Given the genome size of *A. tumefaciens* C58 (approximately 5.67 Mbps),[39] observation of 28,000 mutants within a single hydrogel was desired to ensure that the genome could be screened to saturation with 99% certainty.[40] Using fluorescence microscopy, it was found that seeding bacteria at a concentration of 3.63×10^7 CFU/mL encapsulated bacteria at a density of 90 CFU/mm^2, meeting this requirement. As shown in Figure 3.3, after encapsulation, cells appeared randomly dispersed and vertical overlap of cells was minimal, which was desired to prevent extraction of multiple colonies during the light exposure step. Hydrogel thicknesses greater than 12.7 µm thick resulted in vertical overlap of cells (Figure 5.7).

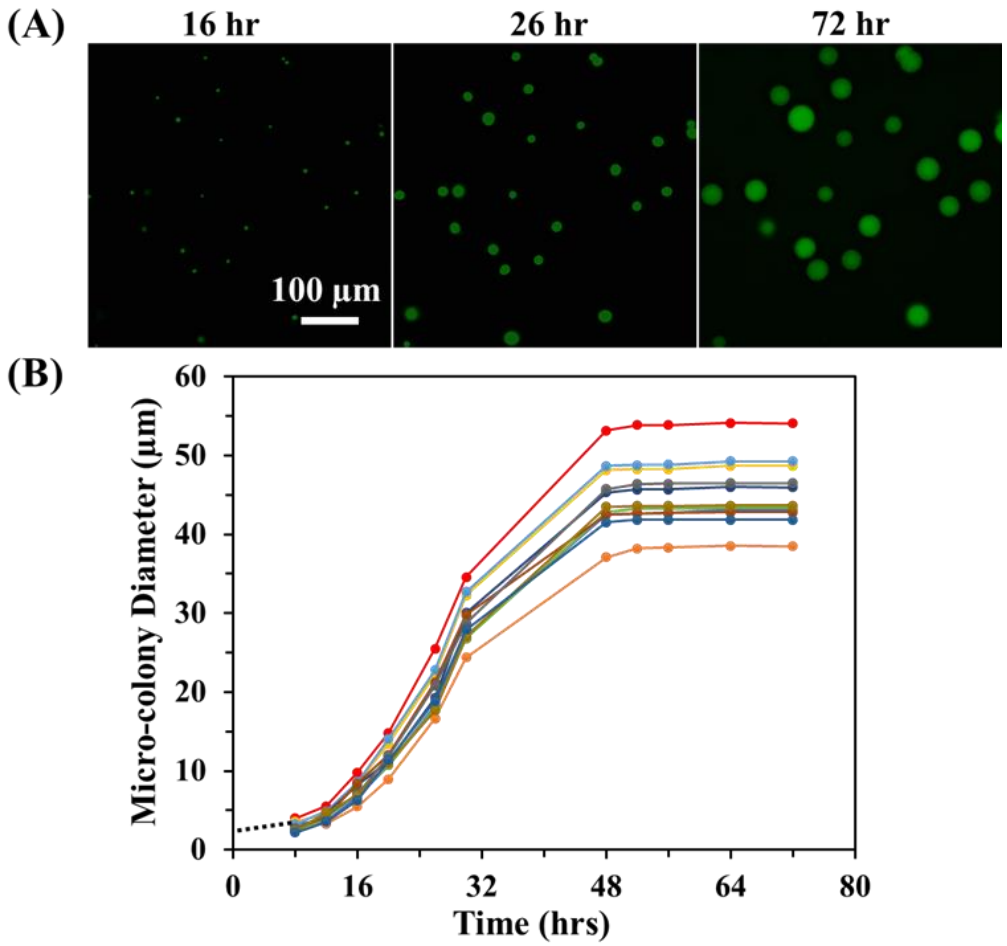

Figure 3.3. Parallel growth monitoring of individual C58 cells into microcolonies within the hydrogel matrix after seeding. (A) Representative fluorescent images of C58 ML microcolonies at different time points. (B) Microcolony growth for 11 sample microcolonies within the hydrogel as a function of time.

After encapsulation, parallel growth tracking of individual cells into microcolonies during culture in ATGN media was achieved. Microcolonies growth reflects a lag phase, here cells were initially not visible under 20X magnification, then a growth phase at 8 hrs, where cell microcolonies became visible. Growth phase ($k = 0.18\ hr^{-1}$) slowed upon entry into stationary phase after 48 hrs (Figure 3.3). These observations suggest that there was sufficient mass transfer to support cell growth. Hydrogel mesh size (ξ), a critical determinant of mass transfer

within the hydrogel,[41] was calculated to be 10 nm based on the equation described by Canal and Peppas,[42] small enough for immobilization of bacteria cells but large enough for diffusive exchange of nutrients (e.g. glucose) and waste products. Similar growth trajectories were observed when monitoring growth of free cells in a 96-well plater reader (Figure 5.9), suggesting that cell confinement or diffusion limitations had a minimal effect on growth within the hydrogel environment. Cells developed into spherical micro-colonies due to deformation of the elastic PEG matrix caused by the local increase in cell numbers and through chemical or enzymatic modes of hydrogel degradation.[43] These measurements were performed several times (n=26) with 92% of the trials resulting in microcolony growth. At later time points (~5 days) bacteria were observed to escape hydrogel encapsulation (Figure 5.11). While chemical hydrolysis of thioether-ester linkages may play a role in hydrogel degredation,[44] follow-up studies have indicated that hydrogels remain capable of immobilizing inert, 1 μm fluorescent beads at neutral pH over 5 days (Figure 5.11). Others have also reported minimal mass loss in similar thiol-acrylate PEG hydrogels over a 5-day time period at neutral pH.[45] This suggests that bacteria within the microcolonies were the cause of eventual breakdown of the hydrogel matrix.

Characterization of cell release and cell viability

Using light for extraction has the advantage of spatiotemporal control of cell release, as the patterned illumination tool allows for projection of user-defined, two-dimensional patterns over any microcolony within the hydrogel. Here, the arrangement of cells released into solution after exposure with different patterns was investigated. Microscale patterns including lines,

rings that outline the microcolony perimeter, a cross, or a broken cross pattern were investigated. Patterns with greater coverage of the colony such as circles were avoided to minimize unnecessary UV light exposure in effort to preserve bacteria viability and DNA quality. The recovered cells present in the extract solution were then imaged in brightfield and fluorescence modes to examine cell arrangement (Figure 3.4).

Light patterning offered control of the arrangement for cells liberated from the hydrogel interface. Ring patterns degraded the hydrogel immediately surrounding the microcolony, forming a hydrogel island that immediately detached from interface and into solution. Examination of the extract solution revealed that cells remained encapsulated as microcolonies in the free hydrogel (Figure 3.4). This pattern offers the advantage that extracted cells are not directly exposed to UV light and that they remain preserved in a larger, protective PEG layer, potentially useful for downstream separation or processing steps. Cross patterns instead appeared to liberate cells as either aggregates or free cells (Figure 3.4), as these exposure patterns etched a direct path for cellular transport out of the hydrogel. Here, it was noted that the entire cell mass was liberated into the media covering the hydrogel as the membrane became compromised (Figure 5.12). Inspection of the recovered cells in the extract solution revealed that broken-cross patterns favored aggregated cells, whereas cross patterns contained extract solutions dominated by free cells. Other patterns, such as individual lines patterned at the microcolony edge, also caused a burst of free cells into solution, however some of the cells appeared to remain in the hydrogel after exposure (Figure 5.12). Because removal of a maximum number of target cells with minimum direct exposure to UV light was desired, the broken cross pattern was selected for further use.

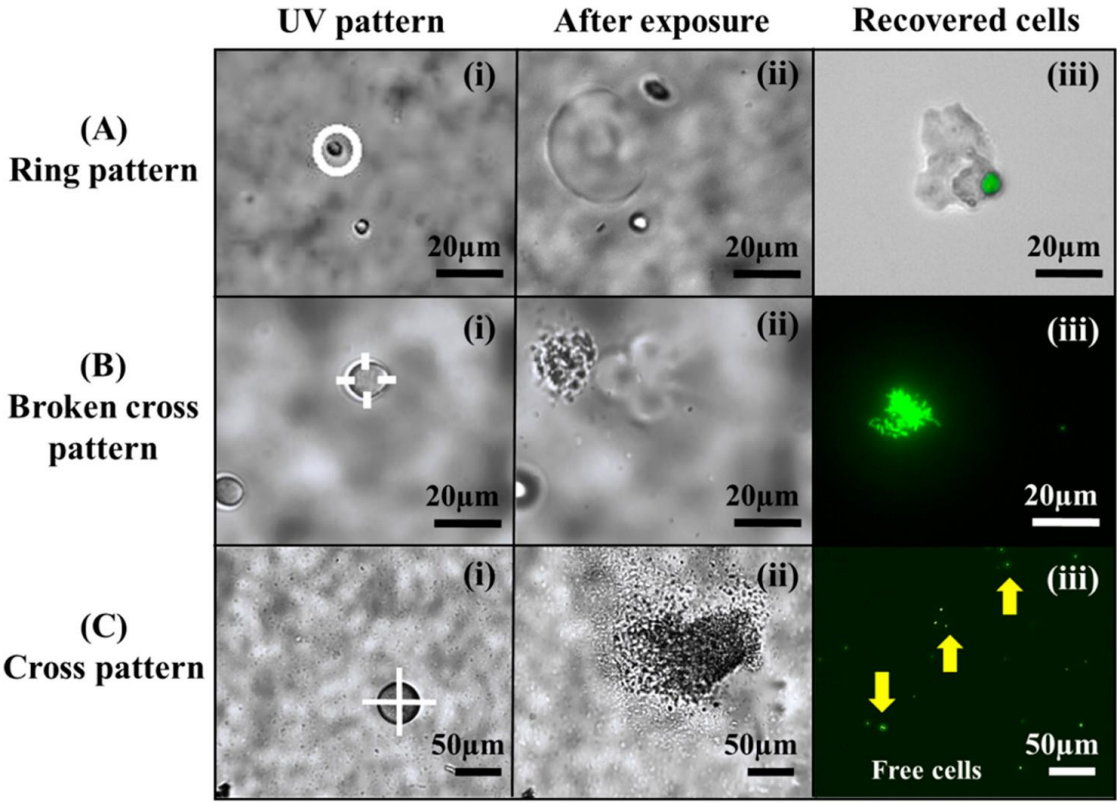

Figure 3.4. C58 ML cell arrangement after release with different light patterns. (A) Ring pattern for the extraction of colonies protected within a PEG layer. (B) Broken cross pattern for the extraction of aggregated cells. (C) Cross pattern for the extraction of predominantly free cells. For each exposure pattern, the following are shown: (i) the projected light pattern (white line) over a targeted colony, (ii) the hydrogel immediately after cell release, and (iii) brightfield and/or fluorescence images of the recovered cells in solution. Patterns were exposed at an intensity of 4.2 mW/mm^2.

After establishing that using broken cross-pattern exposure results in lift off of the entire cell mass, we investigated how varied light intensities affected release time, defined here as exposure time until microcolony burst is observed (Figure 3.5). Step growth hydrogels are characterized by rapid erosion rates due to the low levels of network connectivity,[24] here degradation and cell release were noted in <180 s for all exposure intensities studied. Cell release time showed significant decreases with increasing light intensity up to an intensity of 4.2 mW/mm^2 ($p < 0.05$), this trend was expected as exposure time required for reverse gelation of the hydrogel is inversely proportional to light intensity.[24] Beyond this, only minor decreases in release time were noted and a minimum light dose for release was found at 168 ± 14 mJ/mm^2, corresponding to an intensity of 4.2 mW/mm^2.

Since 365 nm light can be cytotoxic to bacteria through generation of reactive oxygen species,[46] the effect of broken cross pattern exposure (4.2 mW/mm^2, 40 s) on cell viability was characterized using a live/dead assay (Figure 3.5). Here, C58 cells were first seeded within a hydrogel generated with PEG diacrylate without the photocleavable *o*-NB moiety, cultured into micro-colonies, and the colonies were then exposed to broken cross patterns of light. Removal of the *o*-NB group from the network backbone ensured that microcolonies would remain in place during exposure so they could be subsequentially stained and observed with fluorescence microscopy. Comparison of red signal indicating non-viable cells showed no significant difference between unexposed and exposed cells, both of which were significantly less than the dead cell control ($p < 0.01$). This suggests that the majority of cells remain viable during the extraction step for recovery and genomic analysis. Given these findings, these exposure conditions were used in the remaining studies.

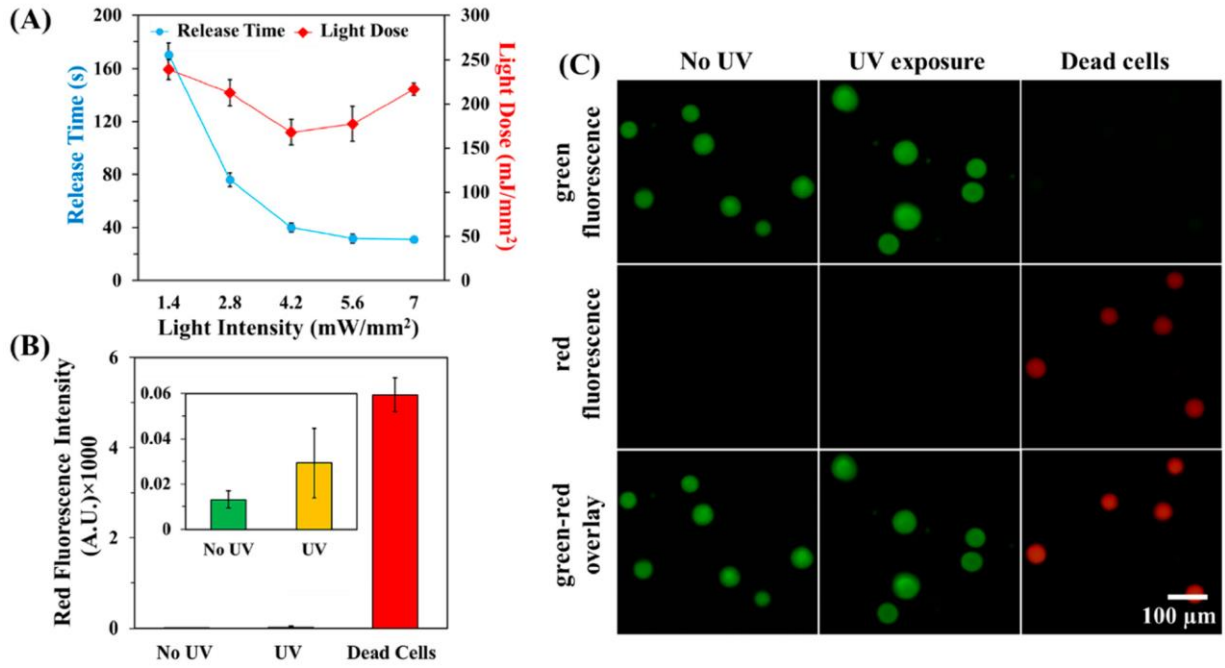

Figure 3.5. (A) Microcolony release time from hydrogels at varied 365 nm light intensity. An entire cell mass lift off effect was noted during broken cross pattern exposure, providing a discrete time point for cell release. (B) Red fluorescence signal after staining with the reagents in the live/dead bacterial viability kit. Microcolonies without UV exposure, with broken cross pattern UV exposure (4.2 mW/mm^2, 40 s), and from chemically treated (70% isopropanol) dead cells are compared. (C) Representative green-red fluorescence images of microcolonies after staining with the live/dead assay. Dead cells with compromised membranes appeared red. ImageJ software was used to adjust the images for color contrast. For each treatment (n = 3 independent trials), 30 different microcolonies were imaged.

Sequential extraction and recovery of individual microcolonies

Isolation of bacteria for pure cultures is one of the most important requirements in microbiological techniques because it enables extraction of pure genetic material, allows for follow-up biological and biochemical testing, and eliminates confounding observations that can arise from other bacteria. Here, the ability to generate pure cultures exclusively from the bacteria targeted for extraction was evaluated. Hydrogels were first seeded and cultured for microcolony development and placed inside a PDMS holder (Figure 5.10). Designated areas of

the hydrogel were exposed to UV light then immediately washed with wash buffer to remove the released cells. Wash solutions were plated on selective media to quantify colony forming units (CFU/mL) in each wash solution. To verify the presence or absence of contaminating bacteria in the media prior to extraction, hydrogels were initially washed prior to light exposure. Additionally, as a negative control, areas of the hydrogel where no colonies were present were exposed to UV light under the same conditions used for cell release. This was done before and after every micro-colony extraction and washing from these blank areas were processed and plated in an identical manner as those solutions containing an extracted microcolony. In this way, carry over and cross-contamination during subsequent microcolony extraction could be identified. Using this approach, the purity of four sequentially extracted microcolonies was accessed (Figure 3.6).

Initial washings of hydrogels and negative controls generated from the opening of hydrogel in areas lacking colonies showed little or no recovery after plating (Figure 3.6). Conversely, solutions extracted from selected microcolonies showed significant growth after plating, with average measurements ranging from 90 ± 28 CFU/mL (MC1) to 260 ± 98 CFU/mL (MC4). The number of cells (CFU/mL) in the wash buffer after microcolony extraction showed no significant association with microcolony size (Figure 5.13). A small amount of carry over (< 5 CFU/mL) was noted in blank solutions after the first microcolony extraction, suggesting that cross-contamination from a previously opened microcolony is a possibility during sequential extraction; however, these levels were minimal, representing < 1% of cells recovered from a typical microcolony. These observations demonstrate that the extraction method allows for

targeted and clean recovery of bacteria colonies, enabling one to sample and isolate multiple colonies from a single screen, if desired.

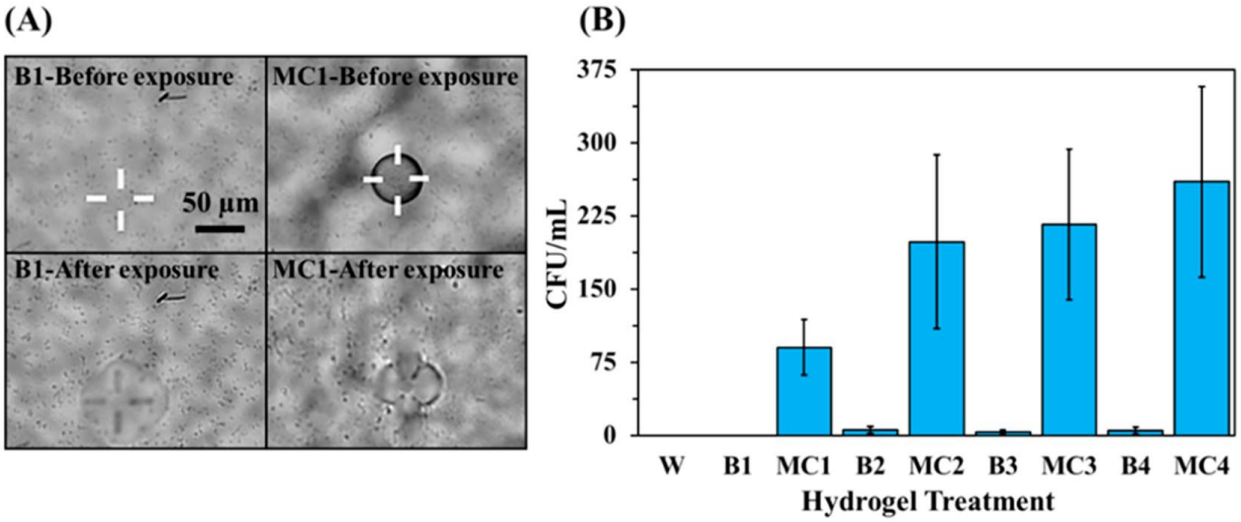

Figure 3.6. Sequential extraction of targeted microcolonies from a hydrogel. (A) Brightfield image of a hydrogel with a sample exposure map (white lines) showing exposure locations targeting a blank area or a microcolony with a broken cross pattern. (B) Colony forming units (CFU/mL) of recovered suspensions after washing the hydrogel at various steps and plating. W = initial wash of the hydrogel; B = hydrogel blank; MC = microcolony. All exposures, wash steps, and plating steps onto selective media were performed under identical conditions (*n* = 3 independent trials).

Screening and identification of rare phenotypes from transposon mutant libraries

Following hydrogel characterizations, the photodegradable hydrogels were evaluated for use in a model ML screening application. The screen involved seeding and culturing C58 ML cells in media supplemented with cell free culture fluid (CFCF) from K84, which contains agrocin 84, a well-known bacteriocin with activity against C58.[26,27] During this screen, three separate hydrogels were prepared from the same hydrogel precursor solution. This included a positive control where C58 ML cells were incubated in liquid ATGN to ensure normal cell growth across

the population (Figure 3.7). This control also allowed for verification that seeding density remained consistent with previous experiments (approximately 90 CFU/mm^2). To quantify the total number of bacteria cells that were screened in any trial, 10 separate areas on the positive control hydrogels were imaged. As a negative control, C58-GFP was also cultured in ATGN/CFCF, where no growth was expected (Figure 3.7), verifying that an inhibitory environment for normal cell growth was present. With these two controls in place, mutants within the seeded ML population that were able to grow in the presence of ATGN/CFCF were identified as candidate agrocin 84 resistant mutants (Figure 3.7).

Once each cell population was encapsulated in the respective hydrogels, they were immersed in ATGN or ATGN/CFCF media and incubated, then imaged using fluorescent microscopy. ML cells seeded in positive control hydrogels consistently grew into fluorescent microcolonies (Figure 3.7) at 28°C within 24 hrs, as expected. C58 ML cells in the positive control were quantified at a density of 90 cells/mm^2 indicating that approximately 28,000 cells were present within the hydrogel. Test hydrogels were immersed in ATGN/CFCF solution for 72 hrs, fresh media was added to this solution every 24 hr. After 72 hrs, the media was changed to ATGN only and incubated for an additional 48 hrs to enable the surviving, agrocin-resistant mutants to fully develop inside the hydrogels (Figure 3.7). Resistant mutants appeared at a density of 0.057 microcolonies/mm^2 (18±7 resistant mutants per hydrogel). The negative control hydrogel, treated the same way as the test hydrogels, rarely produced microcolonies (<0.0011 microcolonies/mm^2), verifying that parental C58-GFP cells very rarely survived when K84 CFCF is present. At the conclusion of the screen, the total number of rare micro-colonies in a representative test hydrogel was 25, representing 0.089% of the cell population. Each rare

colony was extracted from this hydrogel, plated, and recovered for genomic analysis; 23/25 microcolonies were successfully recovered.

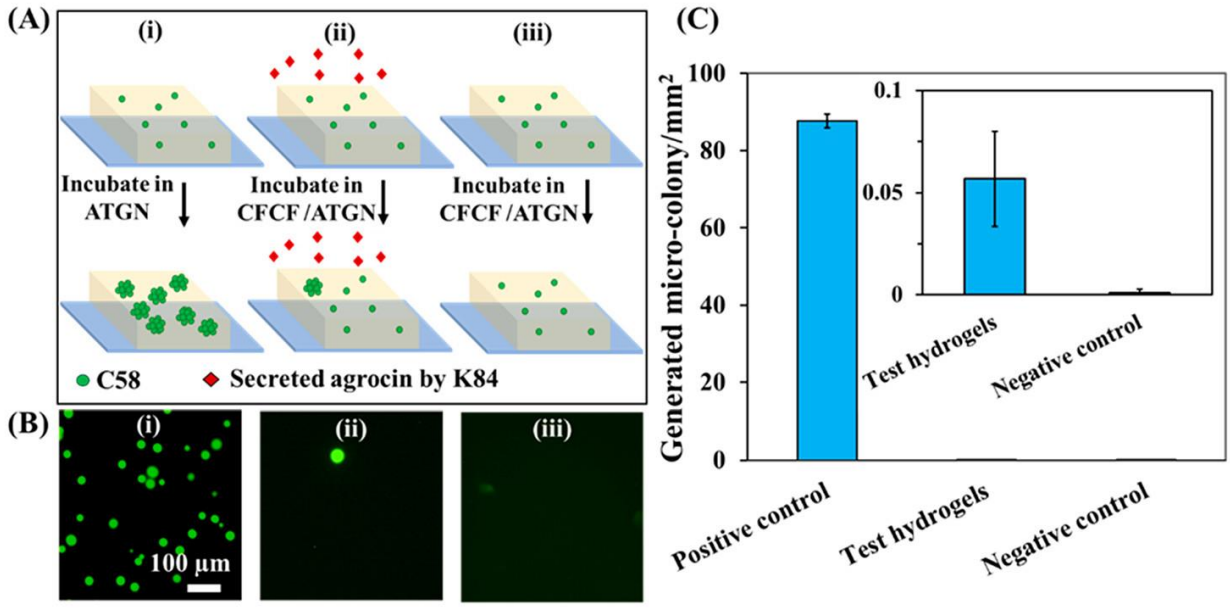

Figure 3.7. (A) Schematic of the ML screen. (i) Positive control: growth of C58 ML cells within the hydrogel; (ii) hydrogel incubation in the presence of CFCF/ATGN for growth of agrocin resistant C58 ML cells; (iii) negative control: C58-GFP incubated in CFCF/ATGN under identical conditions. (B) Representative fluorescence images of the fluorescent microcolonies in the (i) positive control, (ii) test hydrogels, and (iii) negative control. (C) Representative data for generated microcolonies in each treatment (n = 3 independent trials).

Follow-up phenotypic and genotypic analysis of rare cells

Following cell retrieval and recovery, colonies were again streaked onto media containing kanamycin and spectinomycin. To corroborate phenotypic observations in the hydrogel with standard microbiological approaches, the agrocin 84 bioassay was performed as described in the methods.[35,36] For every extracted microcolony, a random subset (n = 5) of recovered colonies that showed resistance to the antibiotics, as well as a set of controls for every isolated mutant (Figure 3.8), was tested for agrocin 84 resistance. Co-culture of C58 with K84 was

included as an agrocin 84 sensitive control for which we expected a zone of inhibition (a region near K84 with no bacterial growth due to inhibition) to form. Additionally, co-culture of *A. tumefaciens* NT1 with K84, a bacterial strain that is known to be resistant to agrocin 84 was used to compare the degree of resistance/susceptibility of the hydrogel isolates.

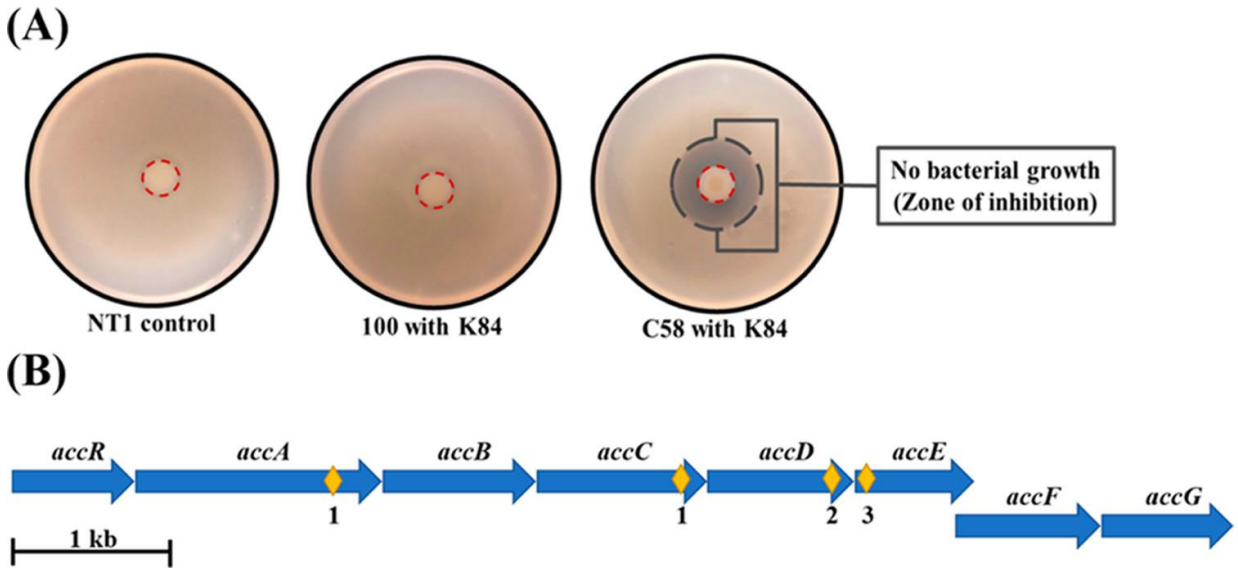

Figure 3.8. Observations of the agrocin 84 bioassay. As expected, NT1 shows no inhibition when co-cultured with K84, and was used as the positive control. The isolated C58 mutant (herein referred to as 100) also shows no inhibition when co-cultured with K84, similar to NT1, while C58 bacteria show a clearing (zone of inhibition) surrounding the K84 at the plate center. K84 bacterial growth is contained inside the red dashed line. The boundary of the zone of inhibition, if present, is denoted by the gray dash line. (B) Most agrocin 84 resistant mutants carry mutations in the *acc* operon. The location of the *acc* operon mutations found in seven of the nine isolated mutants is represented with yellow diamonds, with numbers below indicating how many times a mutation in this position was observed. All *acc* mutants were recovered from different agrocin 84 resistant microcolonies. Mutants with identical mutations were recovered from different hydrogels and so cannot be the result of cross-contamination during recovery. Each gene is shown as an arrow, and they all have been drawn to scale.

The agrocin 84 bioassay verified successful recovery of 9 resistant mutants. Four of these resistant mutants came from two recovered microcolonies and we failed to recover resistant mutants from 16 of the 23 recovered microcolonies. These observations validate the agrocin 84 resistant phenotype observed in the hydrogel screen and also demonstrate that results observed in the screen can be corroborated using follow up tests due to the ability to extract, isolate, and grow colonies of interest from the screening interface.

The final step was to connect the observed phenotype with a genotype of the extracted isolates using whole genome sequencing. Previous work identified that *acc* operon of the Ti plasmid in C58 encodes for utilization of agrocinopines A and B and for susceptibility to agrocin 84 with mutations in this region resulting in agrocin 84 resistant phenotypes.[26,47,48] This gave a clear expectation for the location of genotypic mutations that should be present in the mutants isolated from the hydrogels. Whole genome sequence analysis showed that 78% (7/9) of the isolated mutants that were sequenced from the screen had mutations in genes within the *acc* locus (Figure 3.8). About 20% of the isolated mutants (2/9) lacked a mutation in the *acc* locus, however, they had mutations in membrane transporters. It has been previously shown that inhibitors like agrocin 84 can enter bacterial cells through these transporters, however more research is required to determine the genetic basis of agrocin 84 resistance in these mutant strains. Taken together, our observations verify that successful genotype to phenotype determinations can be made from rare mutants isolated from the hydrogel screen (Figure 3.8).

Conclusion

Photodegradable hydrogels have been widely studied as matrices for biological applications due to their biocompatibility, tunable chemical and physical properties, and crosslinking abilities. These materials offer a unique set of advantages for cell screening applications: viable, high density cell encapsulation and monitoring, molecular exchange for cell growth and function, and spatiotemporal control of matrix degradation for cell release and retrieval when a patterned light source is used. While these materials have been developed extensively towards drug delivery and tissue engineering applications and have been successfully used for capture and on-demand release of rare circulating tumor cells,[49] they have largely remained separate from applications in microbiology. Here, we demonstrate the use of photodegradable hydrogels for high-throughput screening of bacteria populations. To our knowledge, this is also the first successful use of photodegradable hydrogel materials in bacterial cell screening application. The novelty of the approach lies in the combination of high-density culture, allowing for parallel, microscopic observation of tens of thousands of cellular microcolonies, followed by sequential sampling of any desired microcolony at high resolution and with high purity, enabling follow-up genetic characterization of a rare or desired phenotype.

Given the pervasive knowledge gap between bacteria phenotype and genotype, we anticipate that this simple, materials-driven approach to screening and isolation will benefit a variety of different screens. The proof-of-principle for ML screening demonstrated here with a simple growth/no growth phenotype lays the foundation for more complex phenotypic screens, such as using fluorescence or colorimetric reporters to screen for mutations disrupting gene regulation,[14] or growth-based screening of auxotrophic mutants that have loss of enzymatic

function leading to metabolic deficiencies.[50] Using traditional approaches, these screens typically require observations of tens of thousands of macroscopic colonies in hundreds of agar or agarose plates. This throughput can be matched with a single photodegradable hydrogel when combined with a high-throughput image analysis tool to rapidly identify rare cellular phenotypes.[51] The high-throughput nature of our approach, the ease of the screen, along with its repeatability and fast turnaround time also make this approach applicable to other cell separations in microbiomes, clinical samples, and mammalian cell lines.

Acknowledgements

This research was supported by the National Science Foundation (Award 1650187). N.F. would like to acknowledge the National Science Foundation Research Trainee Innovations in Food, Energy, and Water Systems (NRT-INFEWS) program (Award 1828571) and support from the Dr. Larry Erickson Fellowship Award (Kansas State University). P.A.N.- O. would like to acknowledge support from the National Science Foundation Graduate Research Fellowship (Award GGVP004842). We would like to thank Christopher Carter for help with the agrocin 84 bioassays. We also thank the Kansas IDeA Networks of Biomedical Research Excellence (KINBRE) Bioinformatics Core (P20GM103418) for help with using scripts used in the bioinformatic analyses. The computing for this project was performed on the Beocat Research Cluster at Kansas State University, which is funded in part by NSF grants CNS-1006860, EPS1006860, EPS0919443, ACI-1440548, CHE-1726332, and NIH P20GM113109.

Chapter 4 - Conclusion

This dissertation contributes to our understanding of the competitive and cooperative interactions among *Agrobacterium tumefaciens* strains and highlights the effects of these interactions on the evolution of cooperative pathogenesis. The three main focuses of this dissertation were the emergence and effects of cheaters on agrobacterial populations, the use of conjugation of the Ti plasmid as a way of enforcing cooperation, and the development of novel techniques that allow for the study of interactions between microbes.

I addressed the first question in Chapter 1 and showed that agrobacterial cheaters readily emerge *de novo* and can readily displace cooperators in environments where the costly expression of the virulence genes imposes a fitness burden on cooperators. The *de novo* emergence of mutants is constrained by the specific selective environment present and can result in the loss of the genes that allow for breakdown of opines when opines are not present. In contrast, when opines are available, and there is a benefit to keep the plasmid that encodes opine catabolic genes, cooperators often incur targeted mutations that disrupt the virulence genes, but do not affect the genes required for the breakdown of opines. These cheaters genotypes have a fitness advantage over cooperators in host gall-like environments.

In Chapter 2 I addressed a way in which cooperators antagonize cheaters in this system. Agrobacterial cooperators employ conjugation of the Ti plasmid into avirulent mutants to convert them from cheaters to cooperators. This mechanism depends on the expression of TraR, a quorum sensing transcriptional regulator, and on the initial absence of cheaters. When cheaters are initially present, pathogenic agrobacteria cannot use conjugation to antagonize them. However, if they emerge as a result of mutations, conjugation has a significant effect on

the enforcement of cooperation. Antagonism of cheaters via conjugation not only stabilizes cooperation, but it introduces the virulence genes back into avirulent mutants, converting them into pathogenic agrobacteria. I examined the effects of conjugation on two agrobacterial backgrounds; both of which carried a Ti plasmid. It would be interesting to examine the effects of Ti plasmid conjugation into non-agrobacterial backgrounds commonly found in gall environments.

Motivated by the importance of microbial interactions and the limitations of current techniques for the study of said exchanges, the last main objective of this dissertation was to develop new tools for the study of microbial interactions. In Chapter 3, I described a new method that allows for the high-throughput screening of mutant libraries. Using photodegradable hydrogels, I was able to screen the entire genome of *A. tumefaciens* in a single experimental trial. As a proof-of-principle, I studied a well-known interaction between an agrobacterial cheater and an agrobacterial cooperator. I screened a transposon mutant library of *A. tumefaciens*, to see if I could find rare mutants resistant to a bacteriocin produced by a bacterial cheater. Using this method, I was able to screen over 2.8×10^4 mutant cells per hydrogel. Moreover, I isolated rare resistant agrobacterial cells and was able to later characterize the mutations that allowed for their resistance to the bacteriocin. This photodegradable hydrogel offers a high throughput, yet easily accessible screening technique that can be used for the study of many microbial interactions.

This dissertation provides novel biological insights on *Agrobacterium tumefaciens'* population ecology and advances our knowledge in the effects of the interactions between agrobacterial cheaters and cooperators. I highlight the selective pressures that drive the evolution of *A.*

tumefaciens cooperative pathogenesis and identify the types of mutations that drive the emergence of cheaters and saprophytes from cooperative backgrounds. I provided the first evidence that conjugation antagonizes cheater invasion. I also show that conjugation can not only introduce cooperative genes into mutant backgrounds, but it can stabilize pathogenesis in this system. Finally, I collaborated in the development of photodegradable hydrogels, a new technique for high throughput screening of bacterial populations. This technique allows for the simultaneous screening of almost 30,000 cells along with the isolation and characterization of cells with rare phenotypes.

Chapter 5 - Supplemental Data

Chapter 1 Data

Table 5.1. Bacterial strains used in this chapter

Strain	Genotype/Marker	Description	Reference
Escherichia coli			
DH5α/λ*pir*	λpir	Cloning strain	Chiang & Rubin (2002)
S17/λ*pir*	Λpir, Tra^{+}	Cloning host	Kalogeraki & Winans (1997)
S17/λ*pir*	pSW209	P*virB*::*lacZ* reporter	S.C. Winans, Cornell University
Agrobacterium tumefaciens			
15955 (wildtype)	pTi15955	Octopine-type strain	Baek et al. (2003)
TGP101	pTi15955-	15955 derivative	Platt et al. (2012)
TGP103	pTi15955Δ*virA*	15955 derivative	This study
ERM115	pTi15955	$Strep^{R}$, $Spec^{R}$	This study
ERM116	pTi15955-	$Strep^{R}$, $Spec^{R}$	This study
ERM117	pTi15955Δ*virA*	$Strep^{R}$, $Spec^{R}$	This study

Table 5.2. Plasmids used in this study

Plasmid	Features	Reference
pTP103	P15955Δ*virA*	This study
pEM159	pNPTS138::15955 CC with an pHP45 aada omega cassette	This study

Table 5.3. Oligonucleotides used in this study

Primer	Sequence	Reference
15955 pTi virA 5	TACACCGACATGCGCAAA	This study
15955 pTi virA 6	GATATTTTGCCATCCAGCGTC	This study
15955 aadaΩ P1 – NheI	GCTAGCCCACAGCTTGATGCCGAGATAG	This study
15955 aadaΩ P2 – BamHI	CACCACCGTCATGCCGGGG ATCCACTCGACCCGTCGTC	This study
15955 aadaΩ P3 – BamHI	GACGACGGGTCGAGTGGAT CCCCGGCATGACGGTGGTG	This study
15955 aadaΩ P4 – SpeI	ACTAGTGCATGGTCATCGGCGGTTCA	This study

Table 5.4. Genetic changes of evolved strains

Evolution Environment	Genetic changes as a result of evolution		
	Lacks most pTi & pAT	**Loss of *virA* only**	**Small or no changes**
Evolved in E12 P*virB*-	16/16 isolates Total deletions: 458 kb		
Evolved in E14 P*virB*-	3/16 isolates Total deletions: 458 kb	13/16 isolates Total deletions: 3.6 kb	
Evolved in E12 P*virB+*	2/8 isolates Total deletions: 456 kb		6/8 isolates Total deletions: 1 kb
Evolved in E14 P*virB+*			8/8 isolates Total deletions: 0 kb

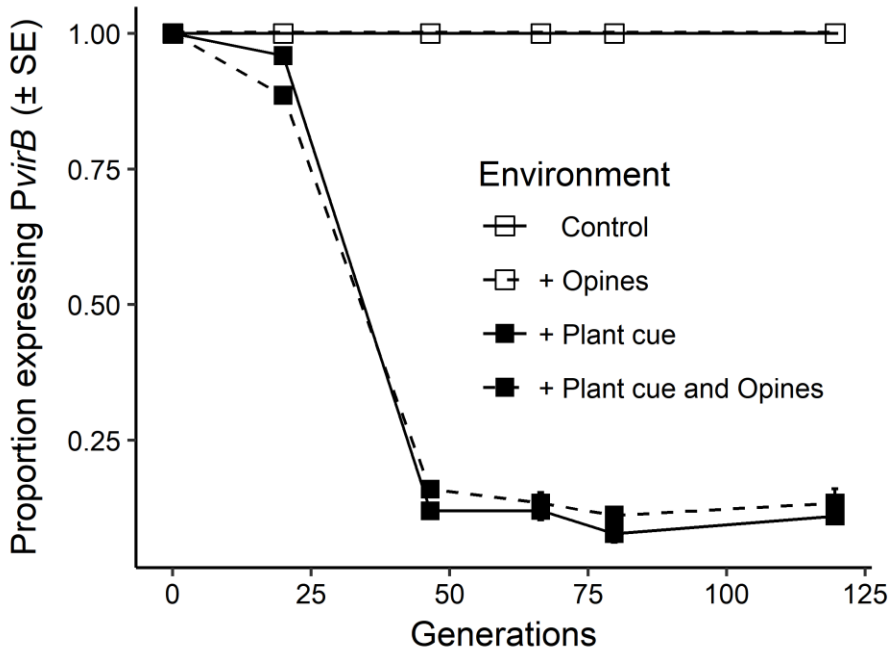

Figure 5.1. Cooperators evolving in the presence of a plant cue lose ability to induce P*virB.*

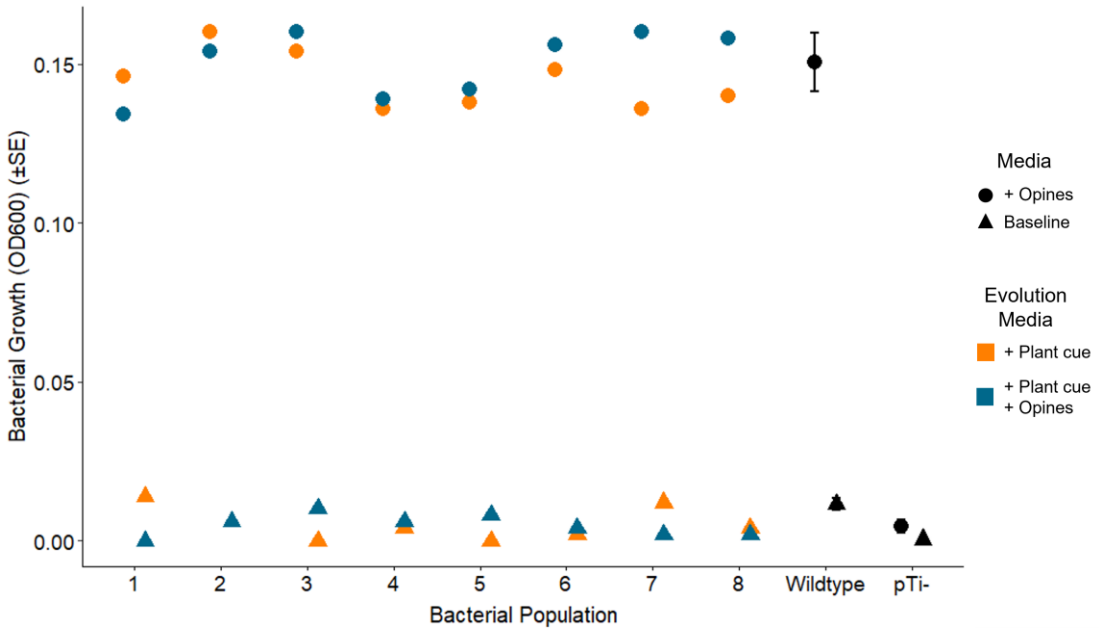

Figure 5.2. Opine catabolic capabilities of 8 independent P*vir*B+ isolates evolved in the presence of 200 µM acetosyringone (+ Plant Cue) and 8 independent isolates evolved in the presence of plant cues acetosyringone and opines 50 mM octopine (+ Plant Cue + Opines).

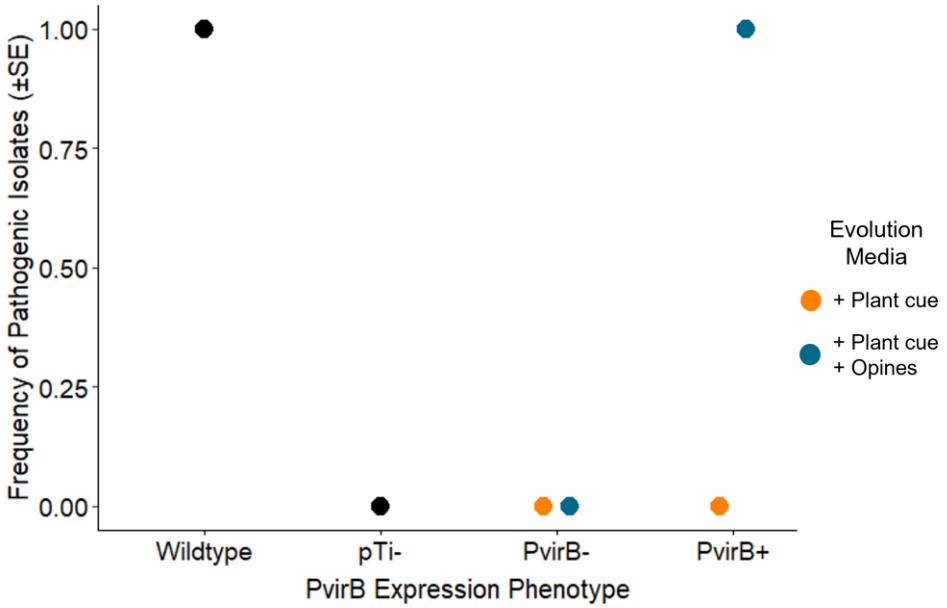

Figure 5.3. Tumorigenesis assay in potato tissue. Wildtype agrobacteria induces tumor production all the time, while a pTi- background does not, because it does not carry the virulence genes. P*vir*B- isolates do not induce tumor production irrespective of the media they were evolved in. When evolved in media supplemented with acetosyringone, P*vir*B+ isolates will not induce tumor production. However, when evolved in media supplemented with acetosyringone and opines, all P*vir*B isolates cause tumor formation.

Chapter 2 Data

Table 5.5. Bacterial strains used in this study

Strain	Genotype/Marker	Description	Reference
Escherichia coli			
DH5α/λ*pir*	λpir	Cloning strain	Chiang & Rubin (2002)
S17/λ*pir*	λpir, Tra$^+$	Cloning host	Kalogeraki & Winans (1997)
S17/λ*pir*	pSW209	P*virB*::*lacZ* reporter	S.C. Winans, Cornell University
S17/λ*pir*	pPG4	pTi15955ΔtraR	This study
S17/λ*pir*	pSRK-Km	Plac-traR pTi	This study
S17/λ*pir*	pSRK-Km	Plac-traR pAT	This study
Agrobacterium tumefaciens			
15955 (wildtype)	pTi15955	Octopine-type strain	Baek et al. (2003)
TGP101	pTi15955-	15955 derivative	Platt et al. (2012)
TGP103	pTi15955Δ*virA*	15955 derivative	This study
PAG1	pTi15955ΔtraR	15955 derivative	Barton et al. (2021)
PAG10	pTi15955-	15955 derivative	This study
PAG12	pTi15955ΔtraR	15955 derivative	This study
IAM1	pAT15955ΔtraR	15955 derivative	Barton et al. (2021)
C58	pTiC58	Nopaline-type strain	Watson et al. (1975)

Table 5.6. Plasmids used in this study

Plasmid	Features	Reference
pIB308	pSRK-Km Plac-traR AT	Barton et al. (2021)
pIB309	pSRK-Km Plac-traR Ti	Barton et al. (2021)
pPG4	pTi15955ΔtraR	This study
pIM4	pAT15955ΔtraR	This study

Table 5.7. Oligonucleotides used in this study

Primer	Sequence	Refence
IBP160	GGACATATGCAACATTGGCT	Barton et al. (2021)
IBP161	AGGACTAGTTCAGATCAGCCCGG	Barton et al. (2021)
IBP162	GGACATATGCAGCACTGGCT	Barton et al. (2021)
IBP163	AGGACTAGTTCAGATGAGTTTCC	Barton et al. (2021)
pTi15955 traR (P1)	GCATGCGCGCTCAATCCCAGACAGAA	This study
pTi15955 traR (P4)	ACTAGTCCTGAACACCTTGATCAGCAT	This study
pAT15955 traR (P1)	GCTAGCACAAAATTTACTGCCACGCGT	This study
pAT15955 traR (P4)	AAGCTTCCCGAGGGTGTGGAAACC	This study

Table 5.8. Genetic consequences of the Ti plasmid conjugation

	C58 AT	C58 Ti	15955 Ti
E11 Observed Mutations	2/12 had major mutations in 85 kb (throughout the genome). 10/12 isolates had no major mutations.	2/12 showed major mutations in TraG, virB4, virB9 10/12 isolates had no major mutations.	2/12 isolates have the plasmid. 10/12 isolates are lacking the plasmid.
E12 Observed Mutations	12/12 isolates had no major mutations.	12/12 isolates had no major mutations.	12/12 isolates are lacking the plasmid
E13 Observed Mutations	2/12 isolates had large-scale deletions. (377kb) 5/12 isolates had mutations throughout the plasmid, but no deletions. 5/12 isolates with no 15955 pTi have no major mutations.	2/12 isolates loss the C58 Ti plasmid. The 5/12 isolates with the 15955 pTi had major mutations in traA, traG and the vir region. 5/12 isolates with no 15955 pTi have no major mutations.	7/12 isolates have the plasmid, but had major mutations in the vir region, trbE, traA, and the toxin antidote system 5/12 isolates are lacking the plasmid.
E14 Observed Mutations	2/12 isolates had mutations throughout the plasmid, but no deletions. 10/12 isolates with no 15955 pTi have no major mutations.	The 2/12 isolates with the 15955 pTi had major mutations in traA, traG and the vir region. 10/12 isolates with no 15955 pTi have no major mutations.	2/12 isolates have the plasmid, but had major mutations in the vir region, trbE, and traA. 10/12 isolates are lacking the plasmid.

Chapter 3 Data

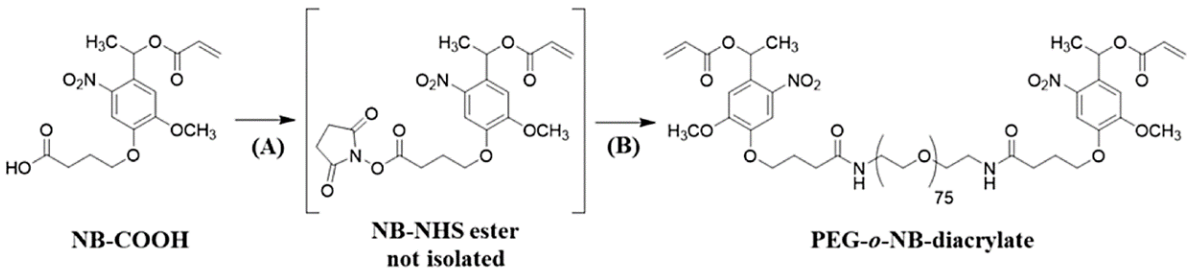

Figure 5.4. Synthesis of PEG-*o*-NB-diacrylate. (A) NHS and DCC, CH2Cl2/DMF, 0°C to room temperature, 21 hr. (B) PEG-diamine and Et3N, CH2Cl2/DMF, 20 h.

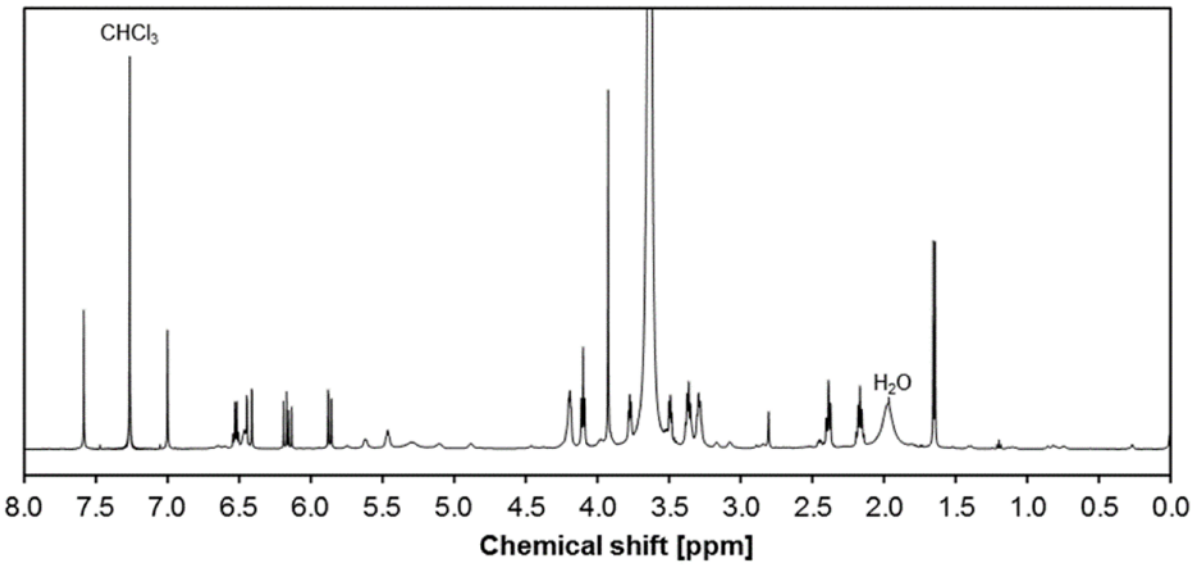

Figure 5.5. 1H NMR spectrum of PEG-*o*-NB-diacrylate in CDCl3.

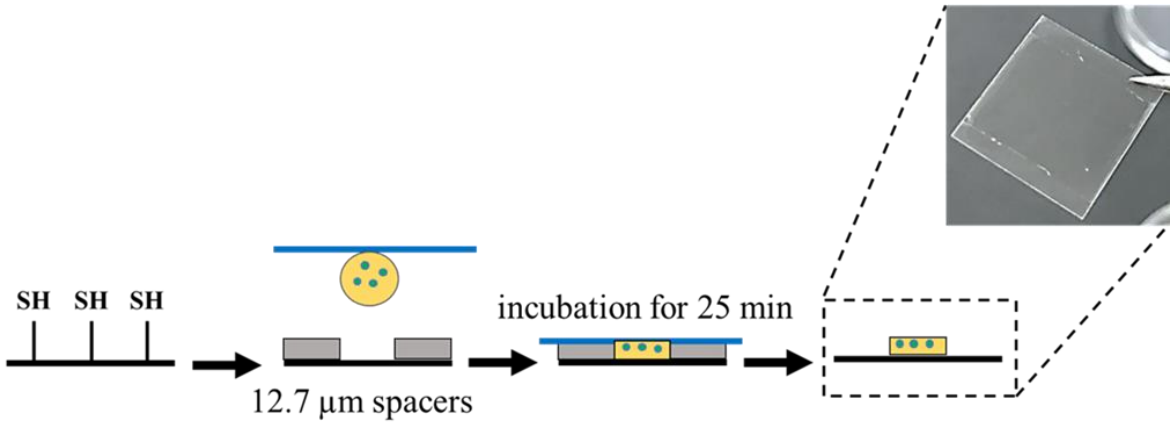

Figure 5.6. Hydrogel preparation. Hydrogel precursor solution with seeded bacteria is placed on a glass slide which is then placed on a thiol functionalized coverslip with desired spacers for hydrogel formation and cell encapsulation.

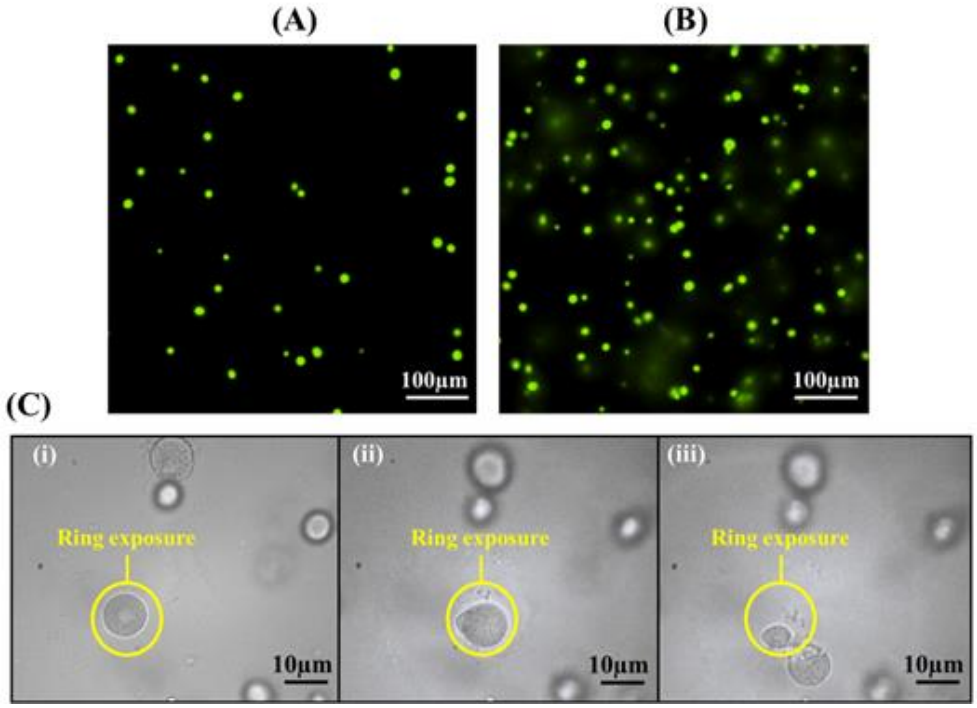

Figure 5.7. Optimization of hydrogel thickness. (A) Using 12.7 µm thick spacers results in formation of colonies in one focal plane. (B) Spacers with thickness greater than 12.7 µm show overlay of colonies within the three-dimensional hydrogel. (C) Overlay of colonies can result in cross-contamination during cell release: (i) Ring pattern exposed on a desired cell colony, (ii) during light exposure a second colony is observed underneath the target colony, and (iii) cells from the non-target colony are also released causing cross contamination when colonies are overlayed.

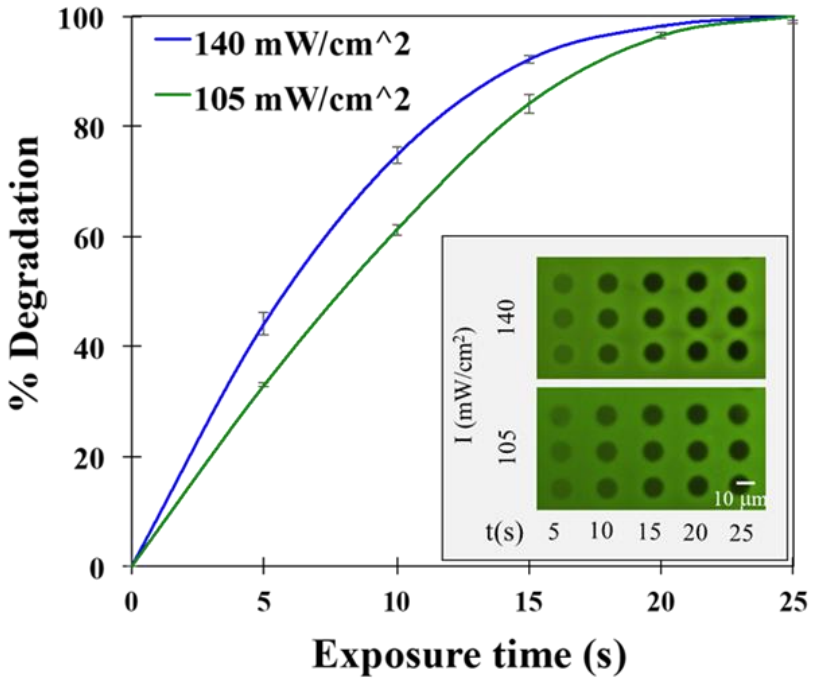

Figure 5.8. Spatial temporal control of hydrogel degradation. The Polygon400 light patterning tool allows for adjustment of UV light intensity and exposure time across a user-defined pattern enabling control of hydrogel degradation. Inset: representative fluorescent images of patterns degraded with two different light intensity and various exposure times. Hydrogels were stained with fluorescein-5-malemide after UV irradiation for visualization.

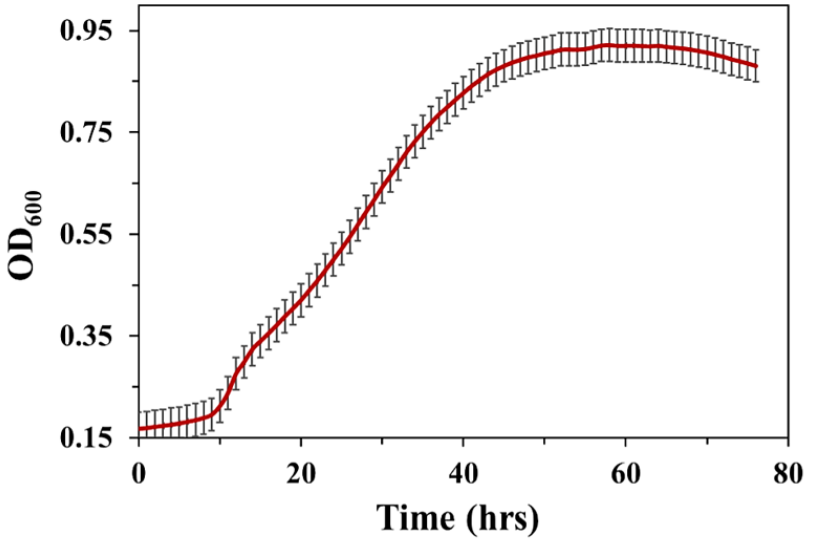

Figure 5.9. Growth curve of C58 ML during culture in ATGN media at 28°C and 282 rpm in 96 well plate format (n = 19).

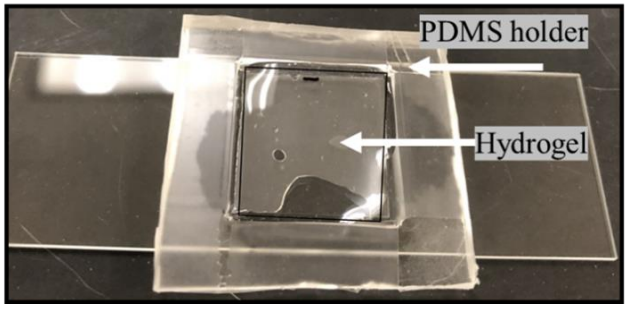

Figure 5.10. Setup used for UV light exposure and cell retrieval. During light exposure for cell release, the hydrogel is placed in a PDMS holder and covered with media to prevent dehydration.

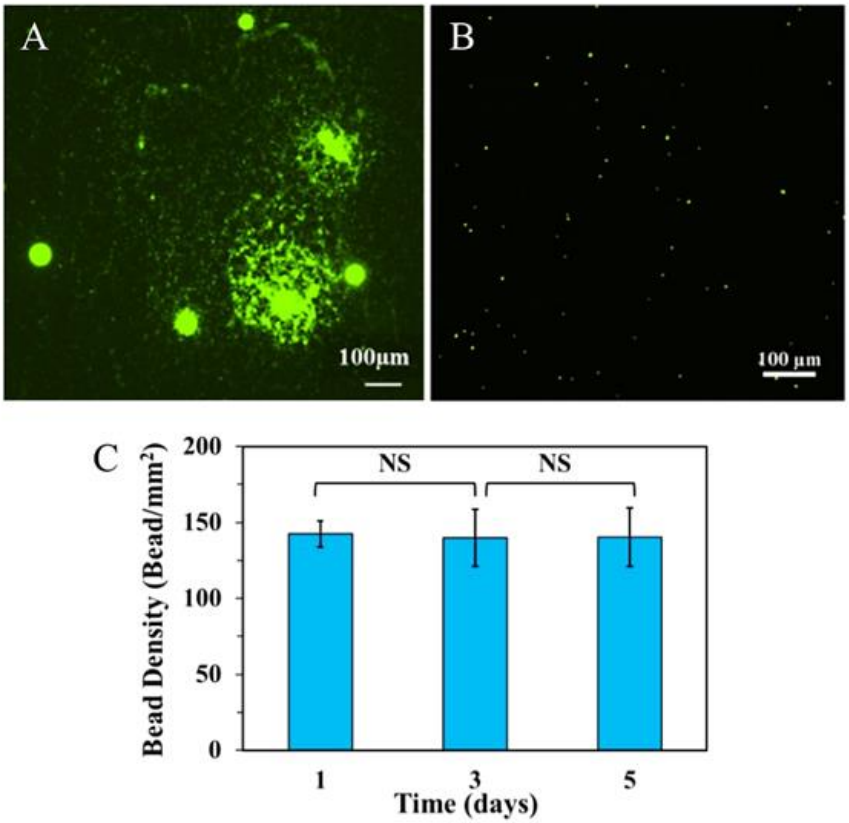

Figure 5.11. Hydrogel degradation after 5 days. (A) Bacteria cells encapsulated within the hydrogel are able to degrade the hydrogel and are released after 5 days incubation in ATGN media (pH 7). (B) 1-um fluorescent beads encapsulated in non-photodegradable hydrogels were used to test hydrogel stability at neutral pH. (C) Bead density in hydrogels after incubation in 1X PBS (pH 7) at different time points. No change in bead density was observed, suggesting that hydrogel degredation in (A) was due to bacteria.

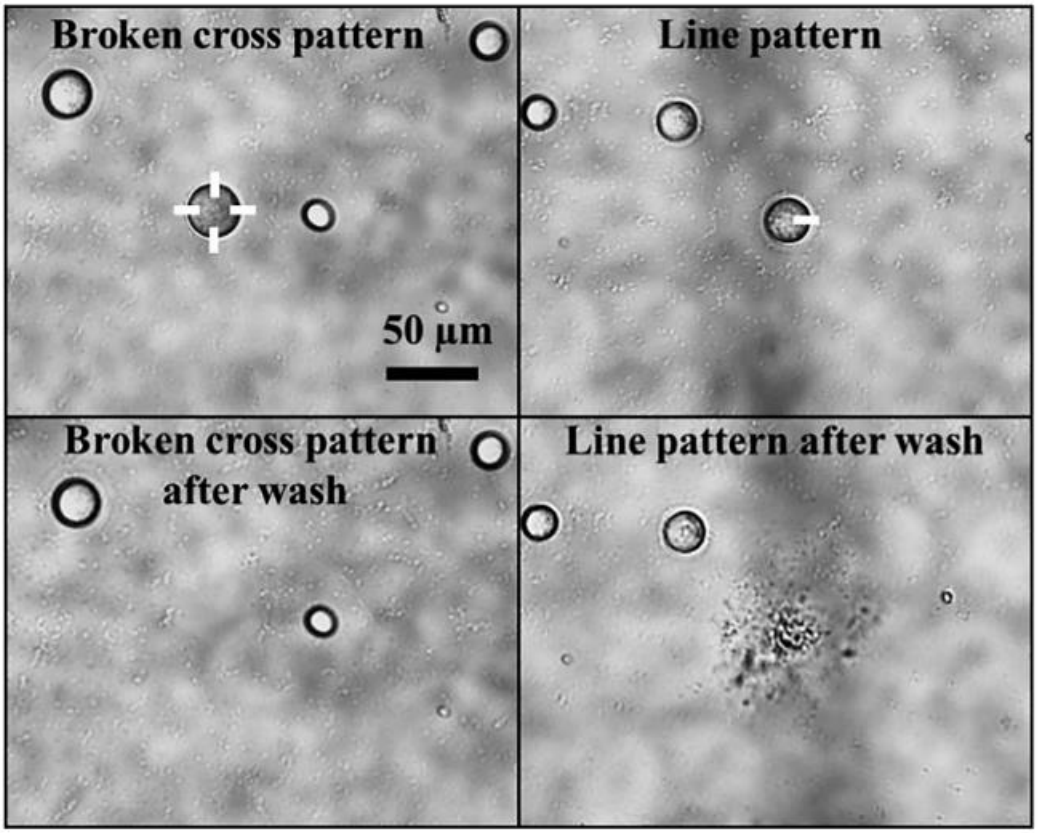

Figure 5.12. The efficiency of a line pattern exposure for cell release compared to a broken cross exposure pattern. Use of a broken cross pattern results in complete release of the microcolony, whereas use of a line exposure pattern results in only partial release of the microcolony.

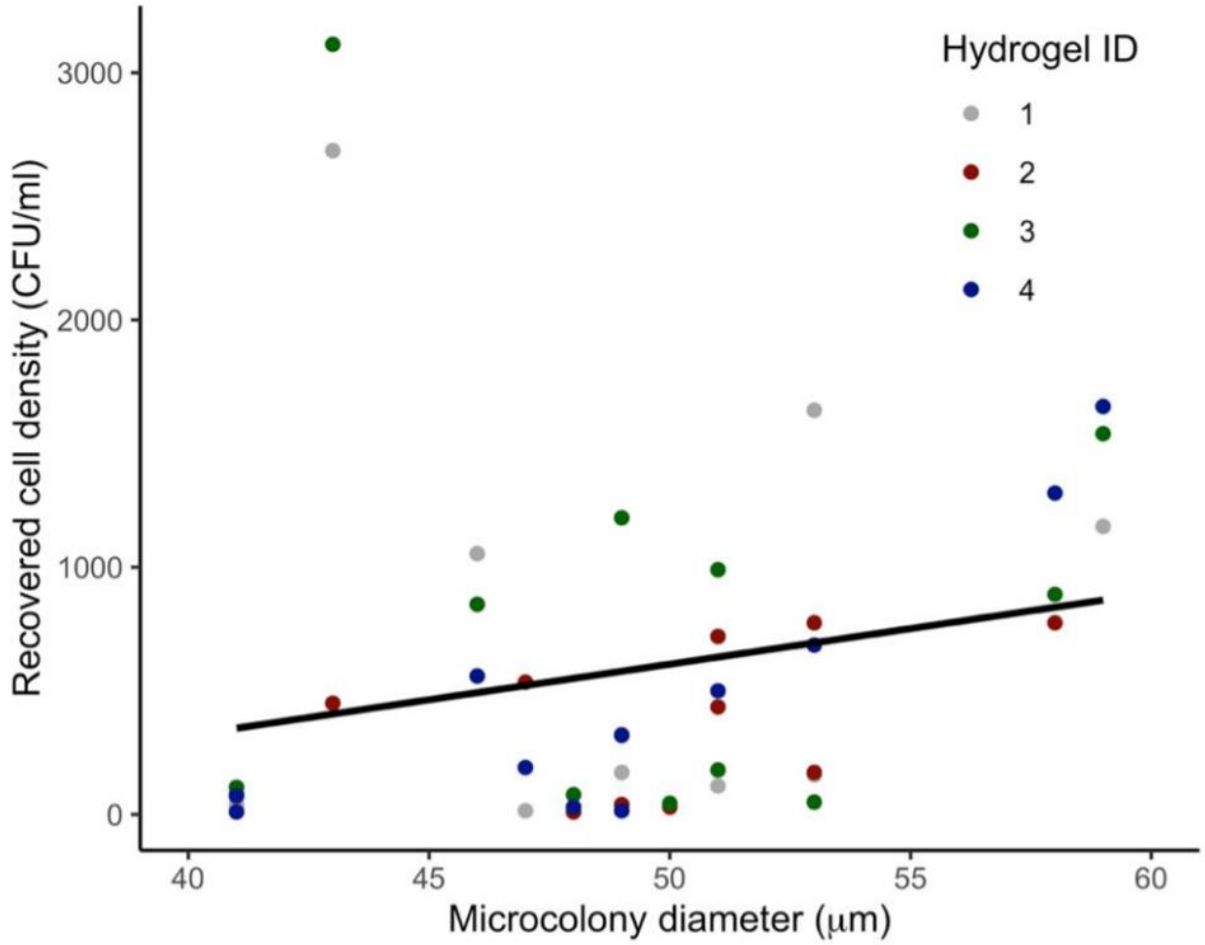

Figure 5.13. The density of recovered cells was not significantly associated with microcolony diameter ($F_{1,42} = 2.03$, $p = 0.16$, adjusted $r^2 = 0.16$; $\beta = 28.78$, $t = 1.42$, $p = 0.16$).

Table 5.9. Strains and plasmids used in this study

Strain/Plasmid	Relevant Features	Reference
Escherichia coli		
S17-1/λ pFD1	Carries pFP1 (used as *Himar1* conjugal donor)	Lampe et al. (1999)
Agrobacterium tumefaciens		
C58	Carries pTiC58 and pAtC58; Agrocin 84 sensitive	Watson et al. (1975)
C58-GFP	Carries pTiC58, pAtC58, and pJZ383; Agrocin 84 sensitive	Danhorn et al. (2004)
NT1	pTiC58- cured derivative of C58; Agrocin 84 resistant	Watson et al. (1975)
Rhizobium rhizogenes		
K84	Carries pAtK84b and pAgK84; Produces agrocin 84	Kerr et al. (1974)
Plasmids		
pFD1	*Himar1* transposon vector	Lampe et al. (1999)
pJZ383	P*tac*::*gfp*mut3	Cormack et al. (1996)

Supplemental Data References

Baek, C. H., Farrand, S. K., Lee, K. E., Park, D. K., Lee, J. K., & Kim, K. S. (2003). Convergent evolution of Amadori opine catabolic systems in plasmids of *Agrobacterium tumefaciens*. *Journal of bacteriology*, *185*(2), 513–524.

Barton, I. S., Eagan, J. L., Nieves-Otero, P. A., Reynolds, I. P., Platt, T. G., & Fuqua, C. (2021). Co-dependent and Interdigitated: dual quorum sensing systems regulate conjugative transfer of the Ti plasmid and the At megaplasmid in *Agrobacterium tumefaciens* 15955. *Frontiers in microbiology*, 3564.

Chiang, S. L., & Rubin, E. J. (2002). Construction of a mariner-based transposon for epitope-tagging and genomic targeting. *Gene*, 296(1-2), 179–185.

Cormack, B. P.; Valdivia, R. H.; Falkow, S. FACS-Optimized Mutants of the Green Fluorescent Protein (GFP). *Gene*. 1996, 173 (1), 33–38.

Danhorn, T.; Hentzer, M.; Givskov, M.; Parsek, M. R.; Fuqua, C. PhosphorusLimitation Enhances Biofilm Formation of the Plant Pathogen *Agrobacterium tumefaciens* through the PhoR-PhoB Regulatory System. *J. Bacteriol.* 2004, *186* (14), 4492–4501.

Kalogeraki, V. S., & Winans, S. C. (1997). Suicide plasmids containing promoterless reporter genes can simultaneously disrupt and create fusions to target genes of diverse bacteria. *Gene*, 188(1), 69-75.

Kerr, A.; Htay, K. Biological Control of Crown Gall through Bacteriocin Production. *Physiol. Plant Pathol.* 1974, *4* (1), 37–44.

Lampe, D. J.; Akerley, B. J.; Rubin, E. J.; Mekalanos, J. J.; Robertson, H. M. Hyperactive Transposase Mutants of the *Himar1* Mariner Transposon. *Proc. Natl. Acad. Sci. U. S. A.* 1999, *96* (20), 11428–11433.

Platt, T. G., Bever, J. D., & Fuqua, C. (2012). A cooperative virulence plasmid imposes a high fitness cost under conditions that induce pathogenesis. *Proceedings of the Royal Society B: Biological Sciences*, 279(1734), 1691-1699.

Watson, B.; Currier, T. C.; Gordon, M. P.; Chilton, M. D.; Nester, E. W. Plasmid Required for Virulence of *Agrobacterium tumefaciens*. *J. Bacteriol.* 1975, *123* (1), 255–264.

References

Preface References

Abisado, R. G., Benomar, S., Klaus, J. R., Dandekar, A. A., & Chandler, J. R. (2018). Bacterial quorum sensing and microbial community interactions. *MBio*, *9*(3), e02331-17.

Buckling, A., Harrison, F., Vos, M., Brockhurst, M. A., Gardner, A., West, S. A., & Griffin, A. (2007). Siderophore-mediated cooperation and virulence in Pseudomonas aeruginosa. *FEMS Microbiology Ecology*, *62*(2), 135–141.

Coyte, K. Z., Schluter, J., & Foster, K. R. (2015). The ecology of the microbiome: Networks, competition, and stability. *Science*, *350*(6261), 663–666.

Faust, K., & Raes, J. (2012). Microbial interactions: From networks to models. *Nature Reviews Microbiology*, *10*(8), 538–550.

Gelvin, S. B. (2003). Agrobacterium-mediated plant transformation: The biology behind the "gene-jockeying" tool. *Microbiology and Molecular Biology Reviews*, *67*(1), 16–37.

Gelvin, S. B. (2006). Agrobacterium virulence gene induction. *Agrobacterium Protocols*, 77–85.

Kobayashi, K. (2021). Diverse LXG toxin and antitoxin systems specifically mediate intraspecies competition in Bacillus subtilis biofilms. *PLoS Genetics*, *17*(7), e1009682.

Moré, M. I., Finger, L. D., Stryker, J. L., Fuqua, C., Eberhard, A., & Winans, S. C. (1996). Enzymatic synthesis of a quorum-sensing autoinducer through use of defined substrates. *Science*, *272*(5268), 1655–1658.

Tshikantwa, T. S., Ullah, M. W., He, F., & Yang, G. (2018). Current trends and potential applications of microbial interactions for human welfare. *Frontiers in Microbiology*, *9*, 1156.

Venturi, V., & Bez, C. (2021). A call to arms for cell–cell interactions between bacteria in the plant microbiome. *Trends in Plant Science*, *26*(11), 1126–1132.

Zhang, H.-B., Wang, L.-H., & Zhang, L.-H. (2002). Genetic control of quorum-sensing signal turnover in Agrobacterium tumefaciens. *Proceedings of the National Academy of Sciences*, *99*(7), 4638–4643.

Chapter 1 References

Andrews, S. (2010). *FastQC: a quality control tool for high throughput sequence data*.

Barton, I. S., Fuqua, C., & Platt, T. G. (2018). Ecological and evolutionary dynamics of a model facultative pathogen: Agrobacterium and crown gall disease of plants. *Environmental Microbiology*, *20*(1), 16–29.

Bauer, M. A., Kainz, K., Carmona-Gutierrez, D., & Madeo, F. (2018). Microbial wars: Competition in ecological niches and within the microbiome. *Microbial Cell*, *5*(5), 215.

Bolger, A. M., Lohse, M., & Usadel, B. (2014). Trimmomatic: A flexible trimmer for Illumina sequence data. *Bioinformatics*, *30*(15), 2114–2120.

Bolton, G. W., Nester, E. W., & Gordon, M. P. (1986). Plant phenolic compounds induce expression of the Agrobacterium tumefaciens loci needed for virulence. *Science*, *232*(4753), 983–985.

Breen, J., Mur, L. A. J., Sivakumaran, A., Akinyemi, A., Wilkinson, M. J., & Lopez, C. M. R. (2016). Botrytis cinerea loss and restoration of virulence during in vitro culture follows flux in global DNA methylation. *Biorxiv*, 059477.

Christie, P. J. (1997). Agrobacterium tumefaciens T-complex transport apparatus: A paradigm for a new family of multifunctional transporters in eubacteria. *Journal of Bacteriology*, *179*(10), 3085–3094.

Cordero, O. X., Ventouras, L.-A., DeLong, E. F., & Polz, M. F. (2012). Public good dynamics drive evolution of iron acquisition strategies in natural bacterioplankton populations. *Proceedings of the National Academy of Sciences*, *109*(49), 20059–20064.

Coyte, K. Z., & Rakoff-Nahoum, S. (2019). Understanding competition and cooperation within the mammalian gut microbiome. *Current Biology*, *29*(11), R538–R544.

Coyte, K. Z., Schluter, J., & Foster, K. R. (2015). The ecology of the microbiome: Networks, competition, and stability. *Science*, *350*(6261), 663–666.

Damore, J. A., & Gore, J. (2012). Understanding microbial cooperation. *Journal of Theoretical Biology*, *299*, 31–41.

Darling, A. C., Mau, B., Blattner, F. R., & Perna, N. T. (2004). Mauve: Multiple alignment of conserved genomic sequence with rearrangements. *Genome Research*, *14*(7), 1394–1403.

De Coster, W., D'Hert, S., Schultz, D. T., Cruts, M., & Van Broeckhoven, C. (2018). NanoPack: Visualizing and processing long-read sequencing data. *Bioinformatics*, *34*(15), 2666–2669.

Escobar, M. A., & Dandekar, A. M. (2003). Agrobacterium tumefaciens as an agent of disease. *Trends in Plant Science*, *8*(8), 380–386.

Fortin, C., Nester, E., & Dion, P. (1992). Growth inhibition and loss of virulence in cultures of Agrobacterium tumefaciens treated with acetosyringone. *Journal of Bacteriology*, *174*(17), 5676–5685.

Gelvin, S. B. (2000). Agrobacterium and plant genes involved in T-DNA transfer and integration. *Annual Review of Plant Biology*, *51*(1), 223–256.

Gelvin, S. B. (2003). Agrobacterium-mediated plant transformation: The biology behind the "gene-jockeying" tool. *Microbiology and Molecular Biology Reviews*, *67*(1), 16–37.

Gelvin, S. B. (2006). Agrobacterium virulence gene induction. *Agrobacterium Protocols*, 77–85.

Gordon, J. E., & Christie, P. J. (2014). The agrobacterium Ti plasmids. *Microbiology Spectrum*, *2*(6), 2–6.

Guyon, P., Petit, A., Tempe, J., & Dessaux, Y. (1993). Transformed plants producing opines specifically promote growth of opine-degrading agrobacteria. *MOLECULAR PLANT MICROBE INTERACTIONS*, *6*, 92–92.

Harrington, K. I., & Sanchez, A. (2014). Eco-evolutionary dynamics of complex social strategies in microbial communities. *Communicative & Integrative Biology*, *7*(1), e28230.

Jin, S., Prusti, R. K., Roitsch, T., Ankenbauer, R. G., & Nester, E. W. (1990). Phosphorylation of the VirG protein of Agrobacterium tumefaciens by the autophosphorylated VirA protein: Essential role in biological activity of VirG. *Journal of Bacteriology*, *172*(9), 4945–4950.

Jin, S., Roitsch, T., Ankenbauer, R., Gordon, M., & Nester, E. (1990). The VirA protein of Agrobacterium tumefaciens is autophosphorylated and is essential for vir gene regulation. *Journal of Bacteriology*, *172*(2), 525–530.

Kruskal, W. H., & Wallis, W. A. (1952). Use of ranks in one-criterion variance analysis. *Journal of the American Statistical Association*, *47*(260), 583–621.

Li, H., & Durbin, R. (2009). Fast and accurate short read alignment with Burrows–Wheeler transform. *Bioinformatics*, *25*(14), 1754–1760.

Li, Y.-H., & Tian, X. (2012). Quorum sensing and bacterial social interactions in biofilms. *Sensors*, *12*(3), 2519–2538.

Mann, H. B., & Whitney, D. R. (1947). On a test of whether one of two random variables is stochastically larger than the other. *The Annals of Mathematical Statistics*, 50–60.

McKenna, A., Hanna, M., Banks, E., Sivachenko, A., Cibulskis, K., Kernytsky, A., Garimella, K., Altshuler, D., Gabriel, S., & Daly, M. (2010). The Genome Analysis Toolkit: A MapReduce

framework for analyzing next-generation DNA sequencing data. *Genome Research*, *20*(9), 1297–1303.

McNally, L., & Brown, S. P. (2015). Building the microbiome in health and disease: Niche construction and social conflict in bacteria. *Philosophical Transactions of the Royal Society B: Biological Sciences*, *370*(1675), 20140298.

Merlo, D. J., & Nester, E. W. (1977). Plasmids in avirulent strains of Agrobacterium. *Journal of Bacteriology*, *129*(1), 76–80.

Morton, E. R., & Fuqua, C. (2012a). Genetic manipulation of Agrobacterium. *Current Protocols in Microbiology*, *25*(1), 3D – 2.

Morton, E. R., & Fuqua, C. (2012b). Laboratory maintenance of Agrobacterium. *Current Protocols in Microbiology*, *24*(1), 3D – 1.

Morton, E. R., Platt, T. G., Fuqua, C., & Bever, J. D. (2014). Non-additive costs and interactions alter the competitive dynamics of co-occurring ecologically distinct plasmids. *Proceedings of the Royal Society B: Biological Sciences*, *281*(1779), 20132173.

Nester, E. W. (2015). Agrobacterium: Nature's genetic engineer. *Frontiers in Plant Science*, *5*, 730.

Oliveira, N. M., Niehus, R., & Foster, K. R. (2014). Evolutionary limits to cooperation in microbial communities. *Proceedings of the National Academy of Sciences*, *111*(50), 17941–17946.

Ostrom, E. (2008). Tragedy of the commons. *The New Palgrave Dictionary of Economics*, *2*.

Platt, T. G., & Bever, J. D. (2009). Kin competition and the evolution of cooperation. *Trends in Ecology & Evolution*, *24*(7), 370–377.

Platt, T. G., Bever, J. D., & Fuqua, C. (2012). A cooperative virulence plasmid imposes a high fitness cost under conditions that induce pathogenesis. *Proceedings of the Royal Society B: Biological Sciences*, *279*(1734), 1691–1699.

Platt, T. G., Fuqua, C., & Bever, J. D. (2012). Resource and competitive dynamics shape the benefits of public goods cooperation in a plant pathogen. *Evolution: International Journal of Organic Evolution*, *66*(6), 1953–1965.

Platt, T. G., Morton, E. R., Barton, I. S., Bever, J. D., & Fuqua, C. (2014). Ecological dynamics and complex interactions of Agrobacterium megaplasmids. *Frontiers in Plant Science*, *5*, 635.

Rainey, P. B., & Rainey, K. (2003). Evolution of cooperation and conflict in experimental bacterial populations. *Nature*, *425*(6953), 72–74.

Rankin, D. J., Bargum, K., & Kokko, H. (2007). The tragedy of the commons in evolutionary biology. *Trends in Ecology & Evolution*, *22*(12), 643–651.

Savka, M. A., & Farrand, S. K. (1997). Modification of rhizobacterial populations by engineering bacterium utilization of a novel plant-produced resource. *Nature Biotechnology*, *15*(4), 363–368.

Schuch, R., & Maurelli, A. T. (1997). Virulence plasmid instability in Shigella flexneri 2a is induced by virulence gene expression. *Infection and Immunity*, *65*(9), 3686–3692.

Seemann, T. (2014). Prokka: Rapid prokaryotic genome annotation. *Bioinformatics*, *30*(14), 2068–2069.

Shams, M., Campillo, T., Lavire, C., Muller, D., Nesme, X., & Vial, L. (2012). Rapid and efficient methods to isolate, type strains and determine species of Agrobacterium spp. In pure culture and complex environments. *Biochemical Testing*, *4*, 3–20.

Smith, P., & Schuster, M. (2019). Public goods and cheating in microbes. *Current Biology*, *29*(11), R442–R447.

Wang, Y., Mukhopadhyay, A., Howitz, V. R., Binns, A. N., & Lynn, D. G. (2000). Construction of an efficient expression system for Agrobacterium tumefaciens based on the coliphage T5 promoter. *Gene*, *242*(1–2), 105–114.

Weisberg, A. J., Davis, E. W., Tabima, J., Belcher, M. S., Miller, M., Kuo, C.-H., Loper, J. E., Grünwald, N. J., Putnam, M. L., & Chang, J. H. (2020). Unexpected conservation and global transmission of agrobacterial virulence plasmids. *Science*, *368*(6495), eaba5256.

Weisberg, A. J., Miller, M., Ream, W., Grünwald, N. J., & Chang, J. H. (2022). Diversification of plasmids in a genus of pathogenic and nitrogen-fixing bacteria. *Philosophical Transactions of the Royal Society B*, *377*(1842), 20200466.

West, S. A., Griffin, A. S., & Gardner, A. (2007). Social semantics: Altruism, cooperation, mutualism, strong reciprocity and group selection. *Journal of Evolutionary Biology*, *20*(2), 415–432.

Wick, R. (2017). *Fitlong: Quality filtering tool for long reads*. https://github.com/rrwick/Filtlong

Wick, R. R., Judd, L. M., Gorrie, C. L., & Holt, K. E. (2017). Unicycler: Resolving bacterial genome assemblies from short and long sequencing reads. *PLoS Computational Biology*, *13*(6), e1005595.

Wick, R., Volkening, J., & Loman, N. (2017). Porechop. *Github Https://Github. Com/Rrwick/Porechop*.

Winans, S. C. (1992). Two-way chemical signaling in Agrobacterium-plant interactions. *Microbiological Reviews*, *56*(1), 12–31.

Winans, S. C., Kerstetter, R. A., & Nester, E. W. (1988). Transcriptional regulation of the virA and virG genes of Agrobacterium tumefaciens. *Journal of Bacteriology*, *170*(9), 4047–4054.

Winans, S., Mantis, N., Chen, C.-Y., Chang, C.-H., & Han, D. C. (1994). Host recognition by the VirA, VirG two-component regulatory proteins of Agrobacterium tumefaciens. *Research in Microbiology*, *145*(5–6), 461–473.

Xavier, J. B., Kim, W., & Foster, K. R. (2011). A molecular mechanism that stabilizes cooperative secretions in Pseudomonas aeruginosa. *Molecular Microbiology*, *79*(1), 166–179.

Chapter 2 References

Abisado, R. G., Benomar, S., Klaus, J. R., Dandekar, A. A., & Chandler, J. R. (2018). Bacterial quorum sensing and microbial community interactions. *MBio*, *9*(3), e02331-17.

Ågren, J. A., Davies, N. G., & Foster, K. R. (2019). Enforcement is central to the evolution of cooperation. *Nature Ecology & Evolution*, *3*(7), 1018–1029.

Barton, I. S., Eagan, J. L., Nieves-Otero, P. A., Reynolds, I. P., Platt, T. G., & Fuqua, C. (2021). Co-dependent and Interdigitated: Dual quorum sensing systems regulate conjugative transfer of the Ti plasmid and the At megaplasmid in Agrobacterium tumefaciens 15955. *Frontiers in Microbiology*, 3564.

Barton, I. S., Fuqua, C., & Platt, T. G. (2018). Ecological and evolutionary dynamics of a model facultative pathogen: Agrobacterium and crown gall disease of plants. *Environmental Microbiology*, *20*(1), 16–29.

Damore, J. A., & Gore, J. (2012). Understanding microbial cooperation. *Journal of Theoretical Biology*, *299*, 31–41.

Dessaux, Y., & Faure, D. (2018). Quorum sensing and quorum quenching in agrobacterium: A "go/no go system"? *Genes*, *9*(4), 210.

Dimitriu, T., Lotton, C., Bénard-Capelle, J., Misevic, D., Brown, S. P., Lindner, A. B., & Taddei, F. (2014). Genetic information transfer promotes cooperation in bacteria. *Proceedings of the National Academy of Sciences*, *111*(30), 11103–11108.

Dimitriu, T., Misevic, D., Capelle, J. B., Lindner, A. B., Brown, S. P., & Taddei, F. (2018). Selection of horizontal gene transfer through public good production. *BioRxiv*, 315960.

Farrand, S. K., Qin, Y., & Oger, P. (2002). Quorum-sensing system of Agrobacterium plasmids: Analysis and utility. In *Methods in enzymology* (Vol. 358, pp. 452–484). Elsevier.

Faure, D., & Lang, J. (2014). Functions and regulation of quorum-sensing in Agrobacterium tumefaciens. *Frontiers in Plant Science*, *5*, 14.

Foster, K. R., Shaulsky, G., Strassmann, J. E., Queller, D. C., & Thompson, C. R. (2004). Pleiotropy as a mechanism to stabilize cooperation. *Nature*, *431*(7009), 693–696.

French, K. E., Zhou, Z., & Terry, N. (2020). Horizontal 'gene drives' harness indigenous bacteria for bioremediation. *Scientific Reports*, *10*(1), 1–11.

Friesen, M. L. (2020). Social Evolution and Cheating in Plant Pathogens. *Annual Review of Phytopathology*, *58*, 55–75.

Fuqua, C., & Winans, S. C. (1996). Conserved cis-acting promoter elements are required for density-dependent transcription of Agrobacterium tumefaciens conjugal transfer genes. *Journal of Bacteriology*, *178*(2), 435–440.

Fuqua, W. C., & Winans, S. C. (1994). A LuxR-LuxI type regulatory system activates Agrobacterium Ti plasmid conjugal transfer in the presence of a plant tumor metabolite. *Journal of Bacteriology*, *176*(10), 2796–2806.

Fuqua, W. C., Winans, S. C., & Greenberg, E. P. (1994). Quorum sensing in bacteria: The LuxR-LuxI family of cell density-responsive transcriptional regulators. *Journal of Bacteriology*, *176*(2), 269–275.

Gallie, D., Hagiya, M., & Kado, C. (1985). Analysis of Agrobacterium tumefaciens plasmid pTiC58 replication region with a novel high-copy-number derivative. *Journal of Bacteriology*, *161*(3), 1034–1041.

Gelvin, S. B. (2003). Agrobacterium-mediated plant transformation: The biology behind the "gene-jockeying" tool. *Microbiology and Molecular Biology Reviews*, *67*(1), 16–37.

Gelvin, S. B. (2006). Agrobacterium virulence gene induction. *Agrobacterium Protocols*, 77–85.

Gordon, J. E., & Christie, P. J. (2014). The agrobacterium Ti plasmids. *Microbiology Spectrum*, *2*(6), 2–6.

Hamilton, W. D. (1964). The genetical evolution of social behaviour. II. *Journal of Theoretical Biology*, *7*(1), 17–52.

Jin, S., Roitsch, T., Ankenbauer, R., Gordon, M., & Nester, E. (1990). The VirA protein of Agrobacterium tumefaciens is autophosphorylated and is essential for vir gene regulation. *Journal of Bacteriology*, *172*(2), 525–530.

Kruskal, W. H., & Wallis, W. A. (1952). Use of ranks in one-criterion variance analysis. *Journal of the American Statistical Association*, *47*(260), 583–621.

Lassalle, F., Campillo, T., Vial, L., Baude, J., Costechareyre, D., Chapulliot, D., Shams, M., Abrouk, D., Lavire, C., & Oger-Desfeux, C. (2011). Genomic species are ecological species as revealed by comparative genomics in Agrobacterium tumefaciens. *Genome Biology and Evolution*, *3*, 762–781.

Lee, I. P. A., Eldakar, O. T., Gogarten, J. P., & Andam, C. P. (2021). Bacterial cooperation through horizontal gene transfer. *Trends in Ecology & Evolution*.

Mann, H. B., & Whitney, D. R. (1947). On a test of whether one of two random variables is stochastically larger than the other. *The Annals of Mathematical Statistics*, 50–60.

Mc Ginty, S. E., Rankin, D. J., & Brown, S. P. (2011). Horizontal gene transfer and the evolution of bacterial cooperation. *Evolution: International Journal of Organic Evolution*, *65*(1), 21–32.

Mehdiabadi, N. J., Jack, C. N., Farnham, T. T., Platt, T. G., Kalla, S. E., Shaulsky, G., Queller, D. C., & Strassmann, J. E. (2006). Kin preference in a social microbe. *Nature*, *442*(7105), 881–882.

Moré, M. I., Finger, L. D., Stryker, J. L., Fuqua, C., Eberhard, A., & Winans, S. C. (1996). Enzymatic synthesis of a quorum-sensing autoinducer through use of defined substrates. *Science*, *272*(5268), 1655–1658.

Morton, E. R., & Fuqua, C. (2012a). Genetic manipulation of Agrobacterium. *Current Protocols in Microbiology*, *25*(1), 3D – 2.

Morton, E. R., & Fuqua, C. (2012b). Laboratory maintenance of Agrobacterium. *Current Protocols in Microbiology*, *24*(1), 3D – 1.

Nowak, M. A. (2006). Five rules for the evolution of cooperation. *Science*, *314*(5805), 1560–1563.

Piper, K. R., von Bodman, S. B., & Farrand, S. K. (1993). Conjugation factor of Agrobacterium tumefaciens regulates Ti plasmid transfer by autoinduction. *Nature*, *362*(6419), 448–450.

Shoeb, E., Badar, U., Akhter, J., Shams, H., Sultana, M., & Ansari, M. A. (2012). Horizontal gene transfer of stress resistance genes through plasmid transport. *World Journal of Microbiology and Biotechnology*, *28*(3), 1021–1025.

Smith, J. (2001). The social evolution of bacterial pathogenesis. *Proceedings of the Royal Society of London. Series B: Biological Sciences*, *268*(1462), 61–69.

Strassmann, J. E., & Queller, D. C. (2011). Evolution of cooperation and control of cheating in a social microbe. *Proceedings of the National Academy of Sciences*, *108*(Supplement 2), 10855–10862.

Tatum, E., & Lederberg, J. (1947). Gene recombination in the bacterium Escherichia coli. *Journal of Bacteriology*, *53*(6), 673–684.

Travisano, M., & Velicer, G. J. (2004). Strategies of microbial cheater control. *Trends in Microbiology*, *12*(2), 72–78.

Wang, M., Schaefer, A. L., Dandekar, A. A., & Greenberg, E. P. (2015). Quorum sensing and policing of Pseudomonas aeruginosa social cheaters. *Proceedings of the National Academy of Sciences*, *112*(7), 2187–2191.

Weisberg, A. J., Davis, E. W., Tabima, J., Belcher, M. S., Miller, M., Kuo, C.-H., Loper, J. E., Grünwald, N. J., Putnam, M. L., & Chang, J. H. (2020). Unexpected conservation and global transmission of agrobacterial virulence plasmids. *Science*, *368*(6495), eaba5256.

Weisberg, A. J., Miller, M., Ream, W., Grünwald, N. J., & Chang, J. H. (2022). Diversification of plasmids in a genus of pathogenic and nitrogen-fixing bacteria. *Philosophical Transactions of the Royal Society B*, *377*(1842), 20200466.

West, S. A., Diggle, S. P., Buckling, A., Gardner, A., & Griffin, A. S. (2007). The social lives of microbes. *Annu. Rev. Ecol. Evol. Syst.*, *38*, 53–77.

West, S. A., Griffin, A. S., & Gardner, A. (2007). Social semantics: Altruism, cooperation, mutualism, strong reciprocity and group selection. *Journal of Evolutionary Biology*, *20*(2), 415–432.

Zhang, L., Murphy, P. J., Kerr, A., & Tate, M. E. (1993). Agrobacterium conjugation and gene regulation by N-acyl-L-homoserine lactones. *Nature*, *362*(6419), 446–448.

Chapter 3 References

(1) Ishii, S.; Tago, K.; Senoo, K. Single-Cell Analysis and Isolation for Microbiology and Biotechnology: Methods and Applications. *Appl. Microbiol. Biotechnol*. 2010, 86 (5), 1281–1292. https://doi.org/10.1007/s00253-010-2524-4 .

(2) Welch, J. D.; Williams, L. A.; DiSalvo, M.; Brandt, A. T.; Marayati, R.; Sims, C. E.; Allbritton, N. L.; Prins, J. F.; Yeh, J. J.; Jones, C. D. Selective Single Cell Isolation for Genomics Using Microraft Arrays. *Nucleic Acids Res*. 2016, 44 (17), 8292–8301. https://doi.org/10.1093/nar/gkw700 .

(3) Holland, S. L.; Reader, T.; Dyer, P. S.; Avery, S. V. Phenotypic Heterogeneity Is a Selected Trait in Natural Yeast Populations Subject to Environmental Stress. *Environ. Microbiol*. 2014, 16 (6), 1729–1740. https://doi.org/10.1111/1462-2920.12243 .

(4) Huys, G. R.; Raes, J. Go with the Flow or Solitary Confinement: A Look inside the Single-Cell Toolbox for Isolation of Rare and Uncultured Microbes. *Curr. Opin. Microbiol*. 2018, 44, 1–8. https://doi.org/10.1016/j.mib.2018.05.002 .

(5) Brehm-Stecher, B. F.; Johnson, E. A. Single-Cell Microbiology: Tools, Technologies, and Applications. Microbiol. *Mol. Biol. Rev*. 2004, 68 (3), 538–559. https://doi.org/10.1128/MMBR.68.3.538-559.2004 .

(6) Czechowska, K.; Johnson, D. R.; van der Meer, J. R. Use of Flow Cytometric Methods for Single-Cell Analysis in Environmental Microbiology. *Curr. Opin. Microbiol*. 2008, 11 (3), 205–212. https://doi.org/10.1016/j.mib.2008.04.006 .

(7) Faraghat, S. A.; Hoettges, K. F.; Steinbach, M. K.; Van Der Veen, D. R.; Brackenbury, W. J.; Henslee, E. A.; Labeed, F. H.; Hughes, M. P. High-Throughput, Low-Loss, Low-Cost, and Label-

Free Cell Separation Using Electrophysiology-Activated Cell Enrichment. *Proc. Natl. Acad. Sci. U. S. A.* 2017, 114 (18), 4591–4596. https://doi.org/10.1073/pnas.1700773114 .

(8) Tatematsu, K.; Kuroda, S. Automated Single-Cell Analysis and Isolation System: A Paradigm Shift in Cell Screening Methods for Bio-Medicines. In *Advances in Experimental Medicine and Biology*; Springer New York LLC, 2018; Vol. 1068, pp 7–17. https://doi.org/10.1007/978-981-13-0502-3_2 .

(9) DeMello, A. J. Control and Detection of Chemical Reactions in Microfluidic Systems. *Nature* 2006, 442 (7101), 394–402. https://doi.org/10.1038/nature05062 .

(10) El-Ali, J.; Sorger, P. K.; Jensen, K. F. Cells on Chips. *Nature* 2006, 442 (7101), 403–411. https://doi.org/10.1038/nature05063 .

(11) Psaltis, D.; Quake, S. R.; Yang, C. Developing Optofluidic Technology through the Fusion of Microfluidics and Optics. *Nature* 2006, 442 (7101), 381–386. https://doi.org/10.1038/nature05060 .

(12) Pratt, S. L.; Zath, G. K.; Akiyama, T.; Williamson, K. S.; Franklin, M. J.; Chang, C. B. DropSOAC: Stabilizing Microfluidic Drops for Time-Lapse Quantification of Single-Cell Bacterial Physiology. *Front. Microbiol*. 2019, 10, 2112. https://doi.org/10.3389/fmicb.2019.02112 .

(13) Kou, S.; Cheng, D.; Sun, F.; Hsing, I. M. Microfluidics and Microbial Engineering. *Lab Chip* 2016, 16 (3), 432–446. https://doi.org/10.1039/c5lc01039j .

(14) Lim, J. W.; Shin, K. S.; Moon, J.; Lee, S. K.; Kim, T. A Microfluidic Platform for High-Throughput Screening of Small Mutant Libraries. *Anal. Chem*. 2016, 88 (10), 5234–5242. https://doi.org/10.1021/acs.analchem.6b00317 .

(15) Nam, S.; Stowers, R.; Lou, J.; Xia, Y.; Chaudhuri, O. Varying PEG Density to Control Stress Relaxation in Alginate-PEG Hydrogels for 3D Cell Culture Studies. *Biomaterials* 2019, 200, 15–24. https://doi.org/10.1016/j.biomaterials.2019.02.004 .

(16) Kloxin, A. M.; Kasko, A. M.; Salinas, C. N.; Anseth, K. S. Photodegradable Hydrogels for Dynamic Tuning of Physical and Chemical Properties. *Science* (80-.). 2009, 324 (5923), 59–63. https://doi.org/10.1126/science.1169494 .

(17) Sergeeva, A.; Vikulina, A. S.; Volodkin, D. Porous Alginate Scaffolds Assembled Using Vaterite CaCO3 Crystals. *Micromachines* 2019, 10 (6), 357. https://doi.org/10.3390/mi10060357 .

(18) Duarte, J. M.; Barbier, I.; Schaerli, Y. Bacterial Microcolonies in Gel Beads for High-Throughput Screening of Libraries in Synthetic Biology. *ACS Synth. Biol*. 2017, 6 (11), 1988–1995. https://doi.org/10.1021/acssynbio.7b00111 .

(19) Connell, J. L.; Ritschdorff, E. T.; Whiteley, M.; Shear, J. B. 3D Printing of Microscopic Bacterial Communities. *Proc. Natl. Acad. Sci*. U. S. A. 2013, 110 (46), 18380–18385. https://doi.org/10.1073/pnas.1309729110 .

(20) Zengler, K.; Toledo, G.; Rappé, M.; Elkins, J.; Mathur, E. J.; Short, J. M.; Keller, M. Cultivating the Uncultured. *Proc. Natl. Acad. Sci*. U. S. A. 2002, 99 (24), 15681–15686. https://doi.org/10.1073/pnas.252630999 .

(21) Kloxin, A. M.; Tibbitt, M. W.; Anseth, K. S. Synthesis of Photodegradable Hydrogels as Dynamically Tunable Cell Culture Platforms. *Nat. Protoc*. 2010, 5 (12), 1867–1887. https://doi.org/10.1038/nprot.2010.139 .

(22) Peppas, N. A.; Hilt, J. Z.; Khademhosseini, A.; Langer, R. Hydrogels in Biology and Medicine: From Molecular Principles to Bionanotechnology. *Adv. Mater*. 2006, 18 (11), 1345–1360. https://doi.org/10.1002/adma.200501612 .

(23) Van Der Vlies, A. J.; Barua, N.; Nieves-Otero, P. A.; Platt, T. G.; Hansen, R. R. On Demand Release and Retrieval of Bacteria from Microwell Arrays Using Photodegradable Hydrogel Membranes. *ACS Appl. Bio Mater*. 2019, 2 (1), 266–276. https://doi.org/10.1021/acsabm.8b00592 .

(24) Tibbitt, M. W.; Kloxin, A. M.; Sawicki, L. A.; Anseth, K. S. Mechanical Properties and Degradation of Chain and Step-Polymerized Photodegradable Hydrogels. *Macromolecules* 2013, 46 (7), 2785–2792. https://doi.org/10.1021/ma302522x .

(25) Harrison, J.; Studholme, D. J. Recently Published Streptomyces Genome Sequences. *Microb. Biotechnol*. 2014, 7 (5), 373–380. https://doi.org/10.1111/1751-7915.12143 .

(26) Reader, J. S.; Ordoukhanian, P. T.; Kim, J. C.; De Crécy-Lagard, V.; Hwang, I.; Farrand, S.; Schimmel, P. Major Biocontrol of Plant Tumors Targets tRNA Synthetase. *Science*. 2005, 309 (5740), 1533. https://doi.org/10.1126/science.1116841 .

(27) Holsters, M.; de Waele, D.; Depicker, A.; Messens, E.; van Montagu, M.; Schell, J. Transfection and Transformation of Agrobacterium tumefaciens. *Mol. Gen. Genet*. 1978, 163 (2), 181–187. https://doi.org/10.1007/BF00267408 .

(28) Tempe, J.; Petit, A.; Holsters, M.; Montagu, M. v.; Schell, J. Thermosensitive Step Associated with Transfer of the Ti Plasmid during Conjugation: Possible Relation to Transformation in Crown Gall. *Proc. Natl. Acad. Sci*. U. S. A. 1977, 74 (7), 2848–2849. https://doi.org/10.1073/pnas.74.7.2848 .

(29) Morton, E. R.; Fuqua, C. Genetic Manipulation of Agrobacterium. *Curr. Protoc. Microbiol*. 2012, 25, 3D.2.1-3D.2.15. https://doi.org/10.1002/9780471729259.mc03d02s25 .

(30) Khire, V. S.; Lee, T. Y.; Bowman, C. N. Surface Modification Using Thiol−Acrylate Conjugate Addition Reactions. *Macromolecules* 2007, 40 (16), 5669–5677. https://doi.org/10.1021/ma070146j .

(31) Hu, M.; Noda, S.; Okubo, T.; Yamaguchi, Y.; Komiyama, H. Structure and Morphology of Self-Assembled 3-Mercaptopropyltrimethoxysilane Layers on Silicon Oxide. *Appl. Surf. Sci*. 2001, 181 (3–4), 307–316. https://doi.org/10.1016/S0169-4332(01)00399-3 .

(32) Sprouffske, K.; Wagner, A. Growthcurver: An R Package for Obtaining Interpretable Metrics from Microbial Growth Curves. *BMC Bioinf*. 2016, 17 (1), 172. https://doi.org/10.1186/s12859-016-1016-7 .

(33) Baldwin, A. D.; Kiick, K. L. Tunable Degradation of Maleimide–Thiol Adducts in Reducing Environments. *Bioconjug. Chem*. 2011, 22 (10), 1946–1953. https://doi.org/10.1021/bc200148v

(34) Masigol, M.; Fattahi, N.; Barua, N.; Lokitz, B. S.; Retterer, S. T.; Platt, T. G.; Hansen, R. R. Identification of Critical Surface Parameters Driving Lectin-Mediated Capture of Bacteria from Solution. *Biomacromolecules* 2019, 20 (7), 2852–2863. https://doi.org/10.1021/acs.biomac.9b00609 .

(35) Hayman, G. T.; Farrand, S. K. Characterization and Mapping of the Agrocinopine-Agrocin 84 Locus on the Nopaline Ti Plasmid pTiC58. *J. Bacteriol*. 1988, 170 (4), 1759–1767. https://doi.org/10.1128/jb.170.4.1759-1767.1988 .

(36) Hayman, G. T.; Von Bodman, S. B.; Kim, H.; Jiang, P.; Farrand, S. K. Genetic Analysis of the Agrocinopine Catabolic Region of Agrobacterium tumefaciens Ti Plasmid pTiC58, Which

Encodes Genes Required for Opine and Agrocin 84 Transport. *J. Bacteriol*. 1993, 175 (17), 5575–5584. https://doi.org/10.1128/jb.175.17.5575-5584.1993 .

(37) Li, H.; Durbin, R. Fast and Accurate Short Read Alignment with Burrows-Wheeler Transform. *Bioinformatics* 2009, 25 (14), 1754–1760. https://doi.org/10.1093/bioinformatics/btp324 .

(38) McKenna, A.; Hanna, M.; Banks, E.; Sivachenko, A.; Cibulskis, K.; Kernytsky, A.; Garimella, K.; Altshuler, D.; Gabriel, S.; Daly, M.; DePristo, M. A. The Genome Analysis Toolkit: A MapReduce Framework for Analyzing Next-Generation DNA Sequencing Data. *Genome Res*. 2010, 20 (9), 1297–1303. https://doi.org/10.1101/gr.107524.110 .

(39) Allardet-Servent, A.; Michaux-Charachon, S.; Jumas-Bilak, E.; Karayan, L.; Ramuz, M. Presence of One Linear and One Circular Chromosome in the Agrobacterium tumefaciens C58 Genome. *J. Bacteriol*. 1993, 175 (24), 7869–7874. https://doi.org/10.1128/jb.175.24.7869-7874.1993 .

(40) Sambrook, J.; Russell, D. Molecular Cloning: A Laboratory Manual Fourth Edition Ed *Cold Spring Harbor*. 2001.

(41) Weber, L. M.; Lopez, C. G.; Anseth, K. S. Effects of PEG Hydrogel Crosslinking Density on Protein Diffusion and Encapsulated Islet Survival and Function. *J. Biomed. Mater. Res. Part A* 2009, 90A (3), 720–729. https://doi.org/10.1002/jbm.a.32134 .

(42) Canal, T.; Peppas, N. A. Correlation between Mesh Size and Equilibrium Degree of Swelling of Polymeric Networks. *J. Biomed. Mater. Res*. 1989, 23 (10), 1183–1193. https://doi.org/10.1002/jbm.820231007 .

(43) Zustiak, S. P.; Leach, J. B. Hydrolytically Degradable Poly(Ethylene Glycol) Hydrogel Scaffolds with Tunable Degradation and Mechanical Properties. *Biomacromolecules* 2010, 11 (5), 1348–1357. https://doi.org/10.1021/bm100137q .

(44) Metters, A.; Hubbell, J. Network Formation and Degradation Behavior of Hydrogels Formed by Michael-Type Addition Reactions. *Biomacromolecules* 2005, 6 (1), 290–301. https://doi.org/10.1021/bm049607o .

(45) Khan, A. H.; Cook, J. K.; Wortmann, W. J.; Kersker, N. D.; Rao, A.; Pojman, J. A.; Melvin, A. T. Synthesis and Characterization of Thiol-Acrylate Hydrogels Using a Base-Catalyzed Michael Addition for 3D Cell Culture Applications. *J. Biomed. Mater. Res. - Part B Appl. Biomater*. 2020, 108 (5), 2294–2307. https://doi.org/10.1002/jbm.b.34565 .

(46) Rastogi, R. P.; Richa; Kumar, A.; Tyagi, M. B.; Sinha, R. P. Molecular Mechanisms of Ultraviolet Radiation-Induced DNA Damage and Repair. *J. Nucleic Acids* 2010, 2010, 592980. https://doi.org/10.4061/2010/592980 .

(47) Hayman, G. T.; Farrand, S. K. Agrobacterium Plasmids Encode Structurally and Functionally Different Loci for Catabolism of Agrocinopine-Type Opines. *Mol. Gen. Genet.* 1990, 223 (3), 465–473. https://doi.org/10.1007/BF00264455 .

(48) Kim, H.; Farrand, S. K. Characterization of the acc Operon from the Nopaline-Type Ti Plasmid pTiC58, Which Encodes Utilization of Agrocinopines A and B and Susceptibility to Agrocin 84. *J. Bacteriol*. 1997, 179 (23), 7559–7572. https://doi.org/10.1128/jb.179.23.7559-7572.1997 .

(49) LeValley, P. J.; Tibbitt, M. W.; Noren, B.; Kharkar, P.; Kloxin, A. M.; Anseth, K. S.; Toner, M.; Oakey, J. Immunofunctional Photodegradable Poly(Ethylene Glycol) Hydrogel Surfaces for

the Capture and Release of Rare Cells. *Colloids Surf*., B 2019, 174, 483–492. https://doi.org/10.1016/j.colsurfb.2018.11.049 .

(50) Connon, S. A.; Giovannoni, S. J. High-Throughput Methods for Culturing Microorganisms in Very-Low-Nutrient Media Yield Diverse New Marine Isolates. *Appl. Environ. Microbiol*. 2002, 68 (8), 3878–3885. https://doi.org/10.1128/AEM.68.8.3878-3885.2002 .

(51) Jung, J. H.; Lee, J. E. Real-Time Bacterial Microcolony Counting Using On-Chip Microscopy. *Sci. Rep*. 2016, 6, 21473. https://doi.org/10.1038/srep21473 .

(§) Fattahi, N.; Nieves-Otero, P. A.; Masigol, M.; Van der Vlies, A. J.; Jensen, R. S.; Hansen, R. R.; Platt, T. G. Photodegradable Hydrogels for Rapid Screening, Isolation, and Genetic Characterization of Bacteria with Rare Phenotypes. *Biomacromolecules*. 2020, 21(8), 3140-3151. https://doi.org/10.1021/acs.biomac.0c00543 .